



HAL
open science

Study, Design and Evaluation of an Actuated Knee Implant for Postoperative Ligament Imbalance Correction

Andrea Collo

► **To cite this version:**

Andrea Collo. Study, Design and Evaluation of an Actuated Knee Implant for Postoperative Ligament Imbalance Correction. Mechanics [physics.med-ph]. Télécom Bretagne; Université de Bretagne Occidentale, 2014. English. NNT: . tel-01206287

HAL Id: tel-01206287

<https://hal.science/tel-01206287v1>

Submitted on 28 Sep 2015

HAL is a multi-disciplinary open access archive for the deposit and dissemination of scientific research documents, whether they are published or not. The documents may come from teaching and research institutions in France or abroad, or from public or private research centers.

L'archive ouverte pluridisciplinaire **HAL**, est destinée au dépôt et à la diffusion de documents scientifiques de niveau recherche, publiés ou non, émanant des établissements d'enseignement et de recherche français ou étrangers, des laboratoires publics ou privés.



THÈSE / Télécom Bretagne

sous le sceau de l'Université européenne de Bretagne

pour obtenir le grade de Docteur de Télécom Bretagne

En accréditation conjointe avec l'Ecole doctorale Sicma

Mention : Sciences et Technologies de l'Information et de la Communication

présentée par

Andrea Collo

préparée dans le département Image et traitement de l'information
Laboratoire Latim et Lirmm

Study, Design and Evaluation of an Actuated Knee Implant for Postoperative Ligament Imbalance Correction

Thèse soutenue le 27 octobre 2014

Devant le jury composé de :

Shabnam Arbab Chirani
Professeur, LBMS – Ecole Nationale d'Ingénieurs de Brest / président

Guillaume Morel
Professeur, ISIR – Université Pierre et Marie Curie / rapporteur

Jérôme Molimard
Professeur, LGF – Ecole des Mines de Saint Etienne / rapporteur

Éric Stindel
PU-PH, Latim – CHRU de Brest / examinateur

Philippe Poinet
Professeur, LIRMM – Université de Montpellier 2 / co-directeur de thèse

Chafaa Hamitouche-Djabou
Professeur, Télécom Bretagne / directrice de thèse

Charles Baur
Senior scientist, Ecole polytechnique fédérale de Lausanne / invité

sous le sceau de l'Université Européenne de Bretagne

Télécom Bretagne

en accréditation conjointe avec l'Ecole Doctorale Sicma

Study, Design and Evaluation of an Actuated Knee Implant for Postoperative Ligament Imbalance Correction

Thèse de Doctorat

Mention : Sciences et Technologies de l'Information et de la Communication (STIC)

Présentée par **Andrea Collo**

Département Image et Traitement de l'Information (ITI)

Laboratoire de Traitement de l'Information Médicale (LaTIM UMR 1101 INSERM)
Laboratoire d'Informatique, de Robotique et de Microélectronique de Montpellier
(LIRMM UMR 5506 CNRS UM2)

Directrice de thèse : Chafiaa Hamitouche-Djabou

Co-directeur de thèse : Philippe Poignet

Soutenue le lundi 27 octobre 2014

Jury :

M. Guillaume Morel, Professeur, <i>ISIR – UPMC</i> , Paris	(Rapporteur)
M. Jérôme Molimard, Professeur, <i>LGF – ENSMSE</i> , Saint-Etienne	(Rapporteur)
Mme Chafiaa Hamitouche-Djabou, Professeur, <i>Télécom Bretagne</i> , Brest	(Directrice de thèse)
M. Philippe Poignet, Professeur, <i>LIRMM – UM2</i> , Montpellier	(Co-directeur de thèse)
M. Eric Stindel, PU-PH, <i>LaTIM – CHRU de Brest</i> , Brest	(Examinateur)
Mme Shabnam Arbab Chirani, Professeur, <i>LBMS – ENIB</i> , Brest	(Examinatrice)
M. Charles Baur, Docteur, <i>EPFL STI IMT INSTANT-LAB</i> , Lausanne	(Invité)

*Non posso cambiare la direzione del vento,
ma posso spiegare le mie vele
in modo tale da giungere sempre a destinazione.*

Mamma e Papà,

se ho ottenuto questo grande risultato è grazie a voi:
mi avete insegnato a mettere passione in tutto ciò che faccio
e mi avete sempre aiutato a far le scelte giuste.
... tutto sommato, siete davvero brava gente.

Andrea

Acknowledgements

Ces trois ans de thèse m'ont appris beaucoup de choses et ont été une expérience formidable. J'ai eu la chance de connaître des personnes très intéressantes, de devenir leur ami, de partager avec elles des moments de bonheur mais aussi de difficulté. Ensemble on a tissé des liens d'amitié que, j'en suis sûr, nous n'allons jamais oublier. Le premier remerciement est donc pour tous mes amis: les bRest friends, la bande de fripouilles de Montpellier, mes colocs (mais pas tous, juste les marins et les chercheurs), mes collègues au LaTIM, à Télécom, au LIRMM et à EuroMov.

Ceux qui me connaissent vraiment savent quelle importance je donne à ma famille et pourquoi. Mes parents m'ont toujours soutenu et encouragé, à distance, à travers les hauts et les bas de ces trois dernières années. Sans leurs conseils je n'aurais pas réussi à faire les bons choix, ou quand même je ne les aurais pas faits au bon moment. Le second remerciement est donc pour ma maman et mon papa, qui sont pour moi une vraie source d'inspiration.

Il y a quatre ans je suis parti en Erasmus à Nantes sans aucune intention d'enchaîner mon Master 2 avec une thèse de doctorat. Heureusement j'ai changé d'idée! Durant cette thèse, les échanges avec mes encadrants m'ont permis d'apprendre à organiser mon travail de manière efficace. Leurs critiques constructives m'ont fait réfléchir à mes erreurs et m'ont permis de mûrir. Donc voilà, le troisième, et dernier, remerciement est pour mes trois encadrants, qui ont contribué à rendre ma thèse une expérience très enrichissante.

Declaration of Authorship

I hereby certify that this thesis has been composed by me and is based on my own work, unless stated otherwise. No other person's work has been used without due acknowledgement in this thesis. All references and verbatim extracts have been quoted, and all sources of information, including graphs and data sets, have been specifically acknowledged.

© 2014 - Andrea Collo

Abstract

Collateral ligaments tensioning is a key achievement of Total Knee Arthroplasty (TKA). This stage, which directly determines the postoperative knee joint function and the implant lifespan, cannot be standardised for all patients and highly relies on the surgeon's experience and perception. Over the last twenty-five years, the design of instrumented knee prostheses has been accepted as a way forward to provide the surgeon with useful pre- and intraoperative assistance. Nevertheless, suboptimal collateral ligaments tension values are practically unavoidable and may lead to severe postoperative complications; in the worst-case scenario, revision surgery might be necessary already a few years after primary TKA. In such framework, this work aims to propose a novel instrumented knee implant able to detect collateral ligaments laxity conditions right after primary TKA and, if needed, compensate for any detected inaccuracy in the postoperative period.

A miniaturised actuation system embedded in the tibial baseplate can be employed to adjust the inclination of the tibial tray and re-tighten a too lax collateral ligament. Such correcting action, carried out to restore optimal balance conditions before the occurrence of more severe complications, is intended to improve the prosthesis lifespan and, contextually, reduce the need for revision surgery. To this end, a compact and robust mechanical structure was dimensioned in order to fulfil the aforementioned clinical needs while facing with technical and technological limitations. Smart design choices resulted in a good system efficiency, as proved by the mechanical model static force analysis. Simulations run on the implant 3D model allowed to perform useful design optimisations and to estimate the components robustness properties. Upon fabrication of the proposed instrumented tibial component full-scale prototype, stability and force sensors tests on a knee simulator were defined to evaluate the actuation system working principle and assess the effectiveness of the proposed design choices under normal working conditions. The very promising results of the experimental validation stage also provided precious indications for future work and improvements.

KEYWORDS

Instrumented Knee Prosthesis,
Knee Ligament Imbalance,
Actuation System,
Miniaturised Mechanical Device

Résumé

Un des objectifs principaux de l'Arthroplastie Totale du Genou (ATG) est la mise en place de conditions appropriées de tension ligamentaire au niveau des deux ligaments collatéraux de l'articulation. Cette étape, qui est effectuée manuellement par le chirurgien, détermine directement la fonctionnalité de l'implant prothétique et sa durée de vie postopératoire. Au cours des deux dernières décennies, plusieurs outils ont été développés en tant qu'outils d'aide au chirurgien pour la phase d'équilibrage ligamentaire. En dépit de cela, les imprécisions peropératoires sont pratiquement inévitables et risquent de donner lieu à des complications postopératoires. Dans le pire des cas, une reprise chirurgicale devient nécessaire pour rétablir des conditions d'équilibre optimales. Dans ce contexte, cette thèse a pour objectif l'étude, la conception et l'analyse d'un modèle original de prothèse instrumentée de genou qui soit capable de détecter toute condition de laxité ligamentaire postopératoire et, si nécessaire, de la compenser.

Un système d'actionnement miniaturisé embarqué dans l'embase tibiale a été proposé pour ajuster l'inclinaison du plateau tibial de façon à retendre un ligament collatéral trop relâché. Cette opération, réalisée avant la survenue de complications plus graves, est suffisante pour rétablir des conditions d'équilibre optimales sans besoin d'une seconde intervention chirurgicale. Pour ce faire, une structure mécanique a été conçue et dimensionnée de façon à répondre aux besoins cliniques tout en faisant face aux contraintes de biocompatibilité imposées par un milieu biologique tel que celui du genou. L'analyse du modèle mécanique du système d'actionnement proposé a confirmé son bon rendement; les simulations effectuées sur le modèle 3D de l'implant ont permis d'en optimiser la conception. Suite à la fabrication d'un prototype à taille réelle de l'implant proposé, des essais expérimentaux ont été conduits à l'aide d'un simulateur du genou pour valider le principe de fonctionnement du système d'actionnement et pour en évaluer les performances lors de la marche. Les résultats très prometteurs de la phase de validation expérimentale ont également fourni des indications précieuses pour l'orientation et la suite de travaux futurs.

MOTS CLÉ

Prothèse Instrumentée de Genou,
Déséquilibre Ligamentaire,
Système d'Actionnement,
Structure Mécanique Miniaturisée

Abbreviations

AP	AnteroPosterior
APD	Anterior-Posterior Displacement
BW	Body Weight
CAD	Computer-Aided Design
CAMI	Computer Assisted Medical Intervention
CAOS	Computer Assisted Orthopaedic Surgery
CoP	Center of Pressure
DoF	Degree of Freedom
FE	Flexion-Extension
IER	Internal-External Rotation
KJ	Knee Joint
LLMA	Lower Limb Mechanical Axis
MA	Mechanical Advantage
ML	MedioLateral
NS	Navigation System
PC	PiezoCeramics
PE	PolyEthylene
RoM	Range of Motion
TKA	Total Knee Arthroplasty
USB	Universal Serial Bus
VMS	Von Mises Stress
VVR	Varus-Valgus Rotation
WL	Wedge-Leadscrew
ZP	Zero Position
3D	Three-Dimensional

Contents

General Introduction	1
1 Introduction	5
1.1 The Knee Joint	5
1.1.1 Definition	5
1.1.2 Biomechanics	7
1.2 Total Knee Arthroplasty	9
1.2.1 Historical Hints	10
1.2.2 Primary TKA	11
1.2.3 Revision TKA	16
2 Assistive Tools and Devices for TKA	19
2.1 Jigs, Cutting Tools and Spreaders	19
2.2 Navigation Systems	22
2.3 Instrumented Knee Implants	23
2.4 A Novel Instrumented Tibial Component	30
2.4.1 Collateral Ligaments Balance Conditions: an Unsolved Problem	30
2.4.2 A Self-Powered Tibial Component for Postoperative Knee Balance Evaluation	31
2.4.3 Current Achievements and Purpose of This Work	34
3 Tibial Component Actuation Requirements	37

3.1	Envisaged Protocol	37
3.2	Clinical Needs	39
3.3	Constraints	40
3.3.1	Volume	41
3.3.2	Accuracy	42
3.3.3	Robustness	42
3.3.4	Wireless Power Supply and Control	43
3.3.5	Biocompatibility	45
3.4	Possible Actuation Approaches	46
4	Actuation System Design	49
4.1	Working Principle	50
4.2	Components Dimensions	52
4.2.1	Wedge-Leadscrew System	52
4.2.2	Baseplate and Mobile Tray	53
4.3	Mechanical Analysis	55
4.3.1	Static Force Analysis	55
4.3.2	Friction Losses	60
4.3.3	Screw Force	65
4.4	Microactuator Selection	68
4.5	Discussion	69
4.5.1	Locking Issue	69
4.5.2	Fine-Tuning Actuation	72
4.5.3	Materials and Sealing	73
4.5.4	Actuation System Scaling	74
5	Experimental Validation	75
5.1	3D Model Simulations	75

5.1.1	Static Analyses	75
5.1.2	Remarks	79
5.2	Prototyping	80
5.3	Knee Simulator	83
5.4	Stability Tests	84
5.4.1	Experimental Protocol	84
5.4.2	Results	87
5.5	Force Sensors	87
5.5.1	Experimental Protocol	88
5.5.2	Results	92
5.6	Comments	94
6	Conclusion	95
6.1	Conclusions	95
6.2	Perspectives	98
Appendix	Actuated Screws Model	103
A.1	Introduction	103
A.2	Actuation System Design	103
A.3	Mechanical Analysis	106
A.4	Microactuator Selection	107
A.5	Discussion	108
A.5.1	Locking Issue	108
A.5.2	Fine-Tuning Actuation	109
A.5.3	Materials and Sealing	109
A.5.4	Actuation System Scaling and Integration with the Piezoceramics Elements	110
A.6	Experimental Stage	111
A.6.1	3D Model Simulations	111

A.6.2 Prototyping	111
A.7 Conclusions and Perspectives	112
Bibliography	115
Publications	129
List of Figures	131
List of Tables	137

General Introduction

Over the last decades, Computer Assisted Medical Intervention (CAMI) technologies have greatly improved. A set of assistance tools has been made available to clinicians, so as to provide them with further knowledge in both the preoperative and the intraoperative periods. The advantages brought by CAMI techniques are both for clinicians and for patients. In general terms, with respect to classic surgical procedures, better accuracy and safety conditions can be attained, as well as less invasive medical procedures. *“CAMI give clinicians the hardware and software tools to enable them to fully exploit the available multimodal information (prior knowledge, gestures or organ models, medical images, physiological signals, etc.) in order to plan, simulate and perform a diagnostic or therapeutic gesture that is as minimally invasive and effective as possible. This field is thematically wide and relevant to signal and image processing, data fusion as well as modeling and simulation, biomechanics, biomedical engineering or robotics”* [1, p. xii]. For a generic CAMI, it is possible to distinguish three successive stages:

Preoperative Evaluation - The maximum of information as possible is collected about the patient. Different sources of information can be combined, including medical and functional history, physical examinations and, when needed, a detailed assessment of preoperative radiographic data.

Surgical Planning - According to the processed data, the optimal patient-specific strategy to perform the surgical intervention is defined.

Action - The planned operation is performed by the surgeon, possibly assisted by a dedicated navigation system in order to monitor the whole procedure until its completion.

CAMI techniques include the quantitative evaluation and processing of multi-modal medical data and a priori knowledge, the definition of patient-specific acts and the implementation of guidance systems to achieve the planned strategy in the safest way possible. In the postoperative period, after assessing the results and the effectiveness of

the adopted techniques, the whole set of processed data is usually stored for potential follow-up visits. There is no extensive evidence that the application of computer technology to medical procedures results, in the long-term, in a significant improvement in operative outcome: *“determining the cost and time benefits, both before and after an obligatory learning curve, requires a complex interaction of capital investments, time savings and outcome research on both safety and efficacy issues”* [2, p. 171]. Medical quality assessment has to be based on comparative surgical trials between classic and computer assisted procedures. Clinical validation necessarily implies long-term medical observations and the evaluation of postoperative outcomes. Nevertheless, CAMI technologies are considered the future of surgery, as it is clearly shown by the larger and larger investments made nowadays in such direction.

In the case of Computer Assisted Orthopaedic Surgery (CAOS), CAMI techniques are employed to improve the outcome of orthopaedic surgical procedures. Pre-, intra- and postoperatively, the clinician can make use of different assistance tools conceived by the combination of computer and robotics technologies [3]. Such instruments mainly facilitate the preparation of cavities or bone surfaces for prosthesis placement, as well as improve component positioning procedures. Radiographic and anatomic data get synergically combined with additional instrument and implant information, leading to a more accurate patient-centered analysis. The case of a surgery for prosthesis installation can be considered by way of illustration:

- in the preoperative period, CAOS techniques allow the planning of the least invasive bone cuts, as well as the determination of patient-specific prosthetic component dimensions;
- intraoperatively, the surgeon can check in real time the correct positioning of the installed implant and, if required, perform precise measurements and corrections. The better the accuracy during the surgery, the more functional the prosthesis and the longer its expected lifespan;
- postoperatively, the operative outcomes are expected to reflect all the aforementioned advantages: namely, for the considered example, a shorter recovery period for the patient and a reduced risk of postoperative complications.

Total Knee Arthroplasty (TKA) is the surgical operation that is considered in this work. TKA consists in the complete replacement of the knee joint by means of a prosthesis [4]. The great challenge of TKA surgery consists in setting up the optimal compromise between mobility and stability: after surgery, the prosthetic joint should

restore the complex functionality of the knee articulation and, at the same time, guarantee a long-lasting stability, without any imbalance condition [5]. To this purpose, it is common to distinguish two key achievements of TKA: first, the correct alignment of the prosthesis with respect to the lower limb mechanical axis; second, the set up of proper balance conditions for the two collateral ligaments of the knee. Both operations are manually performed in the intraoperative period by the orthopaedic surgeon. Dedicated CAOS systems enable, nowadays, the determination of proper alignment conditions for the different prosthetic components. Concerning ligament balance conditions, they depend on both the bone cuts and the component positioning stages. In order not to give rise to any postoperative joint instability, none of the two collateral ligaments should be laxer (or tighter) than the other. During the first years after TKA surgery, the morphofunctional evolution of the patient (changes in body weight, lifestyle and physiology) may amplify any intraoperative inaccuracy and give rise to severe postoperative complications. Component misalignments and premature wear conditions might be generated in the prosthetic knee. In the worst-case scenario, the only solution is represented by revision surgery: the knee prosthesis, which has become suboptimal, is replaced by a new one, with the purpose of restoring perfect balance conditions. A second surgical operation is clearly demanding, both for the patient and for the surgeon [4]. The prosthetic knee articulation undergoing a postoperative complication is less strong than before and the second rehabilitation period is normally more stressful than the first one. With the incidence of TKA surgery increasing annually, the number of revision surgeries continues to rise [6, 7]. *“At the moment, around one tenth of the operations for artificial knees are prosthesis revisions”* [1, p. 13].

Different instruments have been proposed in order to help the surgeon setting up perfect balance conditions during TKA. Unfortunately, despite the assistance provided by such tools, outcomes still majorly depend on the surgeon's experience and perception. Intraoperative inaccuracies in collateral ligaments tensions are unavoidable [8] and no tool gives the possibility to compensate for them in the postoperative period. To cope with this lack, over the last two decades the orthopaedic community has started looking for a way to reduce the number (and the costs) of implant failures from a different perspective. The development of smart knee implants seems the most promising approach: prosthetic components would no longer be passive metal pieces, but active devices able to cope with unexpected complications. The possibility to compensate for the unavoidable inaccuracies of primary TKA surgery and restore optimal balance conditions in the postoperative period should, in the long term, strongly reduce the need for revision surgery.

This project falls within this framework. The goal of this study is to propose a novel instrumented knee implant able to evaluate knee balance conditions after primary TKA and, if needed, compensate for any detected inaccuracy in collateral ligament tensions. Such correcting action must be performed postoperatively and without resorting to revision surgery. As it will be discussed in the following, this challenging project is strongly multidisciplinary and leads to face with severe constraints and the necessity to find proper compromises between the striving for innovation and the feasibility issues that arise from a biocompatible environment.

1.1 The Knee Joint

1.1.1 Definition

In this work the expression Knee Joint (KJ) addresses the whole human knee articulation, including the bony structures and the set of soft tissues surrounding them. The KJ, which is the largest joint in the human body [9], consists of three bones: the femur, the tibia and the patella (Fig. 1.1).

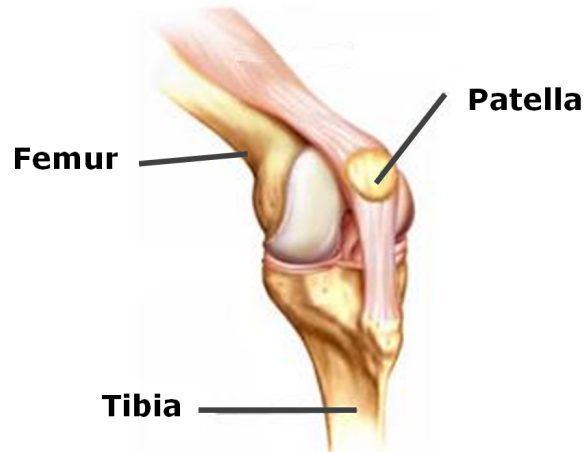


Figure 1.1 – the human Knee Joint (source: unknown)

The femur in the thigh and the tibia in the shin are the two longest bones in the human body. The patella, also called kneecap, is a circular-triangular bone located at the distal end of the femur; embedded within the patellar tendon on the anterior side of the knee, it is the largest sesamoid bone in the human body. Technically, the KJ consists of two sub-parts: the Tibiofemoral Joint (between the tibia and the femur) and the Patellofemoral Joint (between the patella and the femur). The presence of a broad network of soft tissues (ligaments, tendons and cartilages) together with the action of

the main muscles of the leg ensure at the same time the stabilization of the articulation and its complex kinematics. The imaginary line running through the hip joint center to the ankle joint center is defined as the Lower Limb Mechanical Axis (LLMA), as depicted in Fig. 1.2.

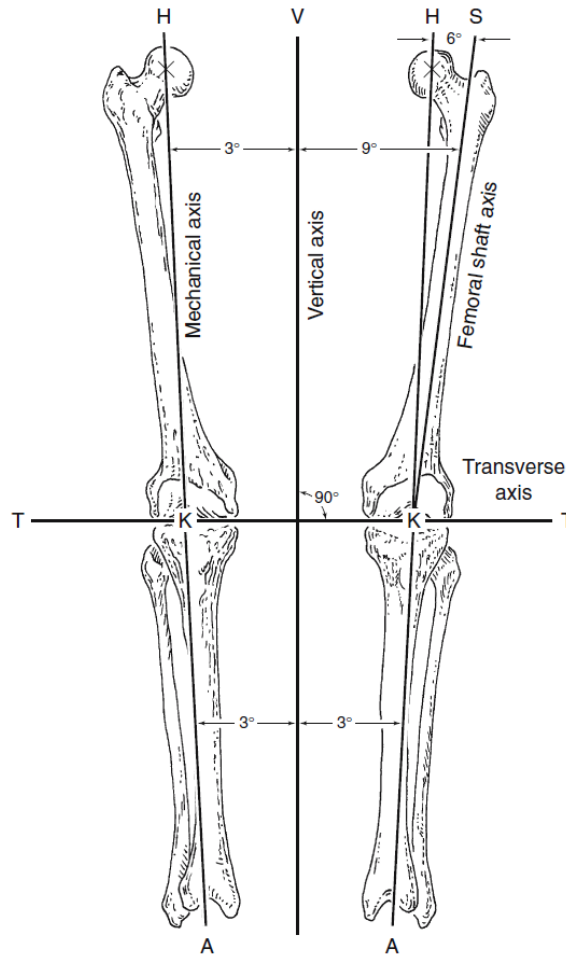


Figure 1.2 – the Lower Limb Mechanical Axis [4]

A natural process of bone transformation takes place during growth [10]. The articular centers of the hip, the knee and the ankle get aligned in such a way that the stresses acting on the KJ get properly distributed. During this process, the distal and proximal surfaces of respectively the femur and the tibia functionally adapt their shapes in order to achieve a maximum level of robustness. This adaptability is optimised for human bipedalism and leads to a specific orientation of the collagen fibers inside the bones. Knee ligaments are involved in this adaptation process and ensure a homogeneous distribution of all the efforts on the articular surfaces. In these terms, ligaments play a key role for proper KJ stabilization. Knee soft tissues intersect on different layers and encapsulate the distal femur with the proximal tibia. The result of such folded configuration is called knee capsule, which holds the synovial fluid that bathes the joint.

According to the type of effort that the articulation undergoes, the articular tissues are differently stressed. Any ligament distortion that may occur poses a serious threat to the whole articulation; for instance, any unnatural ligament elongation might allow undesired movements in the joint, thus reducing its stability. Knee ligaments also play a very important proprioceptive role: according to their tension conditions, they participate in tuning muscular responses. This is a complex task, if one considers that muscles show different mechanical behaviours according to their shape and insertion points.

1.1.2 Biomechanics

The biomechanics of the human KJ can be described by means of a set of basic anatomical terms. Fig. 1.3 shows the three reference anatomical planes (sagittal, frontal and horizontal), as well as six descriptive terms related to them (anterior and posterior, inferior and superior, left and right). Fig. 1.4 illustrates the concept of body midline and introduces four more terms (distal and proximal, medial and lateral).

Being a synovial joint, the KJ permits a variety of movements. From a biomechanical point of view, the KJ kinematics is described by six degrees of freedom, three rotational and three linear. However, due to the single relative mobility of each articular component and to the interactions between muscles and ligaments, that stabilize the

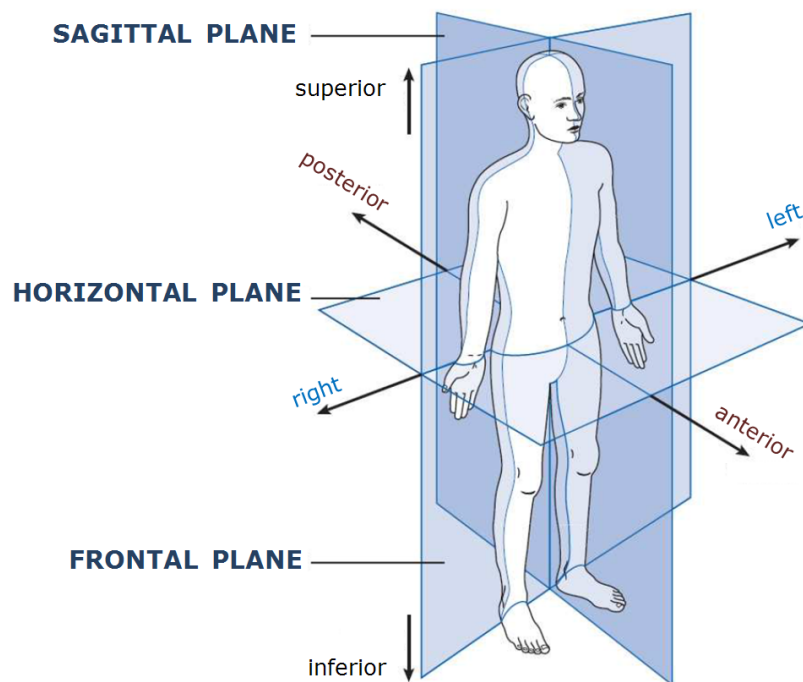


Figure 1.3 – the anatomical planes of the human body (source: unknown)

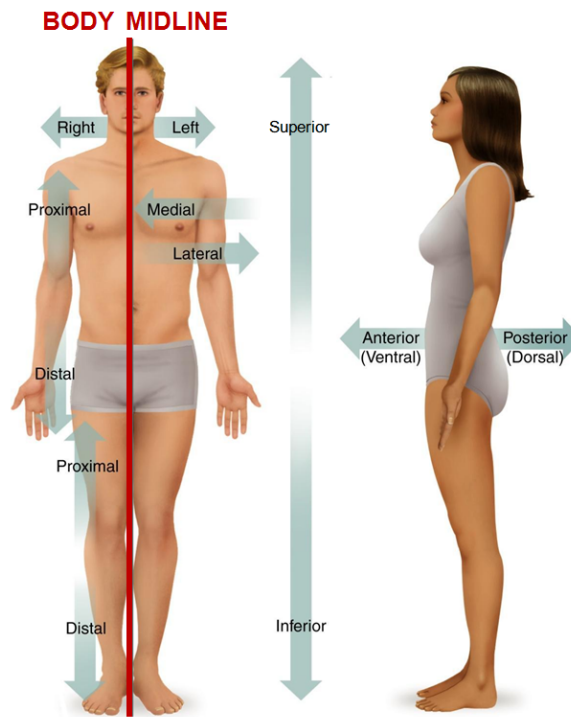


Figure 1.4 – the concept of body midline (source: unknown)

joint respectively in a dynamic and a static way, the overall joint mobility is restricted to four main Degrees of Freedom (DoF), as shown in Fig. 1.5 [11]:

Flexion-Extension (FE) It is the main movement, the rotation of the tibia with respect to the femur about the knee MedioLateral (ML) axis. Knee FE is described by the relative angle between the tibial and femoral axes. On average, the Range of motion (RoM) of knee FE varies from 0 degrees (complete extension, when femur and tibia are aligned) to 135 degrees (complete flexion). Such values may vary among individuals, mainly due to ligament stiffness.

Internal-External Rotation (IER) It is the rotation of the tibia with respect to the femur about the tibial internal axis. This movement is free throughout the whole FE range, except for the cases of complete flexion and complete extension: in such limit positions, in fact, the morphology of the femur and the tibia leads to an automatic rotation of the bones that blocks the articulation in the horizontal plane. Also for IER large individual variations exist: on average, normal internal rotation reaches about 20 degrees, while external rotation gets to 30 degrees.

Anterior-Posterior Displacement (APD) The tibia and the femur can glide with respect to each other along the knee AnteroPosterior (AP) axis. This slight trans-

lation (2 to 3 mm on average) is limited by the anterior and posterior cruciate ligaments, which prevent knee dislocation.

Varus-Valgus Rotation (VVR) It is a movement that results in the displacement of the leg segments on the frontal plane. By rotating about the knee AP axis, the KJ moves towards (Varus) or away from (Valgus) the body midline. Such movements are allowed by the KJ rotational flexibility, which mainly depends on the laxity and passive stiffness properties of knee collateral ligaments.

“The normal knee is aligned with a femorotibial angle of 6 to 7 degrees valgus, has a full range of motion and may be slightly more lax in flexion” [4, p. 41].

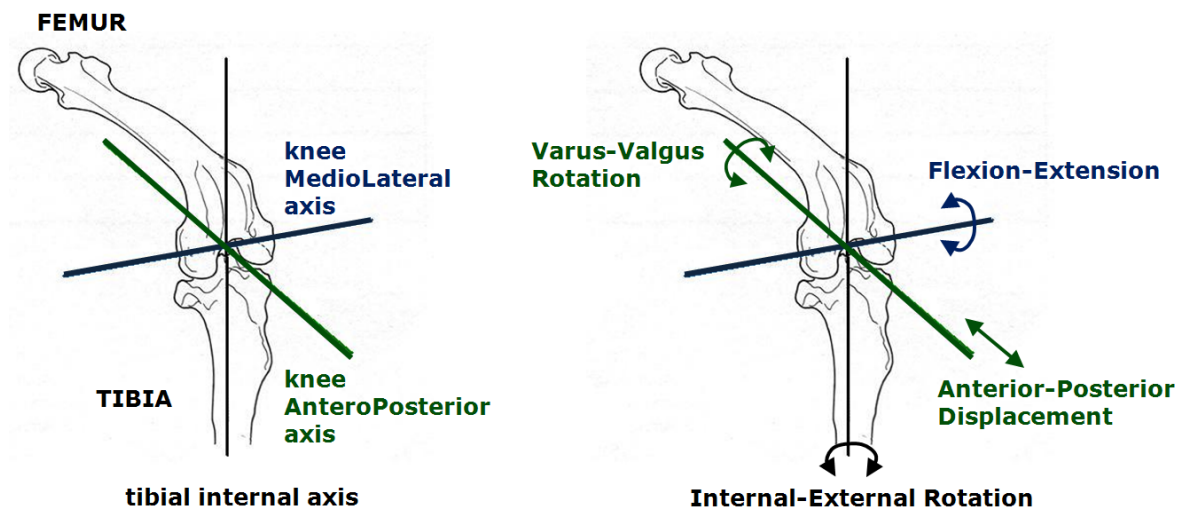


Figure 1.5 – the four degrees of freedom of the human Knee Joint (source: unknown)

1.2 Total Knee Arthroplasty

Degenerative diseases such as osteoarthritis, rheumatoid arthritis and psoriatic arthritis may lead to a substantial loss of the KJ function [12]. Bone and cartilage losses may take place on the KJ weight-bearing surfaces, which therefore undergo severe deformations. Such adaptive changes might give rise to instabilities and lead to suboptimal working conditions of the articulation. Also accidents and bone fractures can be at the origin of damages, deteriorations and excessive KJ wear conditions, thus resulting in reduced joint mobility conditions. In all cases, an inflammation process naturally takes place in the knee capsule [13], as depicted in Fig. 1.6. The patient experiences debilitating pain and disabilities, in order to relieve which the only solution is represented by TKA surgery. The orthopaedic surgeon makes use of specific prosthetic components to

replace the patient's diseased or damaged KJ surfaces; by correcting the bony structures deformities, reliable pain relief is provided and the normal KJ function is effectively restored. Even if TKA surgery is by far one of the most successful and commonly performed surgical procedures [14], it is considered only in the case of advanced and long-standing disease conditions. The substantial postoperative pain and the stressful rehabilitation period that inevitably follow the surgery suggest, if possible, to resort to less drastic solutions for the treatment of knee pain.

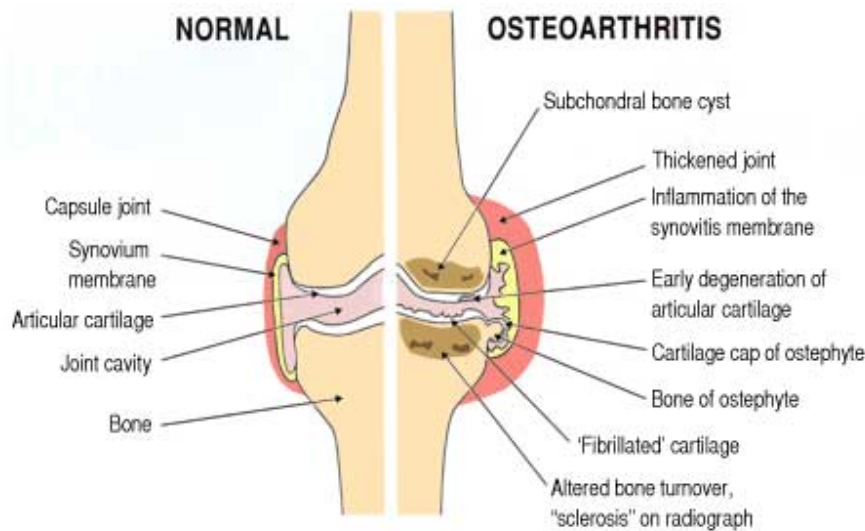


Figure 1.6 – comparison between normal and osteoarthritis conditions in human knee
(source: unknown)

1.2.1 Historical Hints

It was in the late 1860s that the possibility to resurface or replace the KJ was considered for the first time [15]. The concept of knee arthroplasty was then developed in the first half of the twentieth century, when early surgeries performed with simple hand implements started giving encouraging results [16, 17]. Early replacements, called membrane arthroplasties, relied entirely upon ligament stability [18]. The significant improvement of knee implants design that took place in the 1950s had to face with the problem of fixation. In order to effectively keep the prosthetic device in the planned position, bulky metal surfaces were directly fixed onto the bone surfaces. Hinge knee prostheses (Fig. 1.7) were employed to partially restore KJ function and relieve discomfort [19], but generally led to serious postoperative complications such as components loosening and infections.

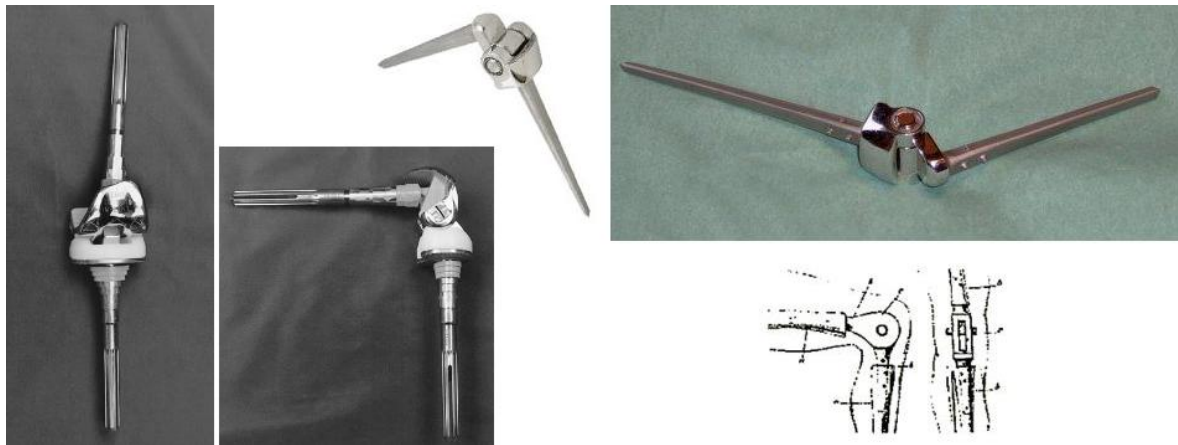


Figure 1.7 – examples of hinge knee prosthesis [4]

This was before 1969, when it was first introduced the use of PolyMethylMethacrylate and PolyEthylene (PE) inserts [20], currently employed in most TKA implants. With the introduction of cement to improve components fixation, the design of prosthetic devices rapidly developed during the 1980s [21]. Nowadays, a knee prosthesis for TKA is generally composed of a femoral component, fixed to the distal femur, and a tibial component, installed on the proximal tibia [4]. The former has a complex shape that reproduces the geometry of the two femoral condyles, while the latter is more simply a platform that gets firmly inserted into the tibial bone. If needed, a small patellar component can be employed to properly resurface the patella and improve FE mechanism performances. The prosthesis design is optimised so as to allow normal KJ dynamics: the femoral component will have to cyclically glide with respect to the load-bearing surface of the tibial platform. In order to improve the prosthetic knee RoM, as well as the implant lifespan, the contact between the two aforementioned components is not direct; a plastic insert, usually made of PE, fits the free space inside the articulation left by the removed soft tissues, so as to smooth the relative movements between the prosthetic parts and absorb most of the shocks (Fig. 1.8). The choice of PE is made for biocompatibility reasons, as well as for the Cobalt-Chrome or Titanium alloys employed for the prosthetic components. In addition to this, thanks to the intraoperative assistance provided by cutting guides and the use of patient-specific prosthetic components, TKA surgery fully restores the KJ function, thus ensuring the normal RoM and stability of the articulation.

1.2.2 Primary TKA

Primary TKA surgery is preceded by a set of preoperative evaluations and physical examinations on the knee that will be operated. This stage must be performed very

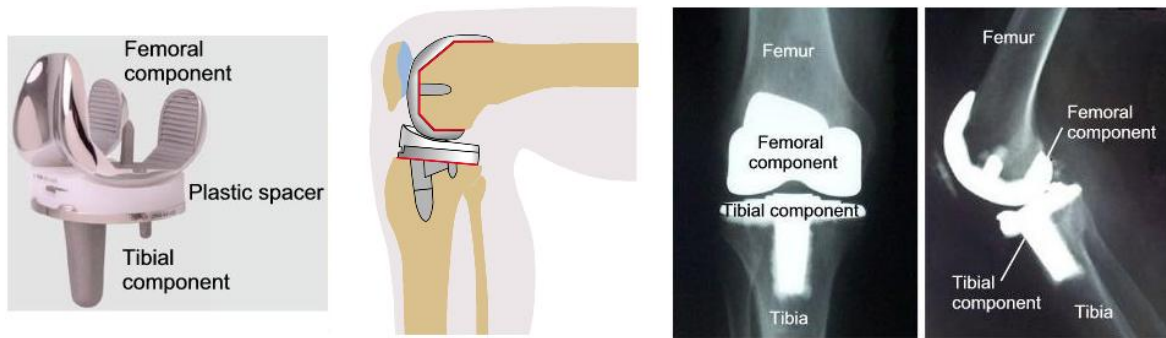


Figure 1.8 – current model of total knee prosthesis before and after primary TKA surgery www.yoursurgery.com

carefully by the surgeon, in order to assess the patient's knee RoM and the stability and strength of ligaments and muscles. Ideally, the prosthesis will completely reproduce the mechanical function of the bony parts and soft tissues that it replaces (Fig. 1.9). Moreover, the surgery must be planned so as to result in the least stressful recovering period for the patient, whose neuromuscular system will have to accept the presence of an artificial implant (that will be initially treated like an external perturbation [22]). In these terms, the preoperative evaluation stage is the first key step for a successful surgery. In primary TKA, *“the clinical results are influenced by the surgical technique. Adherence to the basic principles of the surgical technique ensures a successful outcome. The goal of primary TKA is to reestablish the normal mechanical axis with a stable prosthesis that is well fixed. This is achieved by both the bone resection and the soft tissue balance”* [4, p. 1].



Figure 1.9 – TKA surgery restores full KJ function www.jcl.com

Once in the operating room, anaesthesia is administered to the patient, whose vital signs (blood pressure, oxygenation level, heart rate and body temperature) will be continuously checked throughout the whole surgery (which lasts about two hours). For

sterility reasons, the skin over the operated knee is repeatedly cleansed with antiseptic solutions. After this, the surgeon makes an incision (20 to 25 cm long) down the center of the knee to access the articulation. Successive cuts are performed to remove the damaged soft tissues. This is usually done with the knee bent to 90 degrees flexion, in order to allow better access to the joint. Before any bone cut, the surgeon addresses each bony structure as an independent entity. The orientation of each prosthetic component must be properly defined in order to result in the prosthesis alignment to the LLMA and this determines the entity of bone resections. As a basic rule, the quantity of bone that is resected must be the same dimension as that of the prosthetic component that will replace it. According to this principle, the cuts are planned by means of landmark points that are usually readily palpable [23]. Such references, used to fix intra- and extra-medullary rods, have their own variability. *“There are a total of 7 bone cuts in a typical TKA: distal femur, anterior femur, posterior femur, anterior chamfer, posterior chamfer, tibia, and patella. Each of these cuts has its own special science, and each cut can affect the other cuts and potentially the outcome of the TKA”* [24]. Fig. 1.10 shows a simplified representation of the aforementioned bone cuts.

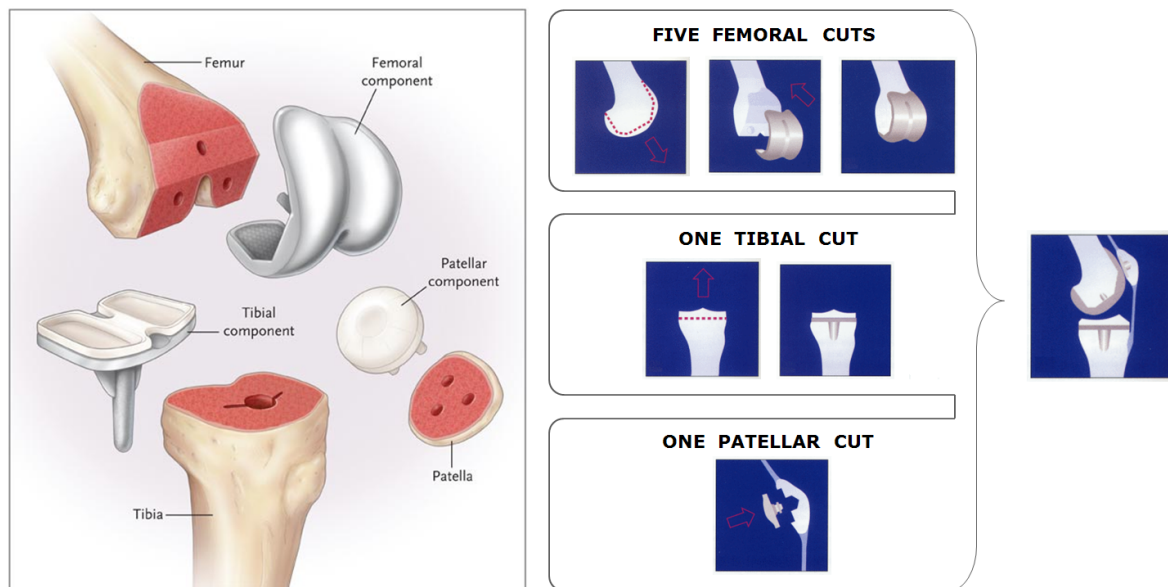


Figure 1.10 – bone resection in TKA surgery includes seven different bone cuts
www.orthopaedics.co.uk

The femoral preparation, which includes five different cuts, is the most delicate resection step [4]. The first cut is made on the distal femur, generally by means of an intramedullary instrument. By adding specific cutting blocks to the same instrument, the anterior and posterior femoral cuts are then performed without changing the reference system. The two smaller anterior and posterior chamfer cuts are performed last

and leave a precisely shaped and sized support for the femoral component, which will fit better the resected bone surface.

The next cut is tibial resection. An extramedullary guide is usually fixed to the bone in order for the cut to be performed perpendicular to the longitudinal tibial shaft axis. The tibial component baseplate should ensure maximum coverage of the sized bone, possibly without overhanging, in order to avoid postoperative complications [25]. To this aim, the use of an asymmetric tibial tray is commonly recognized as an optimal solution [4]. The same negative effects origin from a tibial over-resection that might be performed in the attempt to compensate for bony defects: as already said, the least amount of bone should be sacrificed for the installation of prosthetic components [4].

The last bone cut is the patella resection. Such operation is optional, but it is considered appropriate for most TKA surgeries since it generally improves the prosthetic joint RoM after surgery [26]. During a knee flexion movement manually performed by the surgeon, the patellofemoral ligaments are released while the patella is everted and dislocated laterally. A measured resection of the patella is then performed to properly strengthen and resurface the small bone. It has been shown [27] that patella resurfacing generally results in improved pain relief and lower implant failure risk.

Once the bone resection phase is completed, the knee balancing procedure starts. The surgeon considers now the bony structures as an integrated unit and performs the release of the remaining soft tissues (usually the two collateral ligaments). This is a critical step in that it directly determines the knee mechanical axis and, thus, the postoperative joint kinematics conditions. The surgeon evaluates the distance between the resected femur and tibia throughout FE movements, by defining:

Flexion gap - with the knee in full flexion, it is the space between the tibial cut and the posterior femur cut;

Extension gap - with the knee in full extension, it is the space between the tibial cut and the distal femur cut.

A common technique consists in carrying out the soft tissues release in stages, by continuously checking flexion and extension gaps: *“release is performed in a step-by-step controlled fashion and reassessed with laminar spreaders after each step. The endpoint of release is when the mechanical axis passes through the center of the knee and the flexion and extension gaps are equal and symmetrical”* [4, p. 46]. In order to ensure ligament balance and joint stability, the flexion and extension gaps should be both rectangular and the same size (Fig. 1.11). For instance, a prosthetic knee with a trapezoidal flexion space would have one collateral ligament too tight and the other one too lax. It

is recognized that knee stability depends on equally balanced gaps, so it is imperative to repeatedly assess this condition: any inaccuracy may give rise to component misalignments and suboptimal load distribution, which in turn might cause the implant failure. Since soft tissue balance should be assessed without modifying the bone cuts, spacer blocks are commonly employed intraoperatively to compensate for inaccuracies and reestablish proper flexion and extension gaps [28].

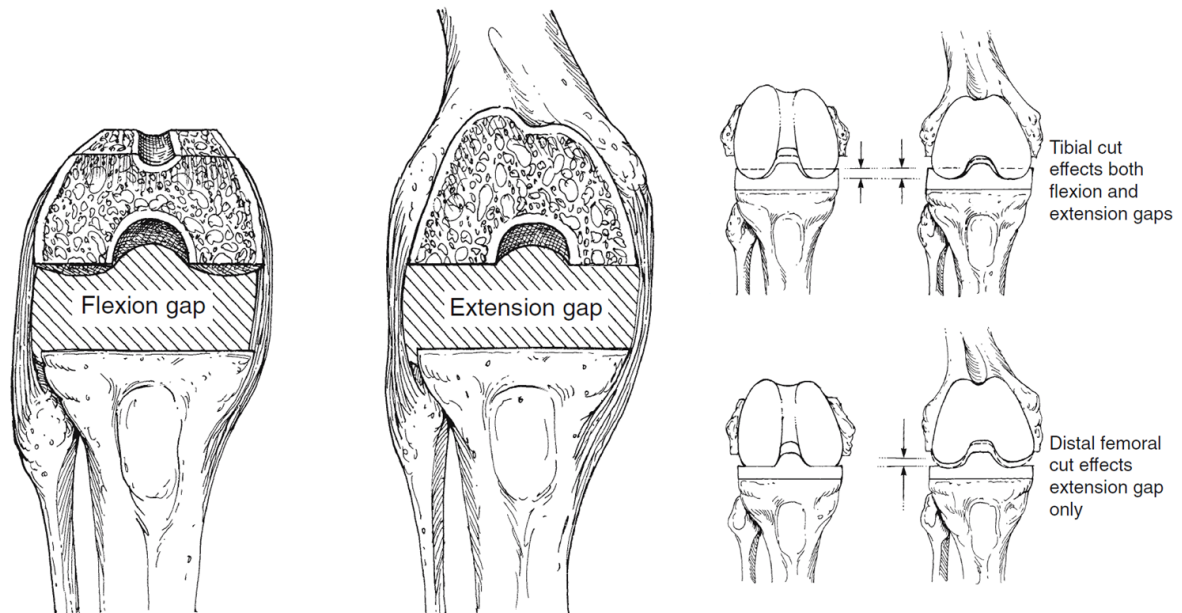


Figure 1.11 – optimal flexion and extension gaps are rectangular and same size [4]

Upon achievement of the bone cuts and the soft tissues release procedures, the surgeon proceeds with the installation of the prosthetic components. The use of cement to improve fixation is optional and mainly depends on the requirements of the surgeon's surgical technique, with individual adjustments according to the operating room conditions (such as temperature and humidity, which affect the cement solidification process [29, 30]). Intraoperatively, cemented and cementless fixations imply very similar requirements in terms of alignment, ligament balancing and bone resection accuracy. Postoperatively, both techniques show equally effective long-term results and success rate [31, 32]. It exists also a biologic cement, that is the slurry of cancellous bone resulting from the resection procedure: usually spread onto each resected bone surface, it facilitates and improves the quality of prosthesis osseointegration [4].

The last part of the surgical procedure consists in positioning the PE insert between the tibial and femoral components. In order to verify the fit of the installed components and test the RoM of the prosthetic knee, the surgeon manually performs repeated FE movements. If no complications occur, the operated knee is then fully extended and all the tissues that have been cut for the surgery are repaired. Stitches and surgical staples

are employed to close the main incision, on which a sterile bandage is finally applied. The rehabilitation period normally starts in the aftermath of the surgery, after a few days of hospitalisation.

1.2.3 Revision TKA

The normal lifespan of a total knee prosthesis is 15 to 20 years [33]. The patient's bodyweight, activity level and health conditions are all important parameters to be attentively monitored in the postoperative period. As already said, suboptimal surgical procedures and intraoperative inaccuracies, as well as the recurrence of the knee diseases already treated by primary TKA, may lead to the implant dysfunction or early failure already a few years after surgery. Component loosening, misalignment and accelerated wear phenomena can develop very rapidly and strongly limit the joint function, leading to the necessity to undergo a second arthroplasty, called revision TKA. When partial component replacements or specific adjustments are not sufficient to restore the functionality of the prosthesis, the suboptimal implant must be replaced by a new one [34] (Fig. 1.12). *“Significant bone loss can occur with removal of previously well fixed components, making revision arthroplasty indicated only when the soft tissue coverage, the previous implant and stem, or the fracture pattern preclude internal fixation ”* [4, p. 177].



Figure 1.12 – example of revision TKA procedure www.gocomplexjoint.com

As for primary TKA, also revision TKA procedure is rigorously defined so as to ensure the effectiveness of the knee reconstruction process [35]. Again, a series of pre-operative evaluations is necessary to assess the anatomical deficits and functional limitations of the failed knee. According also to the patient's expectations, the surgeon selects a proper surgical treatment that, once more, will have to cope with the problems of stability, mobility, alignment and fixation. The choice of the prosthesis is determined by the severity of bone defects and losses: deficient or even missing bone represent a first major challenge of revision TKA, since the landmark points used as references

during primary TKA may not exist in the failed knee. The impossibility to rely on bony structures might require the use of dedicated instruments, which in turn imply extra surgical skill, experience and preparation (e.g.: practice on laboratory sawbone models). A further and even more challenging issue of revision TKA is represented by the soft tissues release procedure: *“more problematic are the soft tissues. Working with strong concepts and trial components, the surgeon will be able to understand the vagaries of lost, plastically deformed, overly tight and unreleased ligaments”* [4, p. 104].

Revision TKA procedure is basically the same as that of primary TKA, with knee stabilization in both flexion and extension following bone resections and soft tissues release. Intraoperatively, regardless of the cause of failure and of the implant which is planned for the revision, the surgeon must first reestablish the tibial platform, which is considered as *“a foundation to build on”* [4, p. 106]. Being the load-bearing surface of the prosthetic articulation, the tibial component is commonly the part of a failed knee which most suffers from loosening phenomena and needs accurate reconstruction. Particular attention must be paid by the surgeon during the removal of the failed components, cement and unrecoverable bony parts: the new bone cuts that are to be performed to install the permanent components must not sacrifice the remaining good bone, which becomes extremely important if further fixation is needed. The use of custom-designed components and modular implants is a common solution to treat most knee bone damages [36]. Longer component stems, bone grafts, rods and intramedullary nails are usually required to enhance fixation. In these terms, revision TKA strongly relies on the intramedullary areas of both femur and tibia, which usually preserve a good bone quality despite the implant failure. In the case of extensive bone losses or too severe ligament instability conditions, constrained prostheses may represent the only possibility to restore reasonably good KJ function [37] (Fig. 1.13).

From both for the surgeon's and the patient's points of view, revision TKA is clearly much more demanding than primary TKA [7]. In light of the above considerations, the degree of difficulty of the surgical procedure itself is much higher on a failed knee and requires extra skills and dedicated preparation. The cost of hospitalization can also become really important [6]: a joint operated for the second time is more exposed to the risk of infection [38], leading to a longer recovery period in the case of postoperative complications. Finally, rehabilitation after revision TKA is generally more aggressive and stressful for the patient, who might face with a reduced joint RoM and be restricted in movements for several weeks.



Figure 1.13 – comparison of two failed primary TKA implants (left) and their corresponding revisions (right) [37]

Assistive Tools and Devices for TKA

In the last fifty years, advances in technology have strongly impacted the world of medicine. The development of CAMI techniques has greatly improved the quality of the pre- and intraoperative information provided to the surgeon, thereby increasing the accuracy of medical interventions as well as their patient-specific characterization [1]. Despite there is no extensive evidence that the application of computer technology to medical procedures effectively improves, in the long-term, the postoperative outcomes [2], larger and larger investments are made nowadays for the development of tools and devices that could assist surgeons and integrate their skills and perception. The ideal surgical instrument is simple and safe to use, is biocompatible, respects the sterility standards of the operating room and provides useful and processable information. The level of invasiveness of the surgical procedure may impose further constraints concerning the tool size.

This chapter presents an overview of the instrumentation that can be employed by the surgeon during TKA surgery, from standard tools to more technologically advanced computer-assisted devices. The concept of instrumented knee prosthesis is also introduced, with a review of the most interesting implants that can be found in the literature. A novel instrumented tibial component is eventually described, as a basis for the development of the actuated knee prosthesis that this work intends to propose.

2.1 Jigs, Cutting Tools and Spreaders

Early TKA bone resections were performed by means of long oscillating blades and cutting blocks, which ensured both support and proper tool orientation for the achievement of effective bone cuts. The need for better intraoperative accuracy led to the progressive refinement of such instruments, which underwent a natural evolution by taking advan-

tage of technological progress. Cutting blocks were replaced by slots, more suitable for preventing cutting blades from oscillating during the resection. The risk of wobbles was further reduced by the introduction of rotary blades, which could also ensure a more accurate control of the cut depth and reduce the temperature of the resected bone surface [4] (Fig. 2.1).

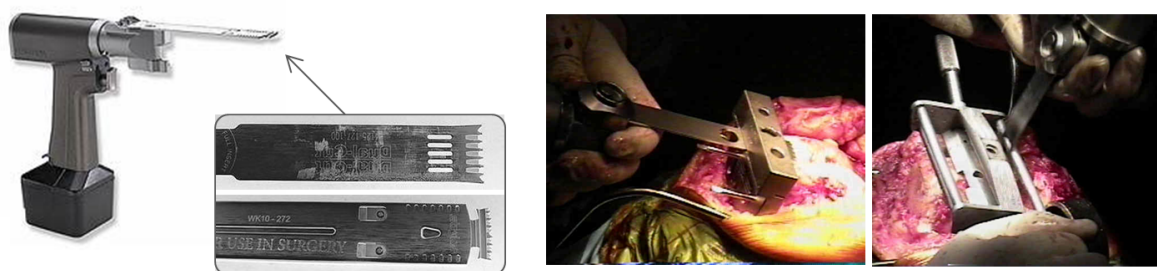


Figure 2.1 – example of a cutting tool for TKA, with details on two different types of oscillating blades, employed with cutting slots during primary TKA [39], www.wheelsonline.com

The quality of support and guiding of the cutting tools was further improved with the development of frames, which consist in base structures on which multiple cutting slots can be applied. Once reliable bone landmark points have been defined as references for effective bone cuts, specific frames, better known as jigs, are rigidly fixed to the bones. Then, the surgeon can perform multiple cuts without the need for repositioning the supports and the guides for cutting tools. This aspect is particularly interesting for the femoral resection, which can be performed in one single surgical step without introducing undesired inaccuracies. Nowadays, bone cuts in standard knee arthroplasty are performed with intra- and extramedullary jigs respectively for the femur and the tibia [4]. The development of custom-made and custom-fit jigs [40] (Fig. 2.2) represents the next promising step towards a further improvement of TKA surgery outcomes [41, 42, 43].

As previously mentioned in this work, besides the bone cuts stage, also the soft tissues release phase has a key importance for a successful TKA. Intraoperatively, the KJ has to be stabilised by equalizing the flexion and extension gaps and progressively tuning the collateral ligaments tension values. During such procedure the surgeon can make use of a distraction device, which is a forceps-like instrument more commonly addressed as spreader, to space the tibia from the femur (Fig. 2.3). The main advantages brought by the use of a spreader are:

- an increased dexterity of the surgeon, who can operate in the open articulation clear space with both free hands;

- a better view of the articular space, with the possibility to perform more precise evaluations of the joint conditions;
- a more accurate control of alignment conditions, bone distances and ligament tensions, which can be progressively adjusted with very high precision.

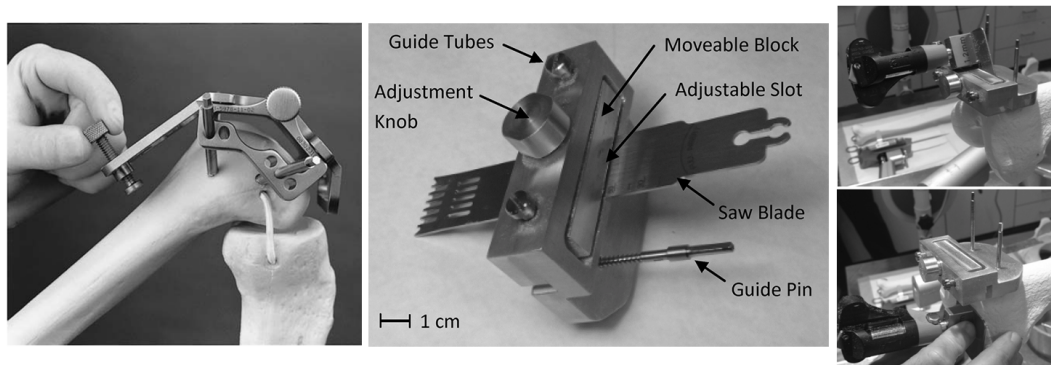


Figure 2.2 – examples of standard frame (left) and customizable frame (center and right) for femur resection [4, 40]

In these terms, knee spreaders can be considered as assistive instruments to perform and confirm the balancing procedure during not only TKA, but also other kind of surgeries (partial replacements, osteotomies, etc.). The complexity of the intervention and its level of invasiveness define the choice of an appropriate spreader, in terms of size and distraction range. A great development of distracting and tensing devices has taken place over the last fifteen years [8], with original mechanical structures that have been proposed towards more “robotized” conceptions and designs [44, 45, 46]. As it will be discussed in chapter 2.2, the interaction between spreaders and navigation systems can effectively assist surgeons in monitoring the evolution of important intraoperative parameters and measures [47, 48] (in the case of TKA: distraction forces, flexion and extension gaps, collateral ligament tension values, etc.).



Figure 2.3 – example of use of knee spreaders for bone resection during primary TKA

2.2 Navigation Systems

Nowadays, the presence of a Navigation System (NS) characterises most CAMIs [1]. In general terms, a NS can be described as a set of different interacting instruments that combine information from multiple sources in order to provide the surgeon with additional intraoperative knowledge. Surgical tools are equipped with reflecting marks in order to be continuously tracked intraoperatively by a dedicated vision system (two or more cameras). Collected data are processed by a central unit, with which the surgeon can interact in real time by means of a graphical user interface.

In the case of TKA, as mentioned in chapter 2.1, the combined use of a NS and a spreader can bring several advantages to the surgeon: intraoperatively, the NS can map anatomical reference points, accurately measure flexion and extension gaps, plan optimal bone cuts and implant positioning and monitor the soft tissues release procedure [49, 50]. In addition to this, by processing the preoperative physiological data of the patient's knee, the diseased joint areas can be represented in 3D and explored in the operating room [44]. For instance, the position and orientation of prosthetic components can be virtually simulated before any bone resection (Fig. 2.4); this can be extremely helpful to discuss the proposed surgical strategy and make fine-tuning adjustments. The bony structures 3D reconstruction is usually performed intraoperatively by means of palpation probes [51]; the accuracy of such stage directly determines the reliability and effectiveness of the data processed by the NS, which evidently is not intended to be employed in the postoperative period. Several studies have already presented the successful outcomes of TKA assisted by a NS [8, 52, 53, 54], while others have enlightened some limitations [55, 56, 57]. Nowadays, thanks to the advances in medical robotics, *“instruments for total knee arthroplasty continue to be refined. There is no question that the more accurate the surgery performed, the better the result and longevity of the prosthesis”* [4, p. 23].

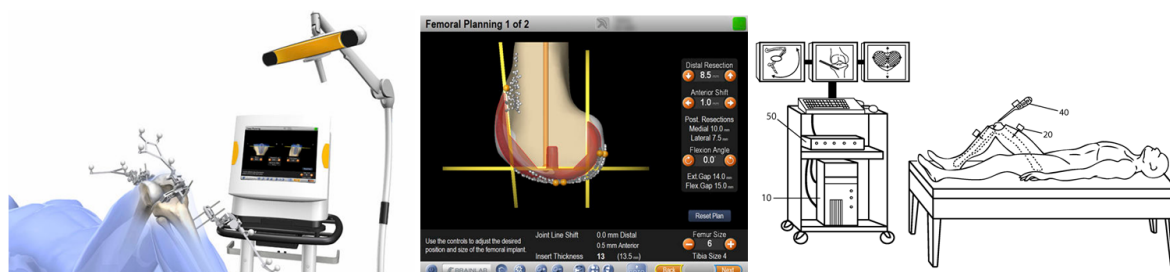


Figure 2.4 – example of combined use of a navigation system and a knee spacer equipped with reflecting marks during TKA www.brainlab.com, [58]

2.3 Instrumented Knee Implants

The application of engineering techniques to improve the design of orthopaedic instrumentation was proposed for the first time twenty-five years ago [59]. The development of instrumented knee prostheses, equipped with embedded sensors and microelectronics, has led to the conception of original prosthetic components able to directly access in vivo measurements of KJ kinematics during and after TKA surgery. The main advantage brought by such kind of implants is to provide significant information to both clinicians and prosthesis designers [60].

In 2004 Marmignon et al. [61] conceived an instrumented tibial baseplate to be employed together with a navigation system during TKA surgery. The device, presented as a robotized spacer, was meant to assist the surgeon in determining optimal prosthesis alignment and collateral ligament balance conditions. In the proposed surgical procedure, the patella was not everted and the tibial cut was performed first. Immediately after, the proposed device was fixed onto the resected tibia surface in order to apply the desired distraction forces. The two femoral condyles were in contact with two mobile femoral plates, each one connected to the baseplate by means of a scissor jack mechanism. The two femoral trays could be raised or lowered independently, always remaining parallel to the resected tibia surface (Fig. 2.5). Miniaturised force-sensing resistances and height sensors embedded in the mobile femoral platforms provided the surgeon with accurate measurements of tibiofemoral forces and flexion and extension gaps. Thanks to the interaction with a navigation system, the collected data were made available in real time to the surgeon, who could intraoperatively evaluate the planned prosthesis implantation.

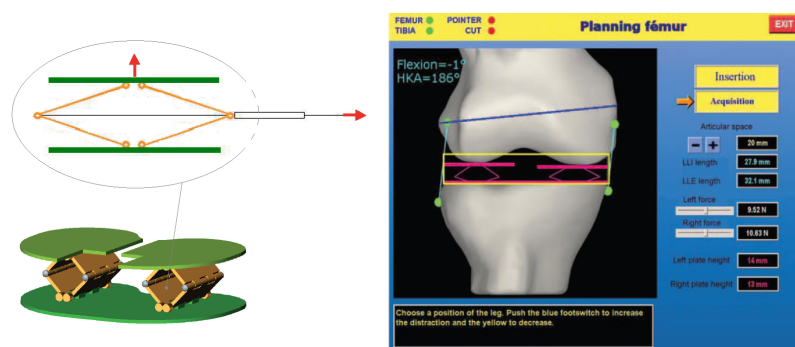


Figure 2.5 – a simplified representation of the robotized spacer employed with a navigation system [61]

In its starting position, the device was 6.1 mm thick and could provide a remarkable distraction range of 15 mm. Repeated tests on sawbones were followed by experiments on two cadaver knees. With respect to standard techniques, a higher level of accuracy

could be achieved; however, a great drawback was the maximum total distraction force that could be produced, only 100 N. Upon discussing with an orthopaedic surgeon, the device was considered not powerful enough and alternative solutions were investigated.

In a successive study [62], the scissor jack mechanisms were replaced by two rubber bladders inflated with a fluid (air or physiological serum). The volume changes were manually controlled and allowed to raise or lower the two femoral plates independently (Fig. 2.6). This design solution doubled the maximum total distraction force (200 N), but reduced the distraction range to 11 mm. Moreover, the stiffness of each bladder was shown not to be constant, but depending on its volume: as a consequence, the contact between each mobile plate and the condyles turned out to be variable and the orientation of the femoral trays could not be controlled.

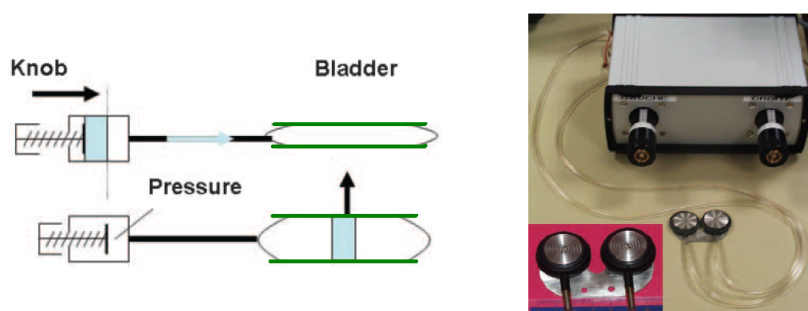


Figure 2.6 – the second version of the robotized spacer [62]

Another instrumented tibial platform was proposed in 2005 by Crottet et al. [63] with the purpose of assisting the surgeon during ligament balancing procedure in TKA. Also in this case, the small force-sensing device (6 mm thick) was conceived to be employed without the need for patellar eversion and right after tibial resection. The upper surface of the platform was divided in two sensitive plates, each one equipped with three deformable bridges instrumented with strain gauges (thick-film piezoresistive sensors). Any tibiofemoral load manually applied by the surgeon during the knee stabilisation procedure developed reaction forces which caused the deformation of the instrumented bridges. The direct measurement of such reaction forces, combined to the knowledge of sensors position, allowed to estimate the location of the applied net tibiofemoral loads acting on the medial and lateral compartments of the tibial baseplate (Fig. 2.7). By performing such operation intraoperatively, the surgeon had the possibility to evaluate joint stability conditions throughout the whole knee kinematics. The proposed device was tested on sawbones and also on a cadaver knee, giving promising results in terms of accuracy and effectiveness. Its flexibility of usage was expected to offer useful quantitative information and assistance to the surgeon, so as to improve the bone cuts planning and the components positioning procedure. However, a major limitation stood

in the way ligaments were modelled for the computations: they were considered as adjustable linear springs, a clearly too strong approximation considering the complexity of multifiber structures [64].

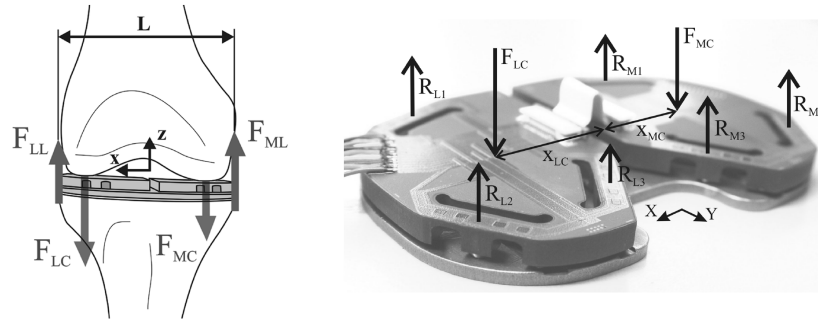


Figure 2.7 – the small force-sensing device and the forces it can measure [63]

A milestone in the literature of instrumented knee implants is the e-Knee, an electronic total knee prosthesis developed to provide the surgeon with postoperative in vivo measurements of KJ forces [65]. The e-Knee was the first assistance tool intended to serve not only during TKA, but also in the postoperative period, being actually one of the permanent prosthetic components. A fully instrumented tibial component was equipped with loadcells and a miniaturised telemetry system; the presence of such embedded components led to a tibial tray 7.5 mm thicker than standard platforms. Wireless power supply and data communication were achieved by means of electromagnetic induction (Fig. 2.8). The first implantation on a patient took place in 2004, after 13 years of research and development [66]. Both intraoperatively and throughout the postoperative period, tibiofemoral force data were collected so as to monitor full KJ kinematics during daily life activities. Load measurements were assessed to be accurate and repeatable; upon further data processing, the e-Knee made it possible to postoperatively monitor the evolution of each single patient's KJ kinematics conditions. As claimed by the authors, such feature was considered “*a technological breakthrough with promise of aiding in the modification of implant design, intraoperative decisions, postoperative rehabilitation programs and assistive devices*” [65, p. 65].

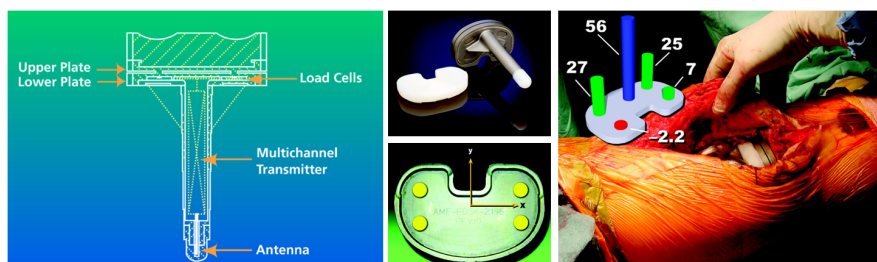


Figure 2.8 – the electronic knee prosthesis e-Knee [65]

In the wake of the e-Knee, the possibility to exploit permanent prosthetic components for collecting postoperative KJ kinematics data took hold in the orthopaedic community. In 2007, Graichen et al. [67] proposed a miniaturised telemetry system especially developed to carry out *in vivo* load measurements in orthopaedic implants. A conventional tibial component for TKA was instrumented with six semiconductor strain gauges, a microtransmitter and an antenna; with respect to standard components, the tibial tray was 5 mm thicker and the tibial stem 3 mm longer (Fig. 2.9). Powered by electromagnetic induction, the device was able to measure knee contact forces and moments and wirelessly transmit the processed data to an external computer (50 cm transmission range). Despite its very low efficiency, the low-power consumption telemetry system (only 5 mW) managed to achieve data communication through the implant metal shielding. Repeated tests on instrumented prototypes of the proposed tibial component allowed to check the measurement accuracy, a key aspect for assessing the reliability of long-term measurements in patients.

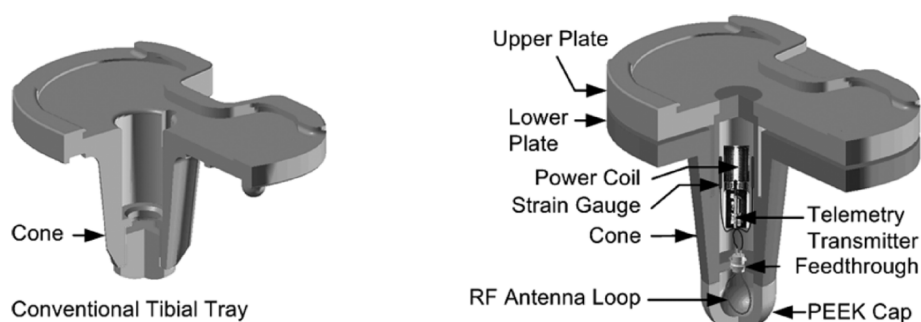


Figure 2.9 – the proposed instrumented tibial component (right) compared to a conventional one (left) [67]

A similar instrumented tibial component was proposed in 2008 by Mündermann et al. [68], who carried out a comprehensive study about the evolution of knee cartilage conditions for patients affected by osteoarthritis or following TKA surgery. The researchers aimed to investigate the relationships among different factors of KJ motion (FE angle, peak load and ML load distribution) during seven different daily life activities. In line with previous studies, four load cells were embedded in the tibial tray so as to serve as force sensors, a miniaturised telemetry system was positioned in the hollow tibial stem and power supply was achieved by means of magnetic coils. The device was implanted on the right knee of a healthy patient who needed to undergo primary TKA and the testing phase started eighteen months after surgery. Data processing consisted in combining the *in vivo* measurements provided by the prosthesis with those of a motion capture system employed throughout the physical tests. *“The results demonstrated that the forces and motion sustained by the knee are highly activity-dependent and that*

the unique loading characteristics for specific activities should be considered for the design of functional and robust total knee replacements, as well as for rehabilitation programs” [68, p. 1167]. For instance, it was concluded that the efforts produced by squat movements might be too demanding with respect to the high flexion values at which they occur (Fig. 2.10), thus they should preferably be avoided during reeducation programs in order not to damage the recovering knee soft tissues.

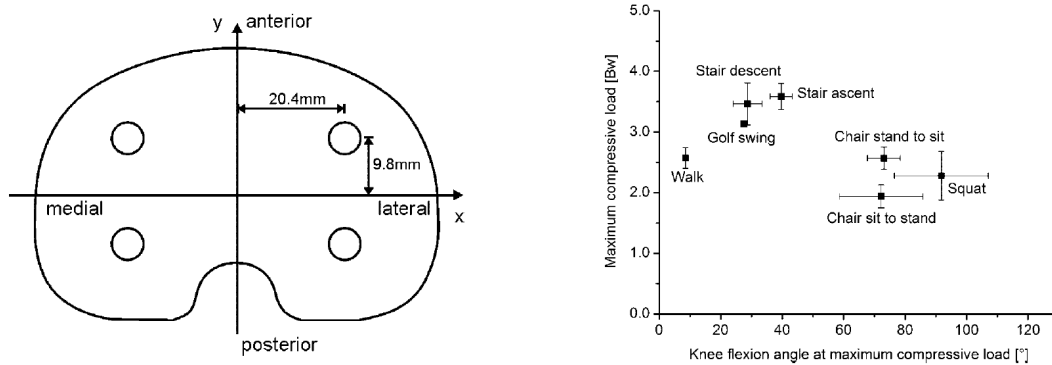


Figure 2.10 – the position of the four load cells embedded in the tibial tray (left) and the analysis of compression loads for the seven considered activities (right) [68]

It is clear that the presence of sensors and microelectronics in the tibial component of a knee prosthesis has been definitively accepted as a way forward to provide the surgeon with further useful knowledge. Besides improving the quality of the intraoperative surgical procedure, the assistance provided by such instrumented implants has turned out to be very helpful to discuss design and material choices, as well as to plan patient-specific rehabilitation programs. In the last five years, other instrumented prostheses similar to those discussed above have been proposed. A further example is the wireless force measurement system developed by Chen et al. [69] in 2010, where tibiofemoral forces measurements were achieved by means of six pressure sensors and a telemetry system embedded in the tray of a TKA tibial component. The great advances in the miniaturisation of low-power consumption devices has allowed (and will allow in the next future) to design tinier and tinier force-sensing systems with greater and greater potential in terms of measuring range and accuracy. In this context, it should not be too implausible to think that not only the tibial component can be exploited to host embedded sensors and microelectronics.

A study by Arami et al. [70] in 2011 presented a smart knee prosthesis with original choices concerning its embedded instrumentation. A permanent magnet was positioned inside the femoral component; a small coil, strain gauges, and anisotropic magneto resistance sensors were located in the PE insert; finally, miniaturised circuitry was hosted in the tibial tray. The working principle was quite simple: during knee motion, the femur

movements with respect to the PE insert produced changes in direction and intensity of the permanent magnet magnetic flux. Such changes, detected by the magneto resistance sensors in the PE, were recorded and processed by the dedicated microelectronics system so as to determine the relative movements between the prosthetic components. In addition to this, also the entity and distribution of tibiofemoral forces were measured in both medial and lateral compartments, as an indicator of soft tissues balance conditions. Power supply and data communication were achieved by means of inductive coupling and, in terms of components size, such minimal sensory system did not require any change with respect to conventional implants (Fig. 2.11). Therefore, the smart proposed design allowed to perform *in vivo* KJ kinematics measurements, thus giving the surgeon the possibility to evaluate the prosthetic joint function after TKA. As claimed by the authors, this implant could serve “also to early detect problems due to knee imbalance and wearing. Furthermore, it can be used for improving patient's treatment during follow up. The system can also be adapted to other kind of prostheses, i.e. shoulder, hip and ankle, broadening the application for similar instrumented devices” [70, p.834]. Further research is currently carried out [71].

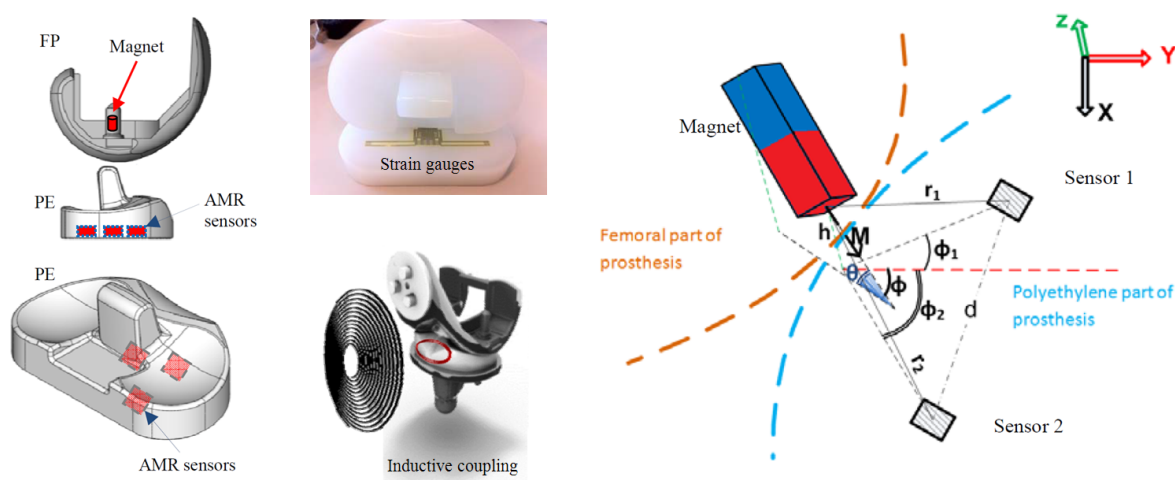


Figure 2.11 – design details and working principle of the smart knee prosthesis [70]

Current research in knee implants follows two main axes in parallel: on the one hand the development of original approaches for prosthetic components instrumentation, on the other the refinement of already existing devices integrated to NSs. In this second case, a last work that is worth mentioning is the genALIGN, a navigated implantation system officially completed by Zimmermann et al. [72] in 2012 after several years of research [73]. By adopting an alternative approach with respect to that of other studies, the researchers addressed more specifically the problem of femoral component alignment to the LLMA, described as a critical achievement for an effective TKA. The key component of the genALIGN system was a sensor-integrated tibial inlay which, once

positioned on the resected tibia and put in contact with the femoral condyles, was able to measure intraoperative tibiofemoral forces and torques. The data collected by six load measurement cells embedded in the platform (three per side) were thus processed to properly orient the femur by means of a dedicated extramedullary mechanical instrument, whose orientation was continuously monitored by a navigation system (Fig. 2.12). Such procedure allowed the surgeon to evaluate the impact of ligament tensions on KJ loads, with the possibility to perform the most effective adjustments in order to set up optimal balance conditions. Laboratory tests on a knee simulator and a study on a cadaver assessed the system feasibility and gave promising results, but a key aspect was the intention of the authors to further improve the system performances by taking advantage of technological advances. Namely, design optimisations prior to clinical trials and the use of more advanced sensors on a microcontroller-based version of the femoral instrument were planned. This confirms the considerations made above about the actual commitment to develop more and more accurate, simple and low-cost assistive tools for TKA, a goal that is made possible by the continuous evolution of technology applied to CAMI techniques.

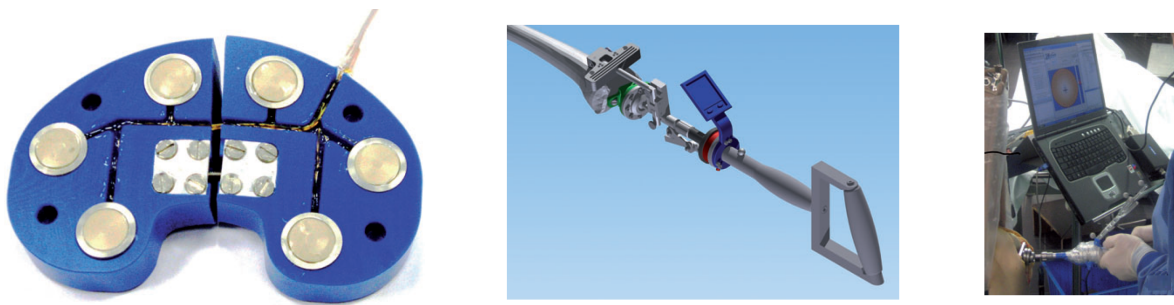


Figure 2.12 – the genALIGN system with the instrumented tibial inlay (left), the femoral instrument (center) and an example of intraoperative use (right)[72]

The most relevant instrumented knee implants that have been developed to date have been described in this chapter. As previously mentioned, research in this field is subjected to such a continuous evolution that it is not easy to keep a constantly up-to-date and exhaustive State of the Art. Nevertheless, it may be observed that most of the models presented here share some recurring elements: specific choices in the proposed surgical procedure, the selection of certain types of sensors preferred to others, the adoption of inductive coupling for power supply and the great importance given to postoperative in vivo measurements. Such common strategies should be reasonably taken into account as a basis for any future study.

2.4 A Novel Instrumented Tibial Component

2.4.1 Collateral Ligaments Balance Conditions: an Unsolved Problem

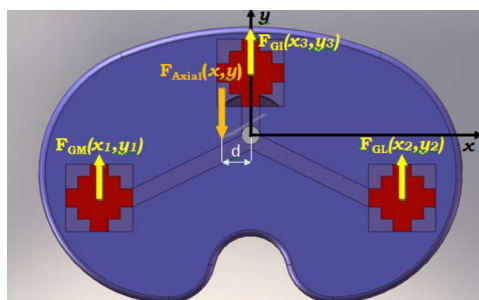
The importance of intraoperative accuracy is a leitmotif for any surgical act, especially in the case of TKA for which *“the more accurate the surgery performed, the better the result and longevity of the prosthesis”* [4, p. 23]. At an early stage, the surgical procedure itself should be planned so as to minimize the risk of introducing inaccuracies. With reference to the assistive tools presented in the previous chapters, the use of instrumented components designed for permanent implantation should be preferred to that of tibial inlays employed only temporarily during the surgery. In any case, the intraoperative information provided by assistive tools is the result of data processing and, as such, its reliability and accuracy largely depend on instruments calibration. Put in other terms, even if the effectiveness of navigated TKA has been largely proved, optimality in instrumentation design is far from being reached and still needs to be extensively validated by means of long-term medical observations [2].

As it has been explained in chapter 1.2.2, during TKA the surgeon has to manually carry out a progressive soft tissues release procedure. This stage is crucial in that it directly influences the postoperative KJ function and the implant lifespan. Proper tension conditions of the two knee collateral ligaments have to be set intraoperatively by evaluating identical flexion and extension gaps, whose geometry depends on the prosthesis alignment to the LLMA and on the performed bone resections. Nowadays, both components positioning and optimal bone cuts planning can be achieved by means of navigated TKA techniques; although, the delicate knee stabilisation process is carried out by evaluating loads that are inevitably variable and user-dependent [72]. This part of the surgery cannot be standardised for all patients and, consequently, its outcomes still highly rely on the surgeon's experience and perception, as well as on the adopted surgical technique [73]. In addition to this, there is no guarantee that the optimal collateral ligaments balance conditions set during TKA remain so after surgery: during the rehabilitation period and in its aftermath, the prosthetic KJ undergoes a natural morphofunctional evolution according to the patient's expected changes in weight and lifestyle. The quality of the restored KJ function and RoM, as well as the interactions that are spontaneously established between the bony structures and the prosthetic components, may affect the collateral ligaments tension values in such a way that unpredictable imbalance conditions might develop in the articulation [28]. The severity of such inaccuracies depends on several factors and varies among individuals.

Postoperative complications caused by suboptimal collateral ligaments balance conditions still represent an unsolved problem [8, 72, 74]. In the case of severe debilitating pain and disabilities experienced by the prosthetic patient, revision surgery is nowadays considered to be the most effective solution [4]. In chapter 1.2.3 revision TKA has already been introduced as a very demanding surgical procedure, both for the patient and for the surgeon. Unfortunately, the incidence of TKA increases annually and also the number of revision surgeries continues to rise [6, 7]: “*at the moment, around one tenth of the operations for artificial knees are prosthesis revisions*” [1, p. 13]. In light of the considerations made above, inaccuracies during and after primary TKA are hereby accepted to be unavoidable. This acknowledgement suggests therefore to consider the possibility to compensate for TKA inaccuracies rather than proposing the umpteenth device to anticipate them. In this context, the main contribution of this work is the design of an original instrumented knee implant able to restore optimal collateral ligaments balance conditions in the postoperative period without resorting to revision TKA.

2.4.2 A Self-Powered Tibial Component for Postoperative Knee Balance Evaluation

Our research team has been working since 2006 on the design of a new generation knee implant able to detect any collateral ligament imbalance condition after TKA. Drawing inspiration from the literature, the first proposed device [75] was a smart tibial baseplate to be employed during TKA soft tissues release procedure (after tibial resection and without the need for patellar eversion). A 4 mm thick tibial tray was instrumented with three strain gauges in order to measure the tibiofemoral loads in the medial, lateral and intermediate parts of the platform. Soft tissues imbalance conditions were evaluated by studying the displacement of the Center of Pressure (CoP) of the total axial force acting on the tibial surface (Fig. 2.13).



$$COP_x = \frac{F_{GM} \cdot x_1 + F_{GL} \cdot x_2 + F_{GI} \cdot x_3}{F_{GM} + F_{GL} + F_{GI}}$$

$$COP_y = \frac{F_{GM} \cdot y_1 + F_{GL} \cdot y_2 + F_{GI} \cdot y_3}{F_{GM} + F_{GL} + F_{GI}}$$

Figure 2.13 – three strain gauges are embedded in the instrumented tibial baseplate for the computation of the CoP of the total axial tibiofemoral load [75]

By means of finite element analysis, twenty-one load cases corresponding to different conditions of ligament imbalance were simulated at 0 degrees of flexion (standing position). Computations assessed the effectiveness of the proposed method and endorsed the concept of considering the CoP displacements as a function of ligament balance conditions. In a successive study [76], the strain gauges were replaced by four PiezoCeramics (PC) elements and the same CoP-based approach was adopted for the design of an original instrumented tibial component. The basic property of PC materials, that is the accumulation of electric charge in response to applied mechanical stress, was exploited for tibiofemoral forces measurement: the PC were positioned in four specific holes grooved in the tibial tray so as to produce low voltages in response to the compression forces exerted by the femoral component via the PE insert. At an early stage, the combined knowledge of the voltage values measured by means of an oscilloscope and of the four PC positions in the baseplate allowed the location of the CoP of the net tibiofemoral force acting on the tibial tray. The idea was to evaluate the CoP average positions during a gait cycle, so as to detect in which part of the tray knee loads were most concentrated; the surgeon could then use this information to detect any imbalance due to collateral ligaments laxity conditions. For instance, a too lax medial collateral ligament would have led to a CoP concentration on the tibial platform lateral compartment. In order to investigate the validity of this method, twelve different imbalance conditions were reproduced during normal gait cycles by means of a knee simulator and the corresponding CoP trajectories were recorded [77] (Fig. 2.14). The same set of imbalance conditions was virtually reproduced on a three-dimensional (3D) model by means of finite element analysis; the CoP trajectories that resulted from such simulations were found to be in reasonably good agreement with the experimental ones. Upon further experimentations, the evaluation of the net tibiofemoral force CoP trajectory was definitely accepted as a reliable and effective metric to evaluate knee collateral ligaments balance conditions.

A truly revolutionary aspect of this instrumented tibial component consisted in the double role played by the PC elements: besides serving as pressure sensors, they were meant to be used also as energy harvesters. In a previous study [78, 79], the possibility to store the electric charge produced by repeated successive compression loads (i.e.: a few steps made by the patient during a follow-up visit) had already been presented as a smart solution towards the development of self-powered knee prostheses. To this purpose, a miniaturised power conditioning system to be embedded inside the tibial component was conceived so as to fully supply a dedicated telemetry system for wireless communication between the prosthesis and the clinician's computer. In order to quantify the electrical energy that could be harvested under conditions of normal walking, the electromechanical model of the PC elements was defined and studied

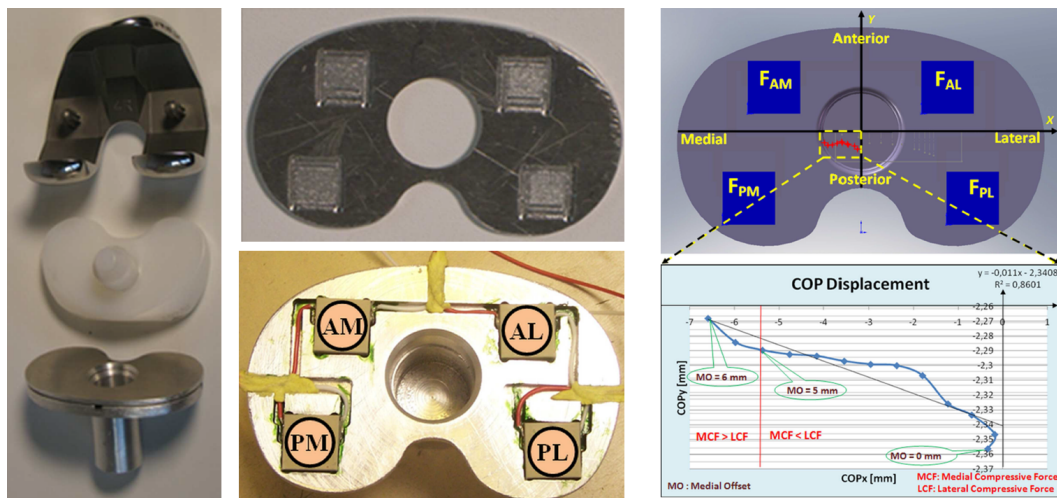


Figure 2.14 – four PC elements are embedded in the instrumented tibial component for the computation of the net tibiofemoral force CoP trajectory [77]

by means of computer simulations and experimental tests. A successive study [80] presented the initial promising results and assessed both the system feasibility and durability (due to the PC elements great lifespan properties). The possible standard use of the proposed instrumented tibial component was outlined as follows:

Intraoperatively - Navigation techniques would allow to achieve optimal prosthesis alignment and bone cuts planning. Throughout a set of passive knee movements, the PC elements embedded in the tibial tray would be employed as pressure sensors in order to evaluate proper collateral ligaments tension values. The microelectronics embedded in the prosthesis, powered by the energy harvested by the PC elements, would allow to measure the average CoP trajectories of the applied loads under conditions of optimal intraoperative balance. Such data would be transmitted wirelessly to the clinician's computer by means of a telemetry system and stored for further processing.

Postoperatively - Throughout the rehabilitation period, with the patient again able to walk autonomously, recording the average CoP trajectories during periodic follow-up visits would allow to build up a set of patient-specific data. Thus, the evolution of the patient's knee balance conditions would be monitored by the surgeon, who would be able to detect any abnormality and, if necessary, to plan appropriate treatments for preventing postoperative complications.

The use of the four PC elements employed as pressure sensors has already been assessed as an effective way to detect the prosthetic KJ balance conditions [80]; ongoing research is currently carried out in order to definitively validate also their role as energy

harvesters. A partner laboratory is currently investigating the possibility to design a low-power consumption system which integrates all the microelectronics necessary for data acquisition, processing and communication, as well as for energy storage. These components are supposed to be embedded in the hollow tibial stem.

The original choice of embedding PC elements in a knee prosthesis was motivated by their biocompatibility and great durability properties [60]. Moreover, with respect to conventional prosthetic components, the presence of the PC elements in the implant did not increase the thickness of the tibial tray (4.5 mm). Hitherto, the results of the experimental tests have been promising and encouraging. The opportunity to carry out in vivo experiments would allow to further improve the measurement system accuracy and perform important design optimisations.

2.4.3 Current Achievements and Purpose of This Work

The proposed instrumented tibial component [81] is able to monitor and assess knee collateral ligaments balance conditions not only during TKA, but also in the postoperative period. Such diagnostic capabilities are ensured by four PC elements that are embedded in the tibial baseplate and act as pressure sensors in response to compression tibiofemoral loads. With respect to other similar devices that can be found in the literature, a unique feature of this implant consists in the fact that it is intended to be completely self-powered, thanks to the energy that can be harvested by the same PC elements under normal walking conditions. By making use of the proposed device, the surgeon can detect any condition of collateral ligament laxity that might develop inside the prosthetic articulation due to the unavoidable inaccuracies of primary TKA. Specific treatment can then be planned in order to cope with such suboptimal conditions, but when too severe debilitating pain and disabilities take place the only solution might be represented by revision TKA.

In this framework, this project aims to develop the first adjustable tibial component able to restore optimal collateral ligament balance conditions in the postoperative period, without the need for a second surgery. As previously explained, according to the information provided by the PC elements, the surgeon can detect if one of the two knee collateral ligaments has become too lax; in order to properly re-tighten it, the idea is to adjust the height and inclination of the tibial tray on the corresponding side, as depicted in Fig. 2.15. This correcting action, which must be performed without impairing the prosthesis alignment to the LLMA achieved during TKA, could compensate for any ligament balance inaccuracies as long as they can be treated and before they give rise to more severe complications. From this point of view, periodic follow-up visits are

of paramount importance in that only a continuous monitoring of the patient's knee balance conditions can allow to plan an effective intervention.

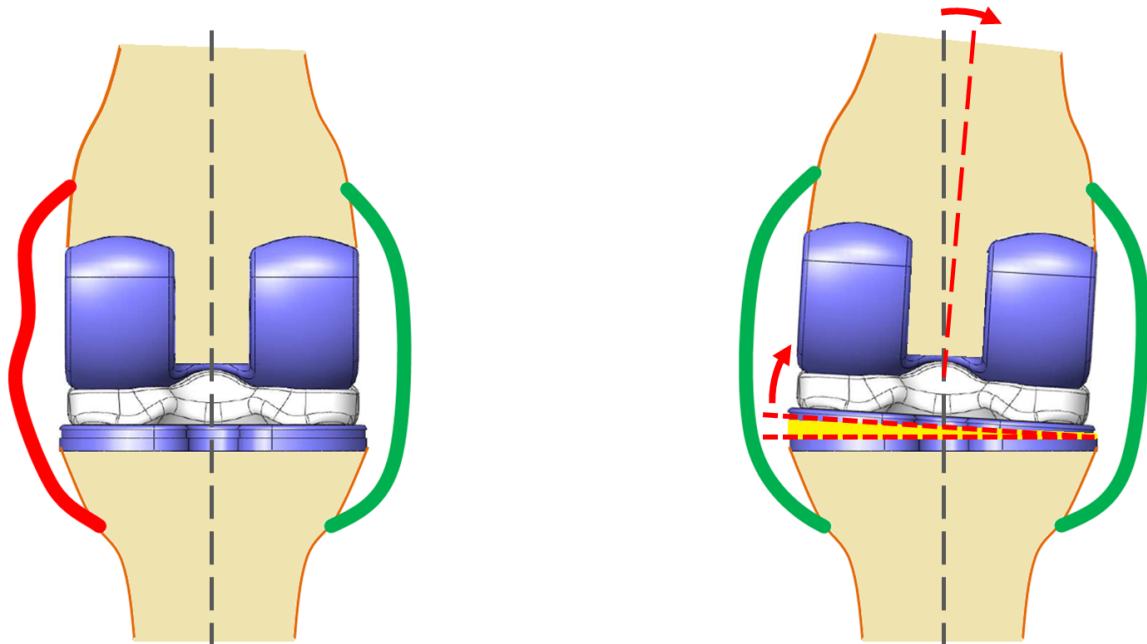


Figure 2.15 – a lax collateral ligament (left) can be properly re-tightened by laterally uplifting the tibial tray on the corresponding side (right)

In conclusion, the main contribution of this work consists in further developing the smart knee implant proposed by our research team by conceiving a miniaturised actuation system able to lift the tibial tray up on either its medial or lateral side. A priori, such system should be sufficiently small in order to be embedded in the tibial component and, at the same time, robust enough to face with the strong cyclic efforts that act inside the KJ. Its power supply and control have to be realised wirelessly by means of biocompatible techniques and its design should allow for an easy integration with the diagnostic part discussed above (the four PC elements embedded in the tibial baseplate). The achievement of all these goals would provide a smart knee prosthesis capable, at the same time, to:

- intraoperatively assist the surgeon to achieve optimal knee balance conditions during TKA soft tissues release procedure;
- monitor the prosthetic patient's KJ evolution after surgery and detect any instability;
- if needed, compensate for the detected imbalances and restore optimal balance conditions without the need for revision TKA.

To our knowledge, no other ongoing study copes with the problem of postoperative knee ligament imbalance with the same approach proposed in this work. As it will be discussed in the next chapters, this project is strongly multidisciplinary and faces with many constraints. If successfully achieved and upon acceptance by the orthopaedic community, the proposed smart knee prosthesis should, in the long term, strongly reduce the need for revision surgery.

Tibial Component Actuation Requirements

This chapter opens with the description of the envisaged protocol for the tibial component actuation. Embedding sensors and microelectronics components inside a knee prosthesis is an operation that faces with many restrictions: the formalization of the clinical needs is therefore followed by the constraints definition. After that, three different approaches for the realisation of the actuation system are proposed and discussed.

3.1 Envisaged Protocol

As mentioned in chapter 2.4.3, this project focuses on the need to postoperatively compensate for undesired knee collateral ligaments laxities. After primary TKA, the prosthetic KJ balance conditions should be evaluated as soon as the patient is able to walk autonomously again. At the very beginning of the rehabilitation period, the average tibiofemoral loads CoP trajectories recorded by the prosthesis still reflect the optimal collateral ligaments tensions achieved during TKA and should be stored as reference data. Afterwards, periodic follow-up visits allow to monitor the prosthetic KJ postoperative function and, by exploiting the diagnostic capabilities of the proposed instrumented tibial component, the surgeon is able to evaluate the evolution of CoP trajectories and detect any abnormality: a non-homogeneous CoP concentration on either the medial or lateral compartment of the tibial tray reveals a laxity condition of the opposite collateral ligament. Once the laxity has been detected, it has to be quantified: this can be achieved by comparing the recently recorded CoP trajectories with the reference ones. This is done by keeping into account the set of patient's knee physiological features, such as ligament stiffness and RoM, that were assessed during TKA surgery. This evaluation cannot be standardised for any patient and clearly depends on the surgeon's perception and experience, just like the soft tissues balance

procedure during TKA (chapter 2.4.1); to cope with such variability, the use of the proposed actuation system during a gradual adjustment procedure allows to effectively restore optimal balance conditions by integrating the surgeon's skills.

The envisaged protocol is depicted in Fig. 3.1. Once the laxity has been assessed, the surgeon quantifies the amount of lateral uplift of the tibial tray that is necessary to properly re-tighten the lax collateral ligament. Then, a progressive fine-tuning correction process is carried out by successive stages: the actuation is performed a first time and the tibial tray is locked in the new raised position. Right after, the patient is asked to walk a few steps, in order to let the PC elements embedded in the tibial platform process the new CoP trajectories and transfer them to the clinician's computer. After comparing the updated data with the reference ones, if needed, the actuation is performed again. In this way, further refinement corrections can be carried out until optimal balance conditions are restored.

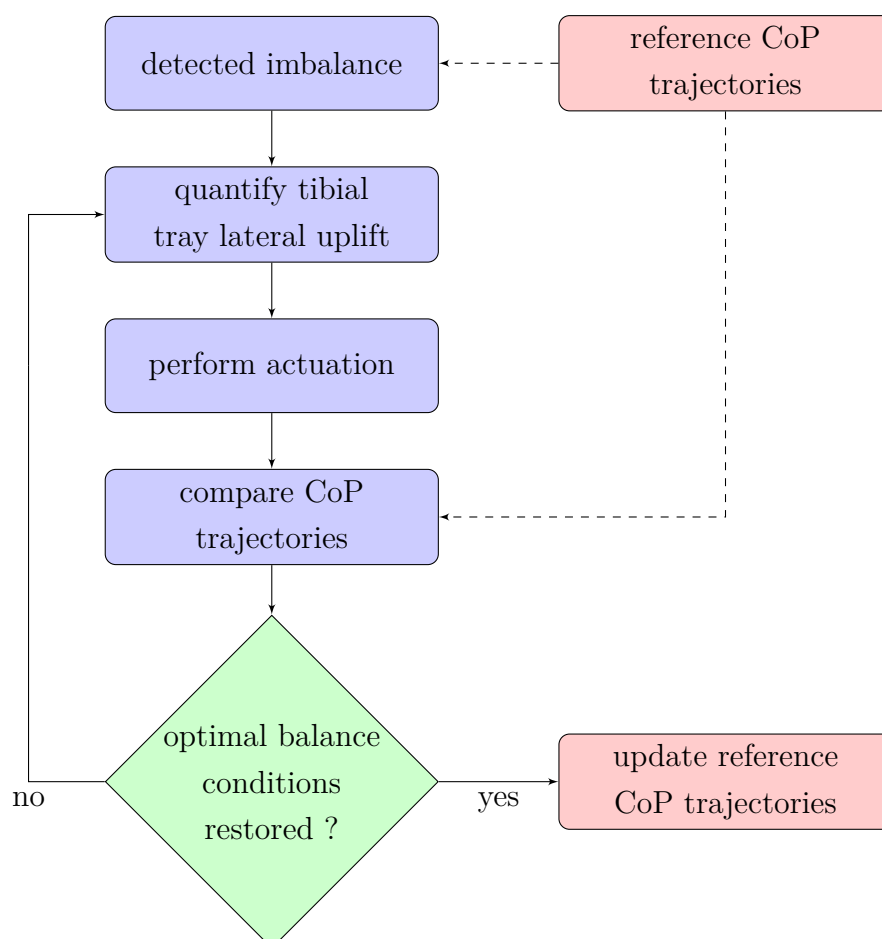


Figure 3.1 – flowchart of the envisaged protocol to restore optimal knee balance conditions

3.2 Clinical Needs

It is very important to properly treat any detected instability as soon as possible; complications can become so severe that postoperative medical treatment may result insufficient to relieve debilitating pain and prevent the patient from disabilities. In such cases, revision TKA could represent the only solution for the restoration of KJ function via a second surgical intervention [6, 7]. As already discussed, only a continuous accurate monitoring of the evolution of the prosthetic KJ stability combined to the use of the proposed implant could allow to restore optimal balance conditions postoperatively, without the need for revision surgery.

After consultation with an orthopaedic surgeon, the correcting action of re-tightening a lax knee collateral ligament in the postoperative period has been accepted as an effective way to restore optimal balance conditions. As suggested in chapter 2.4.3, if acting in good time, residual TKA inaccuracies can be properly treated by slightly lifting the tibial tray up on the side corresponding to the lax ligament. Such uplift must not impair the prosthesis alignment to the LLMA achieved during TKA[4, 5]; thus, it is necessary to determine to which extent it is affordable to perform this actuation without compromising the whole implant functionality. In terms of alignment, the tibial tray lateral uplift is intended to realise the same correcting action performed by spacer blocks and wedges in respectively revision TKA [28] and tibial osteotomy [82]. As depicted in Fig. 3.2, the use of components of predetermined thickness inserted in (or removed from) the tibial bone allows to adjust the tibiofemoral alignment conditions in order to modify loads distribution (and thus CoP trajectories) as required. The thickness of spacers and wedges, on average 5 to 17.5 mm [83], is selected according to the needs of the performed surgery and can produce up to 10 degrees of tibiofemoral angle correction [84, 85].

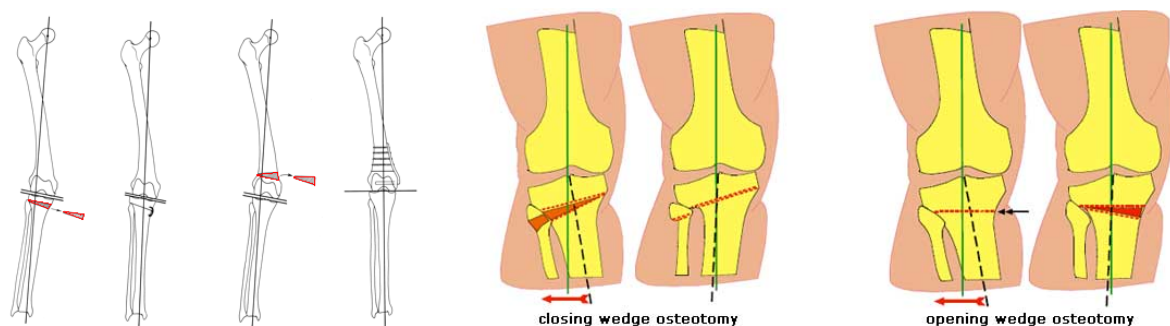


Figure 3.2 – osteotomy results in adjusting tibiofemoral alignment conditions [82],

Knee implants are available in different sizes, according to the standards adopted by each prosthetic manufacturer. In this work, a Genesis 2 Total Knee System [86] of size 6 is considered: the tibial platform dimensions (54 mm AP and 77 mm ML) fit the average male KJ bones size. A simple geometric representation of the prosthetic KJ during the proposed actuation (Fig. 3.3) shows that a 4 mm lateral uplift of the tibial tray results in a 2.9 degrees tibiofemoral angle modification. Such values are consistent with the correction ranges of spacer blocks and wedges mentioned above, thus they should not give rise to dangerous misalignment conditions. Therefore, in order to keep a good margin of safety, the actuation system will be dimensioned considering 4 mm of maximum tibial tray lateral uplift.

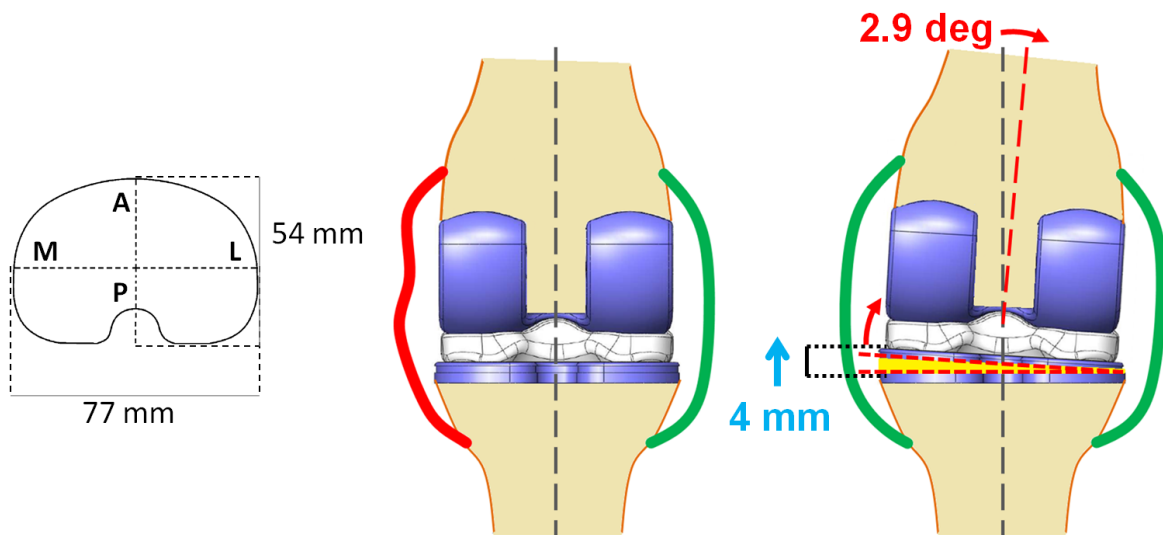


Figure 3.3 – simplified representation of the prosthetic KJ during the proposed actuation

3.3 Constraints

The development of a miniaturised actuation system to be embedded in a knee prosthesis is an ambitious challenge that requires skills in different expertise domains. Design choices have to fulfil clinical needs while facing with technical and technological limitations. The selected components have to meet severe biocompatibility criteria and any proposed solution should be extensively discussed and evaluated in terms of effectiveness and feasibility. All these considerations clearly highlight the multidisciplinary nature of this project; the first step towards the achievement of the defined objectives consists in an accurate definition of the constraints, such as volume, accuracy, robustness, wireless power supply and control, and biocompatibility.

3.3.1 Volume

The tibial tray dimensions are 54 mm AP and 77 mm ML; the presence of the four PC elements leads to a platform thickness of 4.5 mm, in line with the size of conventional implants. The presence of the actuation system, which has to be entirely embedded in the tibial component, will certainly result in an increase of the tibial baseplate thickness. From the perspective of TKA surgical procedure, the implantation of a thicker component entails a greater amount of resected bone; this is acceptable only to a certain extent because, as already mentioned in chapter 1.2.2, bone cuts should be limited to the diseased bony parts without any unnecessary sacrifice of healthy bone. A possible intraoperative measure to get around this drawback and keep optimal tibiofemoral spacing conditions consists in employing a thinner PE insert [4]. In any case, the total volume of the tibial component should be exploited as much as possible for embedding the actuation system (Fig. 3.4); besides the platform thickness, also the hollow cylindrical volume of the tibial stem (17 mm diameter, 40 mm high) can be occupied by miniaturised components. If required, further available volume can be obtained by extra drillings performed in the resected tibial surface around the stem hole; such possibility is not literature-documented and the choice of resorting to it is completely at the discretion of the surgeon. By way of illustration, with the aforementioned dimensions the total exploitable volume offered by the tibial component is about 50 cm³, which is one and a half times the volume of a tennis table ball.

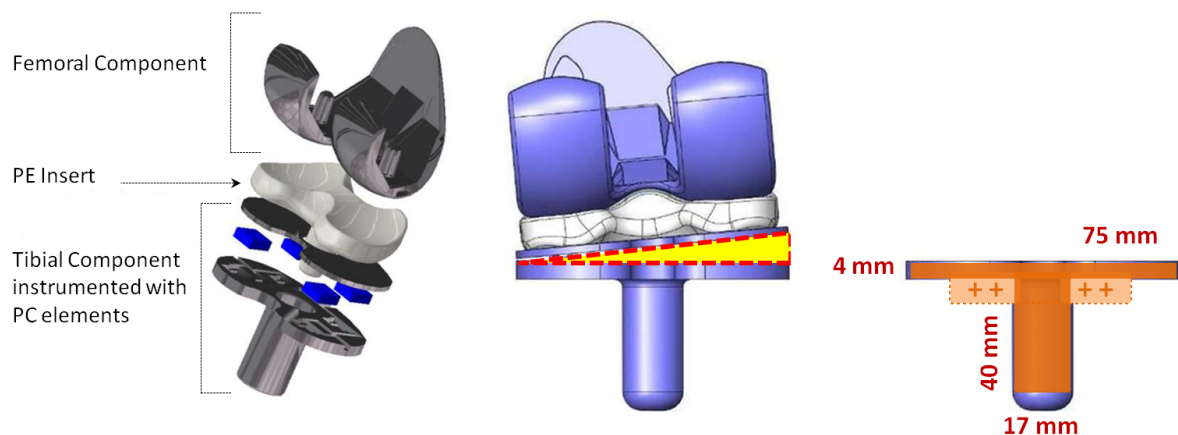


Figure 3.4 – the total available volume offered by the tibial component to embed the actuation system

3.3.2 Accuracy

The envisaged protocol discussed in chapter 3.1 is based on successive adjustments interspersed with measurement phases, that allow to continuously monitor the effects of the performed corrections on the average CoP positions shift. Realistically, a first major tibial tray uplift will be followed by minor fine-tuning adjustments, carried out until optimal balance conditions are restored. It sounds reasonable to design an actuation system able to operate in the range 0-4 mm with submillimetre accuracy.

No standard exists in terms of knee collateral ligaments length and insertion sites, which strongly vary among individuals. A study [87] reported that the average length of knee collateral ligaments was 94.8 mm. According to such value, a condition of full actuation would correspond to a 2.9 degrees tibiofemoral angle modification and a ligament length increase of 4.2 %; likewise, a 0.1 mm tibial tray lateral uplift would result in a 0.07 degrees angle and a 0.1 % ligament elongation. Operatively, there is no need to seek even greater accuracy conditions, for which the surgeon's skills are of major importance.

3.3.3 Robustness

The tibial tray lateral uplift is supposed to be performed with the patient in lying position, so that the Body Weight (BW) can be neglected and the only force acting inside the prosthetic KJ is the passive force of the two collateral ligaments. The value of such force varies among individuals and was estimated [47] as 300 N in total, uniformly distributed on the tibial platform and perpendicular to its surface, as a compression of the femur onto the tibia. According to this, it is assumed that each collateral ligament develops on the corresponding tibial tray compartment a force of 150 N; in this work, this value will be considered as the minimum total force that the actuation system must be able to develop in order to lift the tibial tray up on the desired side. Moreover, considering that *“the collateral ligaments are fully tensed only during extension of the knee joint and they are relaxed during flexion”* [10, p. 179], specific positions of the patient's leg may be evaluated by the surgeon so as to reduce the resistance force opposed by the collateral ligaments and perform the actuation under more favourable conditions.

After surgery the patient should be able to live without any remarkable limitation caused by the presence of the implanted prosthesis. In most everyday life activities, knee prostheses ceaselessly undergo very strong efforts: besides the tibiofemoral loads, uncontrollable vibrations and shear forces generate inside the KJ and act mainly on the

tibial tray. “Knee forces have been reported *in vivo* for a variety of activities including recreation and exercise” [88, p. 97]; Table 3.1 summarizes the peak tibiofemoral forces recorded during daily life activities [89], expressed as multiples of the patient's BW. Another value to keep in mind is that of the peak tibiofemoral force acting inside the prosthetic knee during normal gait cycle, defined by the International Organization for Standardization [90] as 2600 N. As all the aforementioned data suggest, the actuation system embedded in the tibial component must necessarily be robust enough to face with the very strong cyclic efforts that the tibial tray normally undergoes. Considering the very small available volume offered by the tibial component and the need for miniaturised instrumentation, the robustness requirement is not easy to achieve. A smart locking system must be provided in order to block the tibial tray in its uplifted position after actuation; inevitably, proper design choices will have to be made seeking a good compromise between size and soundness.

Activity	Peak Tibiofemoral Force (x BW)
Walking	2.5 ± 0.3
Jogging	4.2 ± 0.2
Stair Climbing (slow)	2.4 ± 0.1
Knee Extension	1.5 ± 0.0
Rowing Machine	0.9 ± 0.1
Stationary Bicycling	1.0 ± 0.5
Golf (lead knee)	4.4 ± 0.1

Table 3.1 – average peak tibiofemoral forces during common daily life activities, expressed as multiples of BW [88]

3.3.4 Wireless Power Supply and Control

Over the last decades, the joint work of prosthetists and implant manufacturers has allowed to combine clinical experience with engineering expertise; the result of such collaboration is a host of instrumented prosthetic implants that provide smart solutions

to a variety of problems. In the case of lower limb implants, almost all the devices that can be found on the market address the problem of amputation, with artificial body parts designed to replace damaged or missing limbs (Fig. 3.5). Nowadays, such prostheses are increasingly exploited as actively powered devices: embedded sensors and microprocessors are employed to enable forms of locomotion that passive implants could not afford, thus enhancing the mobility of the prosthetic patient. The power supply of this kind of implants is achieved by means of batteries (rechargeable or not), which generally can be replaced by the patient for a better ease of use. In a sense, the use of batteries is a prerogative of those implants which are fully or partially removable: the possibility to have a direct access to the device does not imply severe requirements of size and sterility. In the case of a total knee prosthesis, the circumstances are completely different: components miniaturisation is a priority and, because of the high risk of infection, the interface bone-prosthesis should never be exposed to external agents. The patient will never have direct access to the implant and any embedded battery leakage condition would represent a serious threat to the prosthesis lifespan. Consequently, in this work, other techniques should be considered to power the embedded actuation system components.



Figure 3.5 – some examples of lower limb prosthetic implants

Inductive coupling is by far the most widely adopted technique for powering instrumented knee implants. Besides the devices presented in chapter 2.3, many other studies in the literature widely document the effectiveness of such wireless energy transfer technique. A small receiver coil can be placed inside the prosthesis, either located in the tibial stem [91, 92] or embedded in the PE insert [93, 94, 95], and coupled to a bigger external coil positioned around the patient's knee. The presence of specific microelectronics components for power conditioning allows to collect a few tens of mW inside the prosthesis; considering the presence of both the biological tissues and the metal prosthetic components, the efficiency of such energy transfer process mainly depends on the coils dimensions. The two main strengths of inductive coupling are its great biocompatibility and versatility of use. In most applications, the transferred energy is used

to power small telemetry systems for data acquisition, processing and communication (usually achieved by means of radiofrequency techniques).

An alternative choice is represented by the energy that can be produced inside the prosthesis itself. As presented in chapter 2.4.2, a unique feature of the instrumented tibial component that this work aims to further develop is the use of the four PC elements embedded in the tibial tray as energy harvesters. This original choice has been widely discussed by our research team and is currently investigated by other researchers too [96]. The energy collected during a few walking cycles is meant to fully supply a low-power consumption device such as the miniaturised telemetry system located in the tibial stem (Fig. 3.6); in order to be able to exploit the same source of energy, the actuation system should be dimensioned so as to be the least possible power consuming. This cannot be guaranteed a priori and needs to be further discussed during the components selection step.

Another very original approach to the power supply issue could be the exploitation of those power sources that are internal to the human body: chemical, thermal and electric energies are continuously produced by any muscular activity. Although, a very limited amount of energy can be effectively harvested and there is very scarce documentation on this subject [97, 98].

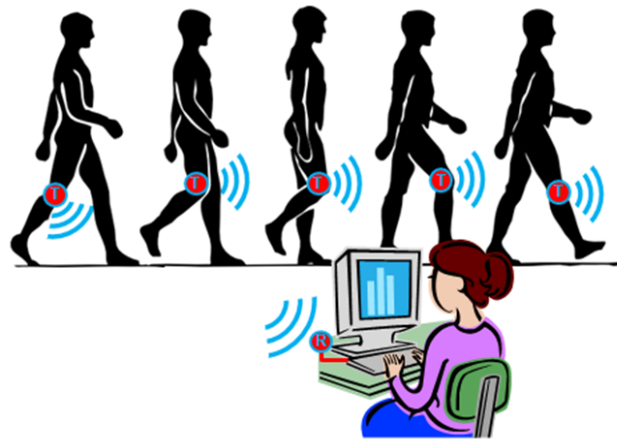


Figure 3.6 – example of wireless interaction between the proposed instrumented knee implant and the clinician's computer during a follow-up visit

3.3.5 Biocompatibility

“The biocompatibility of a long-term implantable medical device refers to the ability of the device to perform its intended function, with the desired degree of incorporation in

the host, without eliciting any undesirable local or systemic effects in that host”[99]. While designing and dimensioning the actuation system, all the constraints that have been discussed above must abide by the biocompatibility requirement. Any component that is supposed to be employed inside the instrumented knee implant must neither jeopardize the integrity of the patient's biological tissues, nor risk to give rise to post-operative complications such as infection processes. The need for biocompatible instrumentation might represent a major limitation also in terms of the powering techniques that can be employed: for instance, as previously mentioned, this is the case of batteries, whose use in permanent prostheses is deprecated because of the risk of power leakages. Most likely, proper design choices and compromises will have to be made in order to find a feasible solution with all the constraints simultaneously satisfied.

3.4 Possible Actuation Approaches

Three different approaches were considered for the realisation of the actuation system. In order to investigate their feasibility, they are presented and discussed hereafter with a pros and cons analysis outlined for each case.

Micromotor - this approach consists in making use of a miniaturised mechanical structure driven by a microactuator; everything should be embedded in the tibial component and allow to adjust the inclination of the tibial tray as required. The great technological advances in terms of miniaturisation allow to select the mechanical structure from a wide variety of possibilities, an aspect which a priori ensures a remarkable design flexibility. Moreover, the micromotor could be controlled very accurately and interact with specific sensors so as to provide extremely reliable measurements. Particular attention should be paid to the choice of the micromotor, which must be small enough to be embedded in the tibial platform and, at the same time, sufficiently powerful to realise the actuation (chapter 3.3.3). For the same reason, it is not conceivable to require the participation of the microactuator to block the tibial tray in the actuated position; a passive locking system should be conceived and provided by smart design solutions. A further drawback of this approach is the fact that also the microelectronics components necessary to control the micromotor should be embedded inside the prosthesis; such components, which must be properly sealed due to biocompatibility reasons, risk being quite power consuming and their wireless supply might turn out to be arduous.

Magnetic Field - this approach is based on achieving the required tibial tray up-lift by means of an external magnetic field. The idea is to adjust the position of

specific ferromagnetic components, properly disposed inside the tibial platform, to be guided from the outside by exploiting a non-contact magnetic interaction. As already repeatedly mentioned in the previous chapters, thanks to their great biocompatibility magnetic fields represent a common choice for powering instrumented knee implants. The design of a ferromagnetic structure to realise the desired actuation may turn out to be quite challenging, especially considering the volume and robustness constraints; although, it is very engaging the possibility to conceive an actuation system actually based on passive components which can be activated when necessary and ensure great durability. Such system passivity, which eliminates the need for power supply, theoretically implies the absence of sensors inside the prosthesis; consequently, it would result more difficult to accurately assess the effectiveness of the performed correcting action. A further minor concern is raised by the ferromagnetic elements, whose permanent presence inside a knee prosthesis has already been discussed [70] and can be considered with all the necessary precautions.

External Tool - this approach involves the use of an external tool to access the prosthesis from the outside, so as to adjust the inclination of the tibial tray by lifting it up on the required side. Via two small skin incisions, the external tool is supposed to be put in contact with the bone-prosthesis interface in order to drive a custom-designed mechanical structure embedded in the tibial baseplate. The most interesting aspect of this approach is its extremely low invasiveness: a priori, general anaesthesia procedure is not required and the actuation would leave no scar or visible trace on the patient's skin. Moreover, the possibility to employ a custom-designed external tool does not require any wireless power supply and should also compensate for the system passivity: despite the absence of sensors, the tool control electronics allows to achieve the tibial tray lateral uplift with very high accuracy. A major drawback of this approach is represented by the risk of infection, too high despite the very reliable sterilisation techniques that are made available nowadays. The introduction of any external body inside the knee articulation after TKA surgery must be avoided, since any bacterium accidentally came in contact with the bone-prosthesis interface might give rise to severe postoperative complications.

The main advantages and drawbacks of the three possible approaches have been discussed [100] and are summarized here in Table 3.2. Upon discussion within our research team, the external tool approach was set aside and it was decided to try to take advantage of the strengths of the other two approaches for the realization of the actuation system. The use of a micromotor was identified as the best choice to

guarantee a highly accurate control of the tibial tray lateral uplift (chapter 3.3.2); inductive coupling techniques could be employed to provide the power supply of the actuator and its electronics, on the basis of what has been proposed by [101] and of the achievements already mentioned in chapter 3.3.4. Striving for innovation, smart design choices necessarily have to be made so as to overcome any technological limitation and find a feasible solution that meets all the constraints.

approach	ADVANTAGES	DRAWBACKS
Microactuator	<ul style="list-style-type: none"> • design flexibility • very high accuracy 	<ul style="list-style-type: none"> • compromise size/power • relatively high energy consumption
Magnetic Field	<ul style="list-style-type: none"> • widely documented biocompatibility • passivity \rightarrow no power supply 	<ul style="list-style-type: none"> • design complexity • no sensors \rightarrow lower accuracy
External Tool	<ul style="list-style-type: none"> • minimal invasiveness • passivity \rightarrow no power supply • custom-designed tool \rightarrow high accuracy 	<ul style="list-style-type: none"> • high risk of infection

Table 3.2 – comparison of the three considered approaches for the realization of the actuation system embedded in the tibial tray

4 Actuation System Design

Bearing in mind all the considerations made in the previous chapter, the actuation system must be based on a compact and robust mechanical structure. Especially the volume constraint compels to set aside bulky components in favour of simpler design solutions. In such context, it should sound reasonable to resort to the use of a simple machine, which is basically an elementary device based on a specific movement that changes the direction or magnitude of a force by providing a mechanical advantage [102]. As defined by [103, p. 112]:

“the Simple Machines are devices used, as a rule, to secure a large force by the application of a smaller force. These machines are the lever, the pulley, the wheel and axle, the inclined plane, the wedge, and the screw”.

The combined use of two or more simple machines can result in an efficient mechanism able to develop great output forces in face of reduced input efforts. In accordance with such principle, different design proposals were extensively discussed [104, 105]. In this current work, two different actuation systems, both able to realise the required tibial tray lateral uplift, are proposed and discussed. The most promising model [106], described in the following, was selected for the fabrication of a steel prototype in order to carry out experimental tests. The other system [107], which was fully developed but then set aside because of its higher invasiveness, is described in the Appendix.

This chapter opens by illustrating the actuation system working principle and describing the components dimensions. The system mechanical analysis, detailed next, highlights the effectiveness of the adopted design choices. The discussion of important issues about the overall feasibility of the proposed tibial component closes the chapter.

4.1 Working Principle

The miniaturised actuation system is based on the smart combination of a wedge and a screw. The wedge has a custom-designed shape and is guided inside a rail grooved in the tibial baseplate (Fig. 4.1). Via a threaded hole, the wedge is coupled to a leadscrew which can only rotate without translating. As in a screw-nut configuration, any lead-screw revolution produces a corresponding wedge translation according to the thread pitch; herein, such assembly will be addressed as a Wedge-Leadscrew (WL) system. For sake of clarity, the description and the figures reported in the following refer to the actuation of only one side of the tibial platform. The reader is invited to keep in mind that the instrumented tibial component actuation is achieved by means of two identical systems, one per each side of the tibial baseplate, positioned symmetrically with respect to the tibial stem axis.

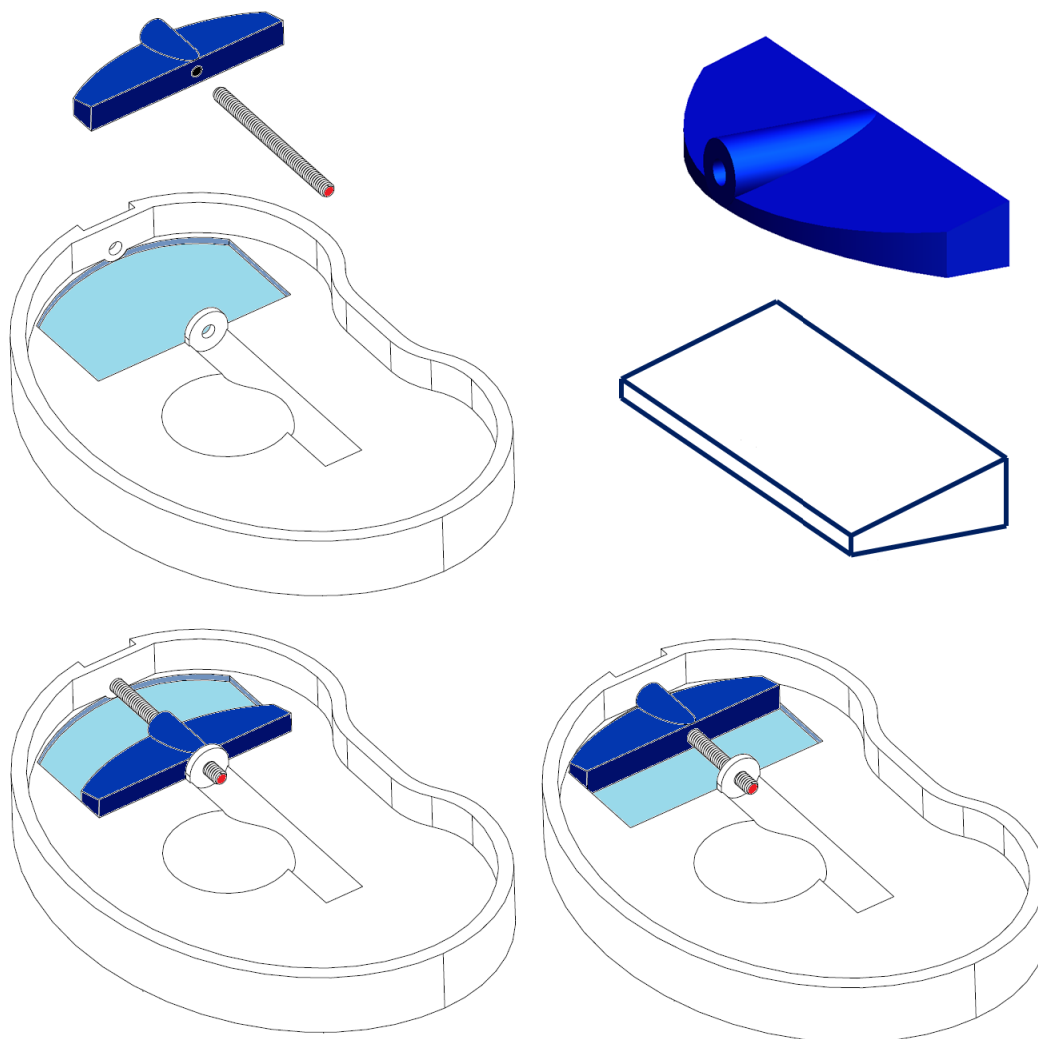


Figure 4.1 – the leadscrew (red) drives the wedge (blue) inside its rail (cyan)

A mobile tibial tray is shaped so as to be positioned from above onto the baseplate and fit the presence of the WL system. As depicted in Fig. 4.2, without any actuation the tray is fully contained inside the baseplate in a configuration that corresponds to that of conventional tibial platforms. In its starting position, the wedge is aligned to the center of the baseplate (null translation).

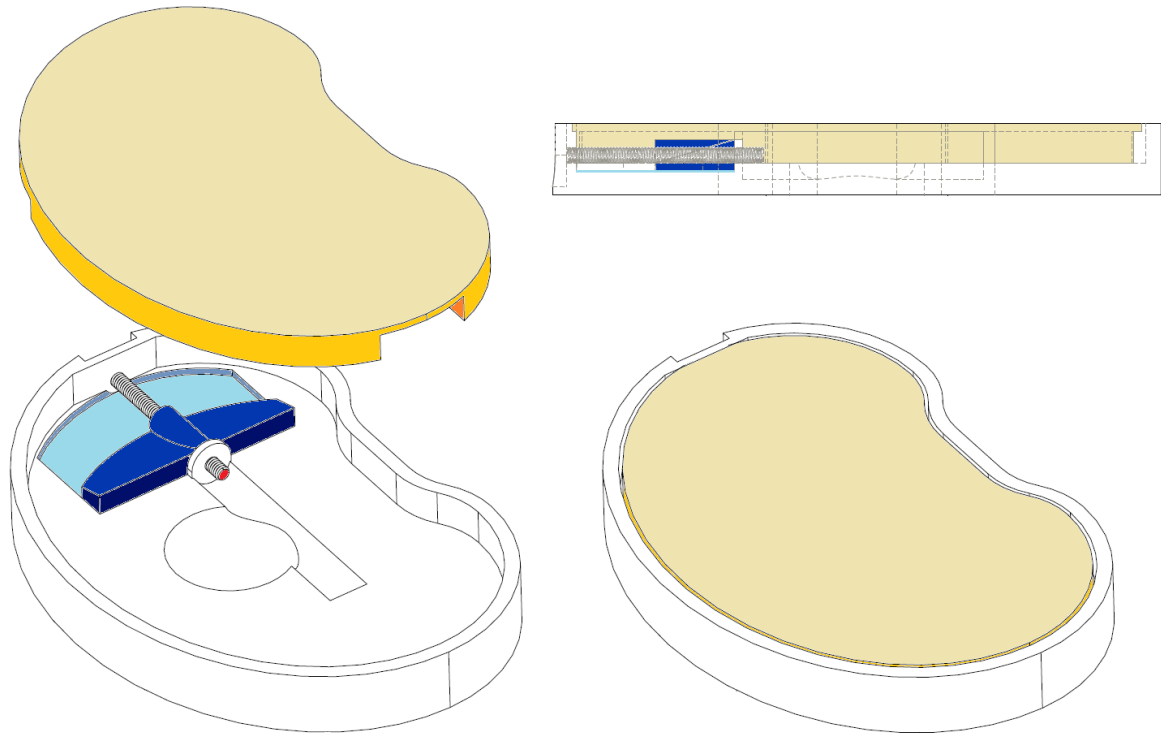


Figure 4.2 – without any actuation, the mobile tibial tray (light brown) is fully contained inside the baseplate

As the leadscrew starts to rotate, the wedge translates laterally, towards the baseplate outer border. By doing this, the wedge slides under the mobile tray and lifts it upwards. The greater the wedge translation, the greater the mobile tray lateral uplift (Fig. 4.3).

The leadscrew is held in place by specific supports and is rigidly fixed to the shaft of a rotary stepper micromotor. As it will be discussed in the following, the actuator is supposed to be entirely embedded in the tibial baseplate; likewise, all the microelectronics components necessary for the system power supply, control and data transmission can be positioned inside the hollow tibial stem.

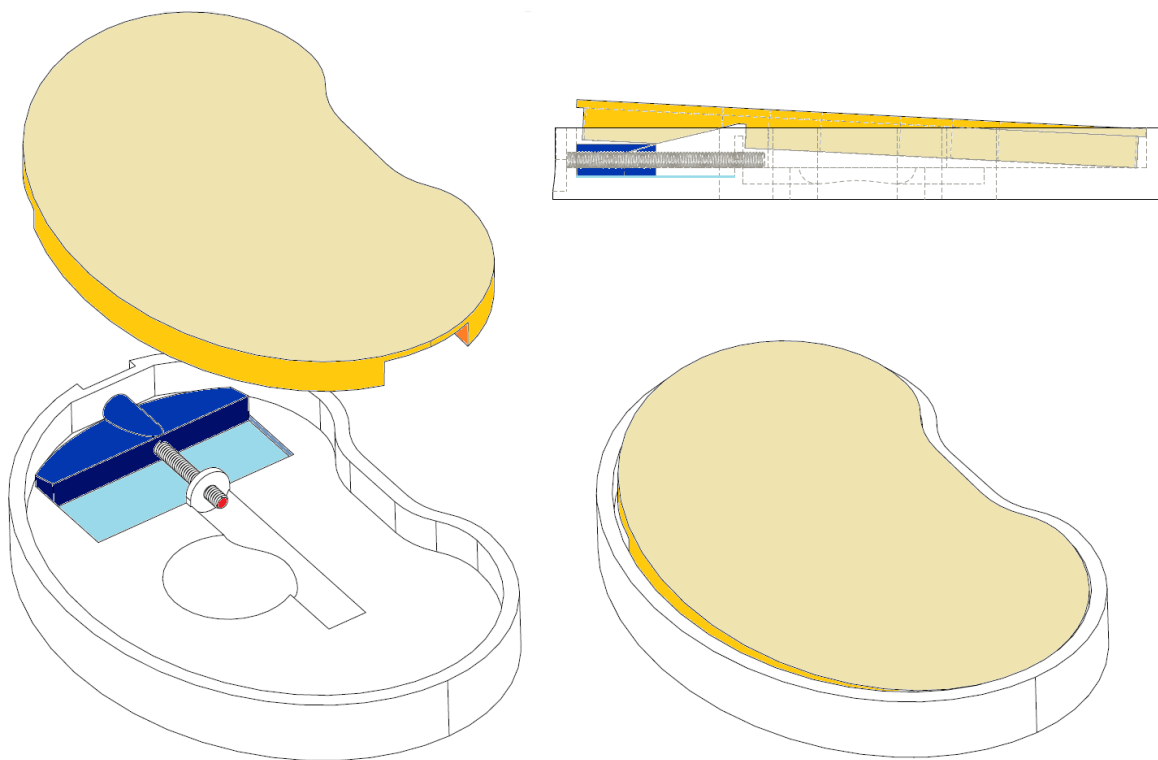


Figure 4.3 – the wedge translation laterally lifts the mobile tray up

4.2 Components Dimensions

4.2.1 Wedge-Leadscrew System

The wedge is the key component of the actuation system. Its custom design is determined by the necessity to fit the rounded outer profile of the tibial baseplate. As depicted in Fig. 4.4, the wedge has a total thickness of 4 mm; the bottom part (1 mm thick) fits a corresponding rail grooved in the tibial baseplate, inside which the wedge translation takes place. Consequently, the actual wedge part (pink-coloured in Fig. 4.4) is 3 and 10 mm respectively high and long. Via a 10 mm long hole drilled along its entire length, the wedge is coupled to the leadscrew by means of a standard M2x0.4 thread profile: 2 mm nominal outer diameter and 0.4 mm pitch, according to the ISO metric design principles [108]. Thanks to specific supports, the leadscrew (25 mm long) can freely rotate about its longitudinal axis and keeps always the same position inside the tibial baseplate.

In such configuration, one complete leadscrew revolution causes the wedge translation of a distance corresponding to the thread pitch, thus 0.4 mm. The profile and the 1 mm depth of the rail inside which the wedge translation takes place prevent any other

undesired movement. The WL system designed in this way is mechanically irreversible: only the leadscrew revolution can produce the wedge translation and not vice versa.

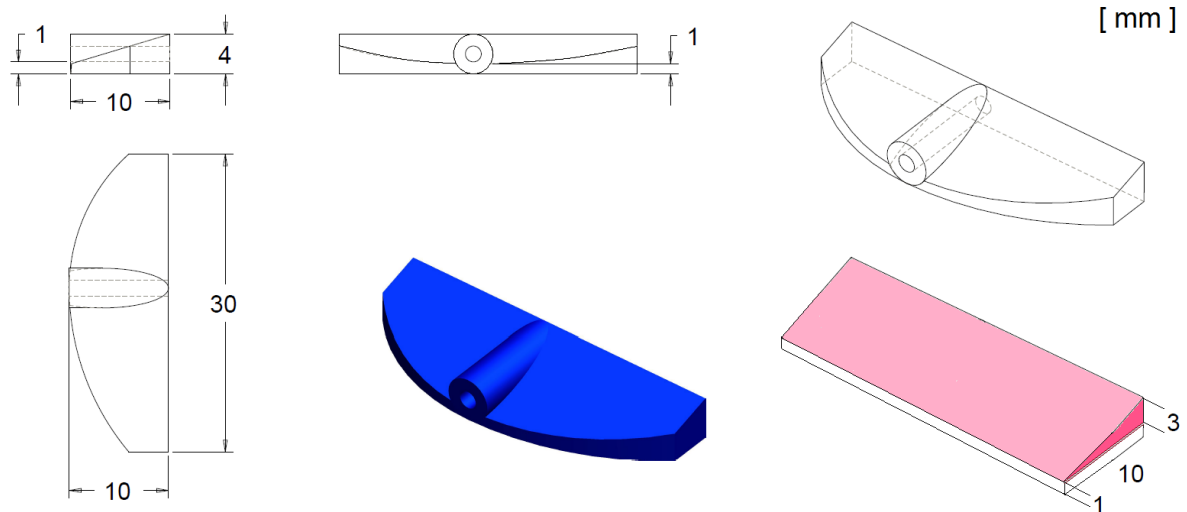


Figure 4.4 – the wedge dimensions (in mm)

4.2.2 Baseplate and Mobile Tray

As already mentioned in chapter 3.2, the reference implant developed in this work is a standard Size 6 knee prosthesis [86]: the tibial tray dimensions are 54 mm AP and 77 mm ML, whereas the tibial stem length is 40 mm. A 30 mm wide and 20 mm long rail is grooved on each side of the tibial baseplate: its shape allows the wedge translation (10 mm maximum stroke) along one single direction (that of the leadscrew longitudinal axis) and prevents from undesired wedge rotation movements. Thanks to a 2 mm thick border extruded all along the baseplate edge, a mobile tibial tray shaped with the same profile (offset by 2 mm) can be positioned from above onto the baseplate and fully contained inside it; in such configuration, when no actuation is performed, the proposed implant is like a conventional one but almost twice as thick. In this work, the necessity to fully embed the actuation system inside the knee prosthesis leads to increase the tibial platform thickness to 9 mm (Fig. 4.5).

The mobile tibial tray is 5 mm thick and is shaped so as to fit the presence of both the WL system and the microactuator embedded inside the baseplate. During the wedge translation, the mobile tray gets laterally lifted up on the actuated side and pivots on the non-actuated one; since its profile corresponds to that of the tibial baseplate, no movement other than the required lateral uplift can take place. Moreover, throughout the actuation process, the baseplate borders always contain the mobile tray,

thus preventing it from experiencing any undesired uncontrollable movement in the ML direction and from changing its orientation on the AP plane.

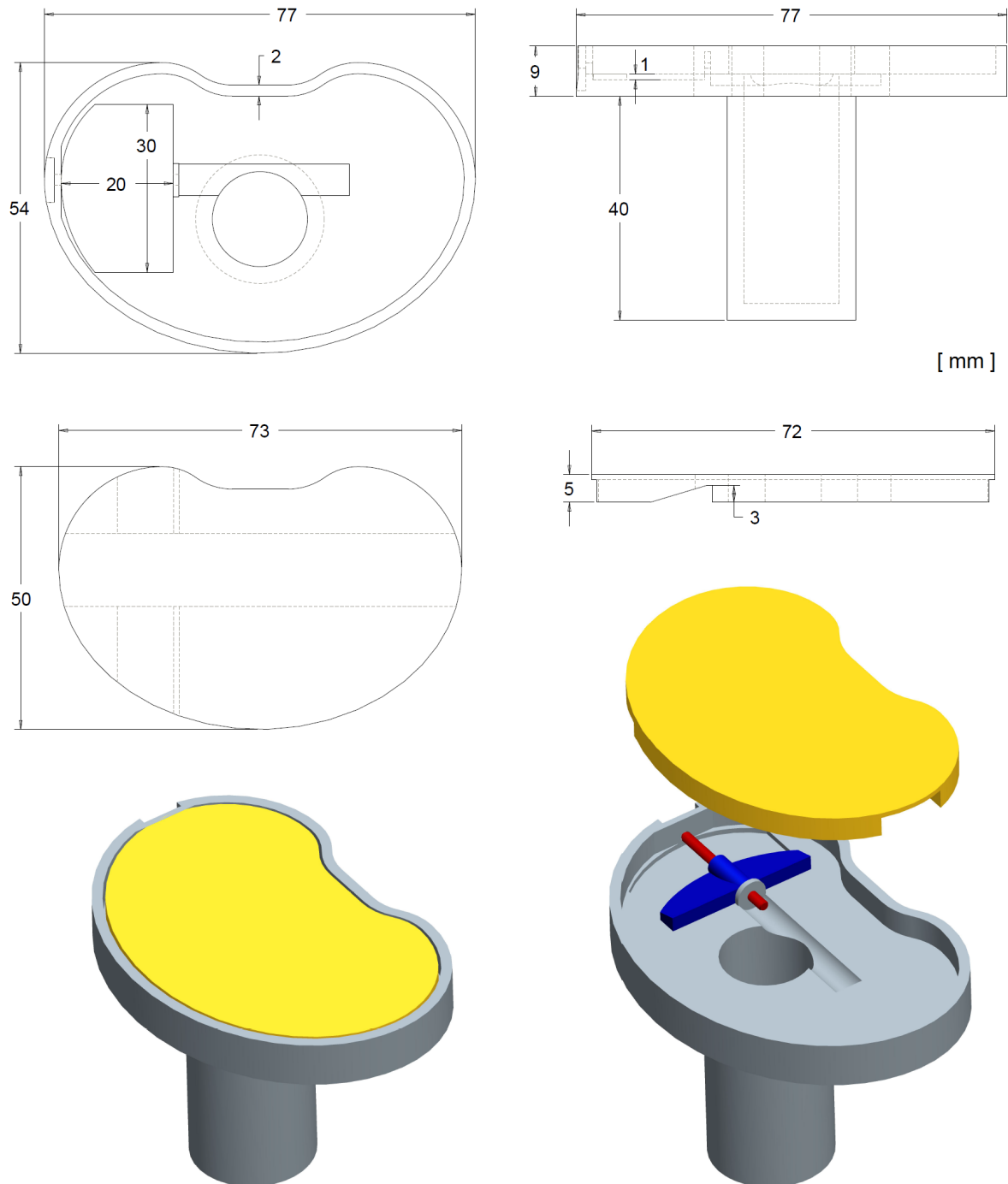


Figure 4.5 – dimensions and assembly of the tibial baseplate and the mobile tibial tray

The components were accurately reproduced and assembled in 3D by means of a CAD software. With the aforementioned dimensions, under full actuation conditions (10 mm wedge translation away from the tibial stem) the mobile tray is 3.6 mm laterally

uplifted. Such achievement is perfectly in line with the primary goal of this work (clinical needs defined in chapter 3.2) for the realization of the required actuation.

4.3 Mechanical Analysis

4.3.1 Static Force Analysis

A standard wedge is defined as a triangular shaped tool that “*can be used to separate two objects or portions of an object, lift up an object, or hold an object in place. It functions by converting a force applied to its blunt end into forces perpendicular (normal) to its inclined surfaces. The mechanical advantage of a wedge is given by the ratio of the length of its slope to its width. Although a short wedge with a wide angle may do a job faster, it requires more force than a long wedge with a narrow angle*” [109, p. 2041]. As depicted in Fig. 4.6, the custom-designed wedge which is part of the proposed actuation system has only one inclined surface, the one which is responsible for lifting the mobile tibial tray up; the opposite side of the wedge is flat and is devoted to constrain its translation inside the rail grooved in the tibial baseplate. With the same notation used in the definition given above, the custom-designed wedge is 10 mm long and 3 mm wide; therefore, its Mechanical Advantage (MA) is $10/3$, or 3.3. This means that any force applied to its blunt end (the black thick arrow in Fig. 4.6) will be converted into an output force more than three times greater (red arrow).

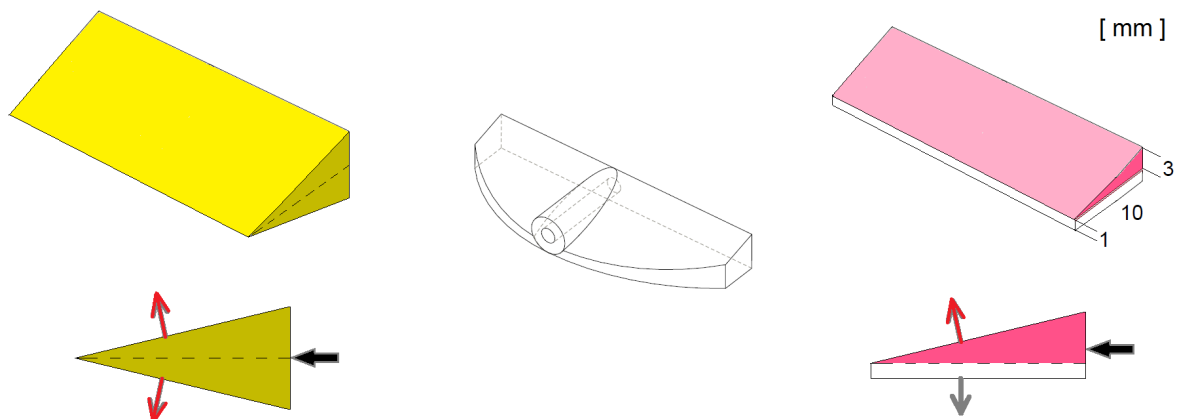


Figure 4.6 – comparison between a standard wedge (yellow, left) and the custom-designed wedge proposed in this work (pink, right)

During the actuation, the output force produced by the wedge translation has a constant direction perpendicular to the wedge inclined surface; such force is responsible for the mobile tibial tray lateral uplift and, as already explained in chapter 3.3.3, has

to cope with the 150 N of resistance force opposed by the collateral ligaments on the actuated side. A priori, considering the wedge MA, the input force exerted on the wedge blunt end is expected to be at least 50 N; this can be verified by means of static force analysis. Fig. 4.7 illustrates the configuration corresponding to a 5 mm wedge translation, which produces a mobile tibial tray lateral uplift of 1.8 mm. Table 4.1 summarizes the terms notation: the point coordinates were measured directly on the 3D model, while the angle values were determined by the components geometry.

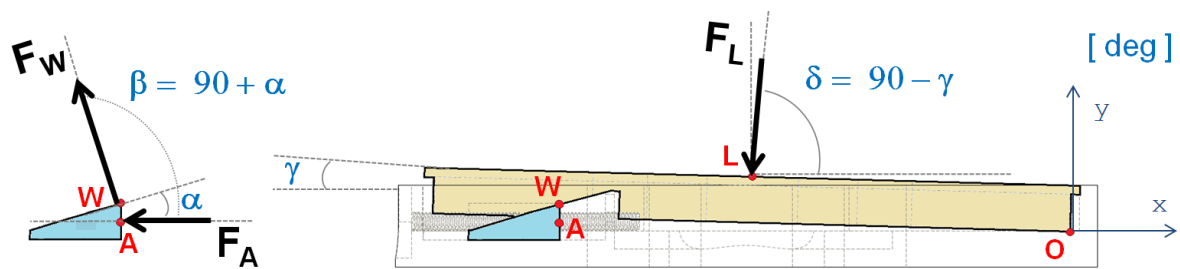


Figure 4.7 – the actuation system configuration selected for the static force analysis

Point A, where the wedge input force is applied, is taken on the wedge threaded hole axis. Point W is the projection on the frontal plane of the contact line shared by the wedge and the mobile tibial tray during actuation. Unlike conventional wedge applications, the mobile tibial tray (uplifted object) does not translate vertically but pivots on the non-actuated side of the tibial baseplate. Such rotation movement, even if limited to a few degrees (2.9 deg maximum, as explained in chapter 3.2), makes the mobile tray slightly change its orientation with respect to the wedge. Therefore, as soon as the wedge translates, the full surface contact that the two components initially share becomes a line contact along the wedge upper edge. Such peculiarity of the WL system is detailed in Fig. 4.8.

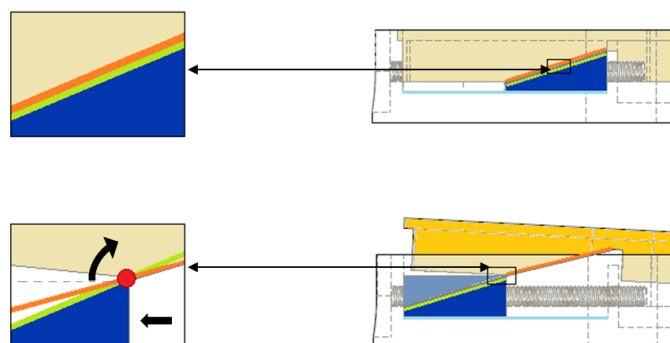


Figure 4.8 – during actuation, the full surface contact between the wedge and the mobile tibial tray becomes a line contact

term	type	value	unit	description
O	point	(0 ; 0)	mm	origin of the coordinate system
A	point	(-56 ; 1)	mm	point of application of the wedge input force (wedge blunt end)
L	point	(-35 ; 6)	mm	point of application of the collateral ligaments passive force (center of the mobile tibial tray)
W	point	(-56 ; 2.5)	mm	point of application of the wedge output force (contact with the mobile tibial tray)
α	angle	16.7	deg	wedge inclined surface angle (constant)
β	angle	106.7	deg	direction of the wedge output force (constant)
γ	angle	1.5	deg	inclination of the mobile tibial tray with respect to the baseplate in the considered configuration
δ	angle	88.5	deg	direction of the collateral ligaments passive force
F_A	force	unknown	N	wedge input force (perpendicular to the wedge blunt end)
F_L	force	300	N	collateral ligaments passive force (perpendicular to the mobile tibial tray upper surface)
F_W	force	unknown	N	wedge output force (perpendicular to the wedge inclined surface)

Table 4.1 – terms notation for the static force analysis

The static force analysis allows to qualitatively evaluate the loading conditions experienced by the system components during actuation. For sake of clarity, numerical approximation was applied when necessary throughout the computations presented in the following.

The coordinate system considered for the static force analysis is centered on the contact point between the mobile tibial tray and the baseplate on the non-actuated side. In order to draw the free-body force diagram of the mobile tibial tray, all the external forces acting on this component must be considered. In the selected system configuration, the mobile tibial tray is subjected to three forces (Fig. 4.9):

- the collateral ligaments passive force, whose direction and magnitude are known (angles are expressed in degrees and forces in Newtons): $F_L = \begin{bmatrix} F_{LX} \\ F_{LY} \end{bmatrix} = \begin{bmatrix} F_L \cdot \cos(180 + \delta) \\ F_L \cdot \sin(180 + \delta) \end{bmatrix} \approx \begin{bmatrix} 0 \\ -F_L \end{bmatrix} = \begin{bmatrix} 0 \\ -300 \end{bmatrix}$;

- the wedge output force $F_W = \begin{bmatrix} F_{WX} \\ F_{WY} \end{bmatrix} = \begin{bmatrix} F_W \cdot \cos(\beta) \\ F_W \cdot \sin(\beta) \end{bmatrix}$, from which we know that $F_{WY} = F_{WX} \cdot \tan(\beta)$, the term $\tan(\beta)$ corresponding to the wedge MA;
- the force $F_B = \begin{bmatrix} F_{BX} \\ F_{BY} \end{bmatrix}$ exerted by the baseplate on the mobile tibial tray, in their contact point B on the non-actuated side; since this force has unknown magnitude and direction (angle ε), its components will be initially considered positive with respect to the chosen coordinate system.

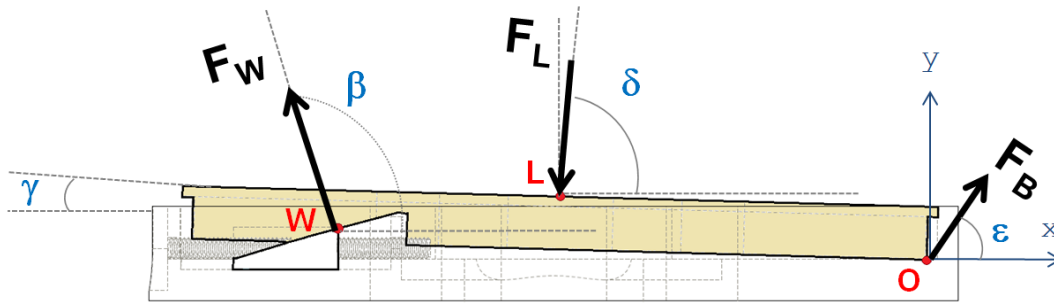


Figure 4.9 – free-body force diagram of the mobile tibial tray

Since the directions of F_L and F_W are known, the mobile tibial tray free-body force diagram can be analysed in some detail so as to deal with simpler computations. It is possible to write the equation for moment equilibrium about point O as follows:

$$\sum \vec{M}_O = \vec{0} \quad \Rightarrow \quad \vec{F}_L \times \vec{OL} + \vec{F}_W \times \vec{OW} = \vec{0}$$

Taking into account the numerical values defined in Table 4.1, the moment equilibrium equation becomes (forces are expressed in Newtons and coordinates in millimetres):

$$\begin{bmatrix} 0 \\ -300 \end{bmatrix} \times \begin{bmatrix} -35 \\ 6 \end{bmatrix} + \begin{bmatrix} F_{WX} \\ F_{WY} \end{bmatrix} \times \begin{bmatrix} -56 \\ 2.5 \end{bmatrix} = \vec{0}$$

The components and magnitude of the wedge output force F_W are then computed as follows (values in Newtons):

$$F_W = \begin{bmatrix} F_{WX} \\ F_{WY} \end{bmatrix} \approx \begin{bmatrix} -57 \\ 190 \end{bmatrix} \quad \text{and} \quad \|F_W\| \approx 198$$

Therefore, 198 N have to be exerted by the wedge in order to lift the mobile tibial tray up under the action of the 300 N collateral ligaments passive force. Considering what was anticipated in chapter 3.3.3 and the fact that, in the considered configuration, force distribution among the prosthetic components is influenced by the inclination of the mobile tibial tray, the computed result is completely realistic and reasonable.

On the non-actuated side, the force F_B exerted by the baseplate on the mobile tibial tray can be obtained from the force equilibrium equation:

$$\sum \vec{F} = \vec{0} \quad \Rightarrow \quad \begin{cases} F_{LX} + F_{WX} + F_{BX} = 0 \\ F_{LY} + F_{WY} + F_{BY} = 0 \end{cases}$$

It is then possible to compute the components, magnitude (in Newtons) and direction (angle ε in degrees) of the force F_B :

$$F_B = \begin{bmatrix} F_{BX} \\ F_{BY} \end{bmatrix} = \begin{bmatrix} 57 \\ 110 \end{bmatrix} \quad , \quad \|F_B\| \approx 124 \quad \text{and} \quad \varepsilon \approx 63$$

It follows that F_B is actually oriented as in Fig. 4.9. Also this result is reasonable, if one takes into account the action-reaction principle (Newton's third law): on the non-actuated side, due to the 300 N collateral ligaments passive force, the inclined mobile tibial tray will realistically exert on the baseplate a force equal and opposite to F_B .

The next step consists in considering the wedge and drawing its free-body force diagram. In the selected system configuration, the wedge experiences three forces (Fig. 4.10):

- the force F_W^M exerted by the mobile tibial tray onto the wedge. According to the action-reaction principle, such force is equal and opposite to F_W and can be defined as (values in Newtons): $F_W^M = \begin{bmatrix} F_{WX}^M \\ F_{WY}^M \end{bmatrix} = -F_W = \begin{bmatrix} 57 \\ -190 \end{bmatrix}$;
- the wedge input force, which is horizontal (perpendicular to the wedge blunt end) and is the major variable of interest in this study: $F_A = \begin{bmatrix} F_{AX} \\ F_{AY} \end{bmatrix} = \begin{bmatrix} F_{AX} \\ 0 \end{bmatrix}$;
- the vertical reaction force exerted by the baseplate on the wedge lower surface, as a consequence of all the aforementioned loads: $R = \begin{bmatrix} R_X \\ R_Y \end{bmatrix} = \begin{bmatrix} 0 \\ R_Y \end{bmatrix}$.

In this case, the force equilibrium equation turns out to be very simple and direct:

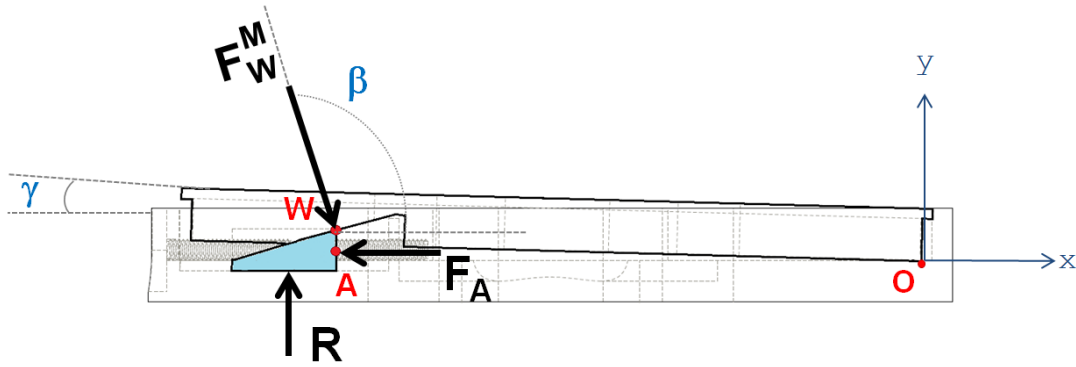


Figure 4.10 – free-body force diagram of the wedge

$$\sum \vec{F} = \vec{0} \quad \Rightarrow \quad \begin{cases} F_{AX} + F_{WX}^M = 0 \\ R + F_{WY}^M = 0 \end{cases}$$

Thus, the wedge input force and the tibial baseplate reaction force can be computed as follows (values in Newtons):

$$F_A = \begin{bmatrix} -57 \\ 0 \end{bmatrix} \quad \text{and} \quad R = \begin{bmatrix} 0 \\ 190 \end{bmatrix}$$

The wedge input force F_A is directed perpendicular to the wedge blunt end and is responsible for the mobile tray lateral uplift. Besides its minus sign, which is consistent with the directions fixed by the chosen coordinate system, the magnitude of F_A is in line with the expected value: a wedge input force of approximately 57 N (to be amplified via the wedge MA) is needed to overcome the 150 N collateral ligaments passive force acting on the actuated tibial tray compartment. Different actuation system configurations may be considered to carry out the static force analysis, which will always lead to similar values of F_A (slight variations might be due to numerical approximation).

4.3.2 Friction Losses

A clear limitation of the static force analysis presented above stands in the fact that friction effects are not taken into account. During actuation, the wedge translation is continuously subjected to the resistance force exerted by the collateral ligaments on the mobile tibial tray; consequently, the system components experience strong efforts mainly in two areas (green-coloured in Fig. 4.11):

- on the wedge inclined surface, along the contact line shared with the mobile tibial tray;

- on the three contact surfaces between the wedge and the rail grooved inside the tibial baseplate.

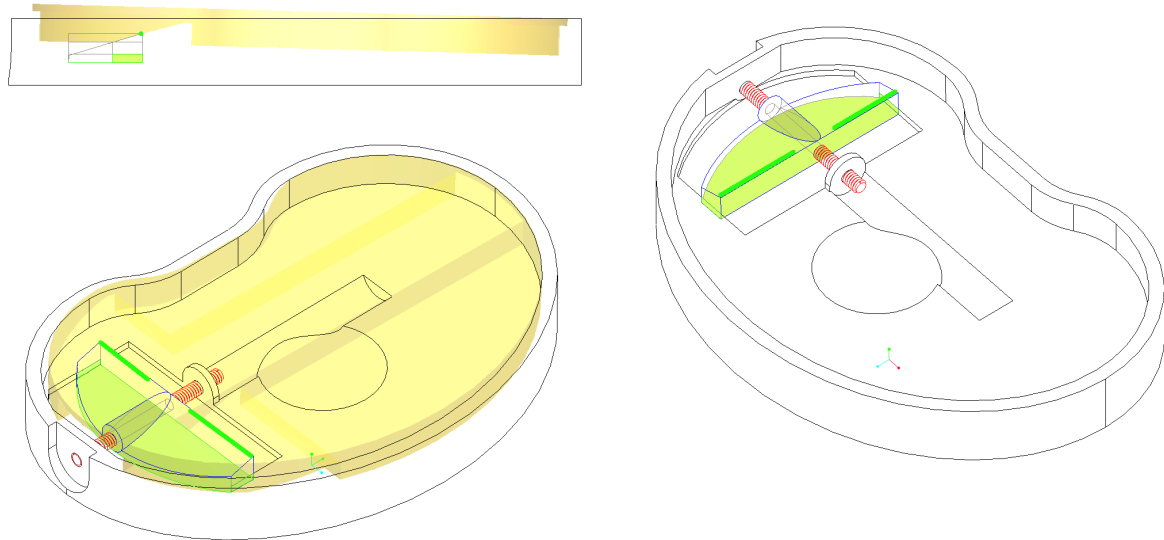


Figure 4.11 – the contact areas (green) among system components during actuation

When trying to determine the total actuation force that needs to be applied onto the wedge blunt end to achieve the required actuation, the friction effects that take place between the moving surfaces of the system components cannot be neglected. Intuitively, friction opposes the wedge translation and increases the effort that has to be made to generate motion inside the prosthesis. Friction forces do not depend on the extent of the contact areas [110], which incidentally, in the case of the proposed actuation system, have complex profiles; moreover, the contact line between the wedge and the mobile tibial tray varies in length with the two components relative position. Consequently, it is difficult to evaluate the entity of friction losses by means of direct computation. A possible solution to this problem consists in approximating the actuation system working principle with an already existing model. As previously mentioned, a wedge is most commonly used to lift up an object (Fig. 4.12); the input force to be applied onto the wedge blunt end is a function of the weight of the object, the wedge shape and the friction coefficients between the two rigid bodies and the ground. Table 4.2 defines the terms of the lifting wedge equation, reported here [111]:

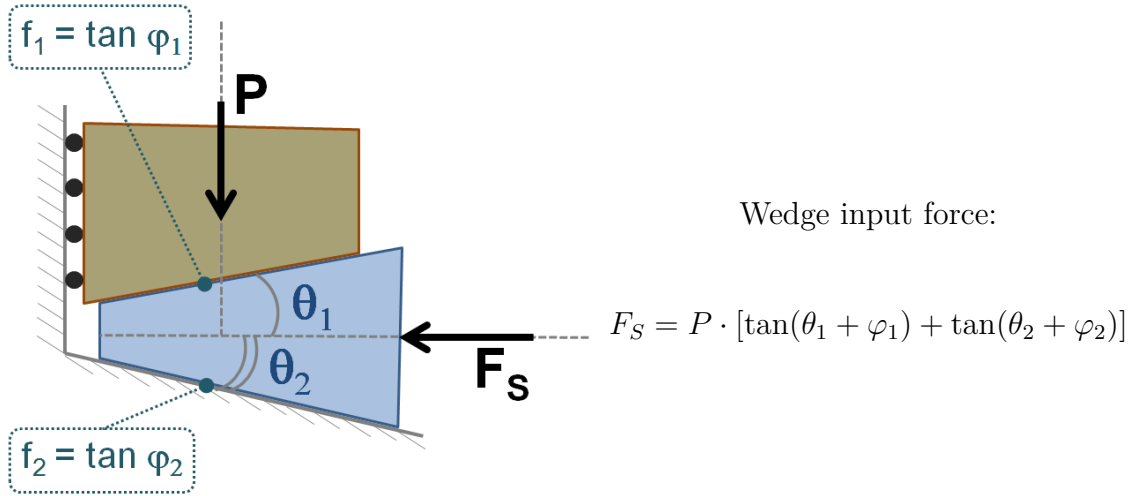


Figure 4.12 – conventional use of a wedge (blue) to lift up an object (brown) [111]

term	type	unit	description
P	force	N	weight of the object to be uplifted
F_S	force	N	wedge input force to be applied to its blunt end
f_1	friction	-	friction coefficient between the wedge and the object
f_2	friction	-	friction coefficient between the wedge and the ground
θ_1, θ_2	angle	deg	angles of the two wedge inclined surfaces

Table 4.2 – terms notation for the lifting wedge equation

In this model, the wedge is pushed by the horizontal input force F_S and translates from right to left; consequently, the object of weight P gets uplifted vertically without changing its orientation. Throughout the entire motion, full surface contact is continuously experienced by the system components at the two interfaces wedge-object and wedge-ground: the friction effects that, according to the material properties, generate in such contact areas play a key role in determining the entity of the input force F_S . Besides the evident similarities between this model and the proposed actuation system (Fig. 4.13), in the latter (as already explained in chapter 4.3.1) the full surface contact between the wedge and the mobile tibial tray is replaced by a line contact (green-coloured in Fig. 4.11). From a practical point of view, it must be considered also that the mobile tibial tray has essentially only one degree of freedom: it is designed so as to be always contained inside the baseplate border and allow only lateral uplift movements. Pushed by the continuous action of tibiofemoral efforts, most likely the mobile tray will infinitesimally adjust its position with respect to the wedge so as

to establish with it the most stable contact possible. Pending experimental verification of this last consideration, the lifting wedge model will be considered here as an effective approximation of the proposed actuation system in order to evaluate to which extent friction losses affect the entity of the required wedge input force. Table 4.3 defines the correspondences among the terms of the two models. Friction coefficients are selected assuming the actuation system components as being made of Titanium Vanadium Alloy (Ti-6Al-4V), a material that is commonly chosen nowadays for knee implants [5].

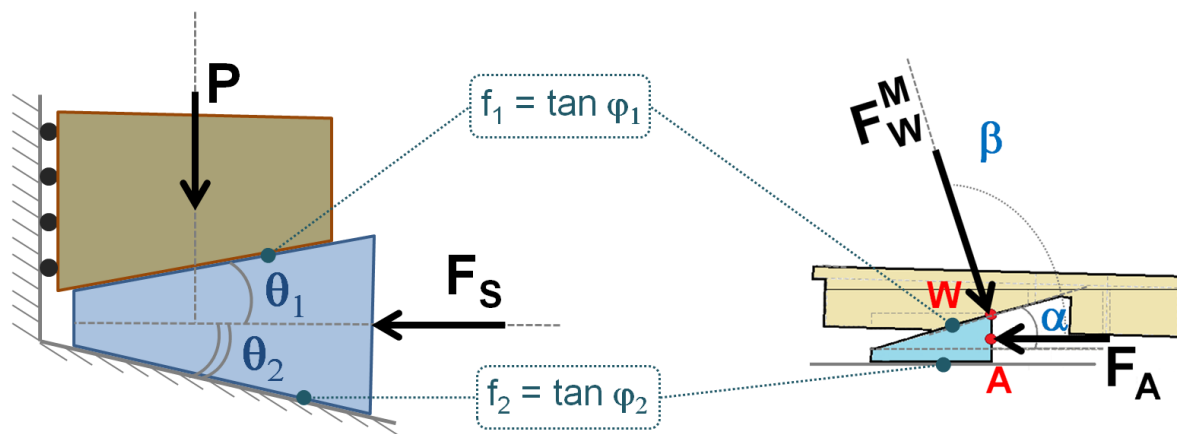


Figure 4.13 – the lifting wedge model (left) approximates the proposed actuation system (right)

LIFTING WEDGE	ACTUATION SYSTEM	value	unit
P	F_W^M	198	N
f_1, f_2	f_1, f_2	0.36	-
θ_1	α	16.7	deg
θ_2	absent	0	deg

Table 4.3 – corresponding terms between the lifting wedge model and the proposed actuation system

The lifting wedge equation computed with the numerical values listed in Table 4.3 results in a wedge input force $F_S \approx 218$ N, which is almost four times greater than the actuation force $F_A = 57$ N that was computed in chapter 4.3.1; such difference is entirely due to the friction effects that take place among the sliding components during actuation. Given the system size and the very limited volume available in the tibial baseplate for embedded components, two hundred Newtons represent unquestionably a huge force to provide. For sake of feasibility, specific design choices have to be made

in order to try to reduce as much as possible the friction losses. It is clear that friction effects cannot be completely zeroed out, but indeed they could be greatly limited by combining the two smart design expedients discussed here.

Anti-friction Coating - In those mechanical applications where lubrication must be achieved without any liquid medium, a common solution consists in resorting to dry lubricants. Basically, fine particles of lubricating pigments are sprayed onto the interested metal surfaces, thus coating them with a very thin film of solid lubricant [112]. The deposited micrometre-thick layer can offer extremely good low-friction and resistance properties; for the proposed actuation system, an anti-friction coating could be put onto all the contact surfaces at the interfaces wedge-baseplate and wedge-mobile tray. Especially in the former, namely the rail grooved inside the tibial baseplate to host the wedge translation, friction losses could be greatly reduced. By way of illustration, the Minilub coating [113] offers a maximum friction coefficient of 0.03, a value which is more than ten times smaller than that of Titanium Vanadium Alloy considered above; the lifting wedge formula applied in this case would result in a wedge input force of approximately 71 N instead of 218 N.

Ball Bearings - Along the lines of the ball and cage assemblies typical of thrust ball bearings, miniaturised balls could be embedded on the wedge contact parts (its bottom surface and upper border) as depicted in Fig. 4.14. Thanks to specific races grooved in the baseplate rail and in the mobile tibial tray, the presence of the ball bearings would not require to increase the components thickness. In general terms, thrust ball bearings are designed to carry large loads while allowing for movement with very little rolling resistance and sliding [114]; for biocompatible applications, *“ceramics can be used in place of steel for ball bearings. Their higher hardness means they are much less susceptible to wear and typically last for triple the lifetime of a steel part. They also deform less under load”* [115] and *“they do not need lubrication to run. Ceramics is non-porous, unlike steel, as a result it is virtually frictionless”* [116]. In the case of the proposed actuation system, the balls number, size and arrangement are to be defined so as to meet the robustness needs (chapter 3.3.3) and to allow theoretically frictionless sliding movements among the system components. By way of illustration, the ball and cage assembly of F3-8M Silicon Nitride Full Ceramic Thrust Ball Bearings [117] contains seven balls of 1 mm diameter each and can support static and dynamic loads of respectively 413 and 695 N.

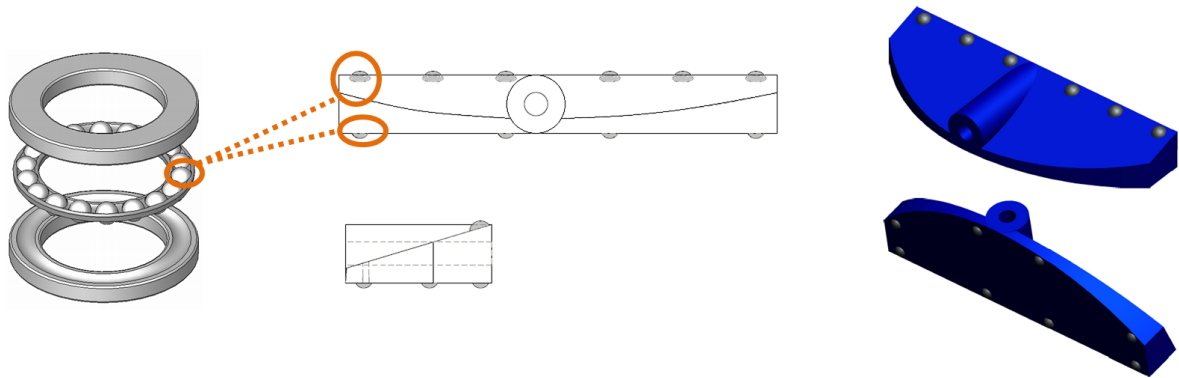


Figure 4.14 – miniaturised balls can be embedded in the wedge in order to minimize friction losses

Having assessed the results of the static force analysis, the value 57 N can reasonably be assumed as the minimum force that needs to be applied to the wedge so as to realise the actuation. Friction losses, which make this value increase, can be minimized by means of ball bearings sliding on surfaces coated with a proper anti-friction material; herein, the force $F_T = 65$ N will be considered as the force to be applied to the wedge to produce its translation and lift the mobile tibial tray up. The most intuitive choice to provide such force would consist in employing a miniaturised linear motor to push the wedge inside its rail; nevertheless, browsing the currently available off-the-shelf solutions, it can be verified that no product meets the needs of the proposed actuation system. Nowadays it does not exist any linear microactuator at the same time sufficiently small to be embedded in the tibial baseplate and able to provide 65 N of force. Again, a smart design expedient needs to be adopted to cope with such technological limitation; the choice of employing a leadscrew is made in this regard.

4.3.3 Screw Force

As already mentioned in chapter 4.1, the wedge is coupled to a leadscrew via a threaded hole (standard M2x0.4 profile). Specific supports keep the leadscrew in place while allowing its free rotation; according to the thread pitch (0.4 mm), any leadscrew revolution produces a corresponding lateral translation of the wedge, whose total stroke is 10 mm (25 complete leadscrew revolutions) as depicted in Fig. 4.15.

The medial end of the leadscrew is supposed to be rigidly fixed to the shaft of a rotary stepper micromotor embedded in the tibial baseplate. The force developed by the wedge during its translation will depend on the torque applied onto the leadscrew by the microactuator; in light of the considerations made previously, such translating force must at least equal $F_T = 65$ N in order to realise the desired actuation.

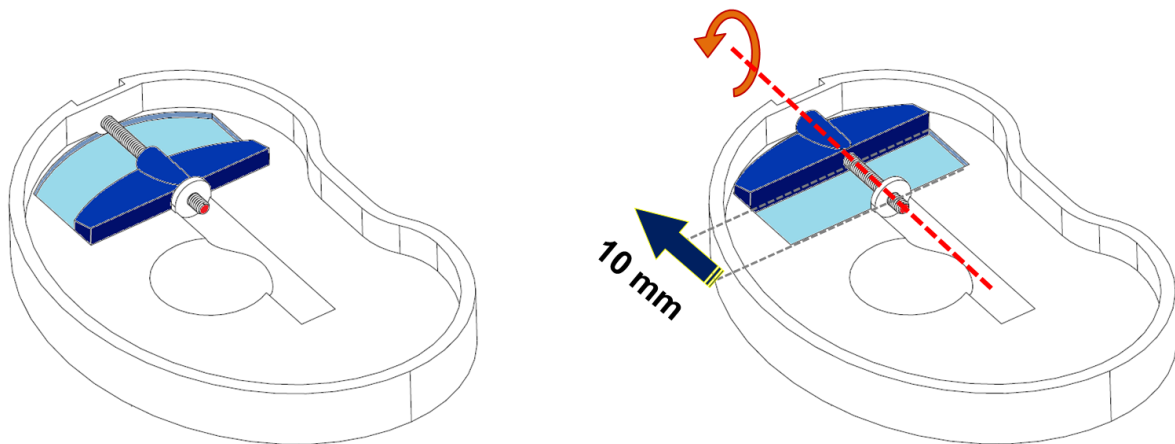
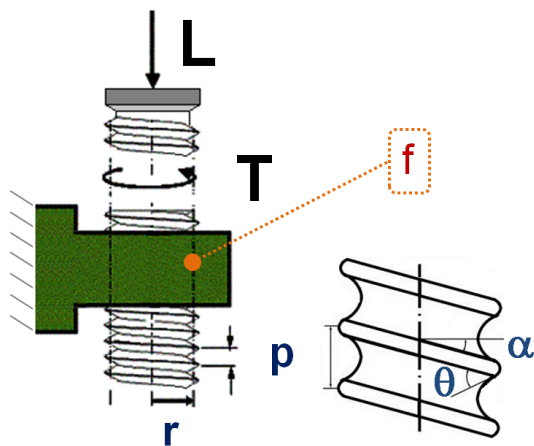


Figure 4.15 – the wedge translation is driven by the leadscrew rotation

Fig. 4.16 shows the case of a standard screw-nut system, where the nut is fixed and the screw rotates and translates; if the screw experiences an axial load L , the torque T needed to unscrew it out of the nut is given by the following equation [111] (the equation terms are described in Table 4.4):



$$T = L \cdot r \cdot \frac{\tan \alpha + f \cdot \lambda}{1 - f \cdot \lambda \cdot \tan \alpha}$$

with:

$$\lambda = \sqrt{1 + \tan^2(\theta/2) \cdot \cos^2(\alpha)}$$

$$\alpha = \arctan\left(\frac{p}{2 \cdot \pi \cdot r}\right)$$

Figure 4.16 – a standard screw-nut system [111]

term	type	unit	description
T	torque	mNm	torque applied to the screw
L	force	N	axial load applied onto the screw
r	distance	mm	screw thread mean radius
f	friction	-	friction coefficient inside the thread
α	angle	deg	thread helix angle
θ	angle	deg	thread profile angle

Table 4.4 – terms notation for the standard screw-nut system equation

Besides taking into account the thread parameters, the screw-nut system equation addresses also the friction effects that take place between the moving parts. This equation can be considered valid also for the proposed WL system: according to the action-reaction principle (Newton's third law), the similarity between the two models is direct if the wedge is considered as a translating nut. Therefore, it is possible to compute the torque T to be applied to the leadscrew in order to produce a wedge translation force F_T , which corresponds to the axial load L to be overcome. The correspondences among the terms of the two models are defined in Table 4.5. Concerning the thread friction coefficient, the worst-case scenario is considered by assuming the WL system as made of Titanium Vanadium Alloy (Ti-6Al-4V).

SCREW-NUT SYSTEM	WL SYSTEM	value	unit
T	torque applied to the leadscrew	unknown	mNm
L	needed wedge translation force F_T	65	N
r	leadscrew thread mean radius	0.87 [108]	mm
f	leadscrew thread friction coefficient	0.36	-
α	leadscrew thread helix angle	4.18 [118]	deg
θ	leadscrew thread profile angle	60 [118]	deg

Table 4.5 – corresponding terms between the screw-nut system and the proposed WL system

The screw-nut system equation computed with the numerical values listed in Table 4.5 results in a torque $T = 28.6$ mNm to be applied to the leadscrew so as to produce a wedge translation force $F_T = 65$ N. Also in this case, friction losses play a key role and may be greatly reduced by coating the threaded profiles of the leadscrew and the wedge with a proper anti-friction material; by way of illustration, the use of the Minilub coating [113] previously mentioned ($f = 0.03$) would allow to obtain the same wedge translation force by applying a torque of only 6.2 mNm. In any case, such torque values can be provided by already existing off-the-shelf solutions; contrary to linear microactuators, rotary micromotors can be employed to drive the actuation system and achieve the mobile tibial tray lateral uplift as required. This choice, in line with the considerations made in chapter 3.4, is discussed in the following in further detail.

4.4 Microactuator Selection

All the computations considered throughout the mechanical analyses described in the previous chapters remain theoretical and should be assessed by means of experimental validation; the values of both the wedge translation force $F_T = 65$ N and the leadscrew torque $T = 28.6$ mNm have been determined relying on the possibility to reduce friction losses among the moving parts. Considering the integration of all the components described so far, as well as the overall system efficiency, the actual operating conditions under which the actuation system works are difficult to predict and, globally, will most likely be more constraining than any a priori evaluation. Consequently, when selecting the microactuator, it may be recommended to consider to over-dimension it as a precautionary measure.

Among the currently available off-the-shelf products, the actuation system requirements are met by the rotary stepper micromotor Faulhaber ADM0620-2R-V2-05 [119]. It occupies a cylindrical volume of 29.6 mm height and 6 mm diameter, therefore it can be easily embedded in the tibial baseplate as depicted in Fig. 4.17. Combined to its integrated planetary gearhead (06/1 K 1024:1 [120]), this microactuator is able to provide up to 35 mNm intermittent torque. By way of illustration, such torque T , reversely used in the screw-nut formula (chapter 4.3.3, Table 4.5), would theoretically produce a wedge translation force $F_T = 79.5$ N. The standard gearhead shaft (1.6 mm diameter) has to be customised in order to be rigidly fixed to the medial leadscrew end. The microactuator wireless power supply and control are supposed to be achieved by means of respectively inductive coupling (already discussed in chapter 3.3.4) and radiofrequency techniques.

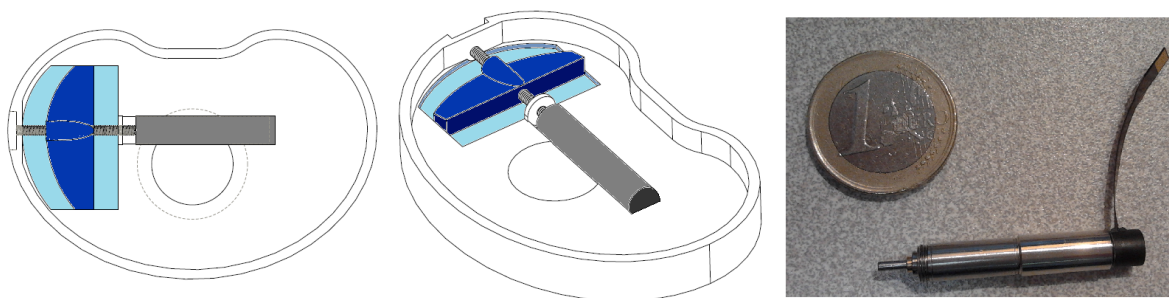


Figure 4.17 – the micromotor (grey) is embedded in the tibial baseplate [119, 120]

4.5 Discussion

This chapter covers a set of important issues about the overall feasibility of the instrumented tibial component proposed in this work. The passive locking system necessary to keep the mobile tibial tray laterally uplifted after actuation is described first. The high accuracy provided by the WL system is then discussed. Some interesting considerations are made about the sealing of the actuation system components and their scaling for knee implants of different size.

4.5.1 Locking Issue

The actuation procedure is carried out with the patient in lying position, so as to cope only with the collateral ligaments passive force; once optimal balance conditions have been restored, the patient is supposed to live a normal life without experiencing any remarkable limitation caused by the presence of the implanted prosthesis. This can be guaranteed only by a robust and durable locking system provided by the instrumented implant, able to keep the mobile tibial tray in the uplifted position. As already anticipated in chapter 3.3.3, the peak tibiofemoral forces acting inside the KJ during daily life activities can be more than four times the patient's BW. In a prosthetic knee, the implant components ceaselessly undergo very strong cyclic efforts; especially the tibial platform, which is the load-bearing surface of the prosthetic articulation, is continuously subjected to repeated vibrations, compression loads and shear forces. To evaluate the order of magnitude of the efforts that generate among the actuation system components under normal working conditions, the static force analysis presented in chapter 4.3.1 can be carried out again by considering the compression load F_L distributed on the mobile tibial tray upper surface as being the 2600 N peak tibiofemoral force acting inside the prosthetic knee during normal gait cycle [90]. Due to the components design, any tibiofemoral effort gives rise to the three main reaction forces depicted in Fig. 4.18 (values are defined in Table 4.6):

- F_B^M exerted by the inclined tibial tray onto the baseplate, at the pivot point on the non-actuated side;
- R_B^W exerted vertically by the wedge onto the baseplate, inside the translation rail;
- F_A^W exerted horizontally by the wedge, along the actuated leadscrew axis.

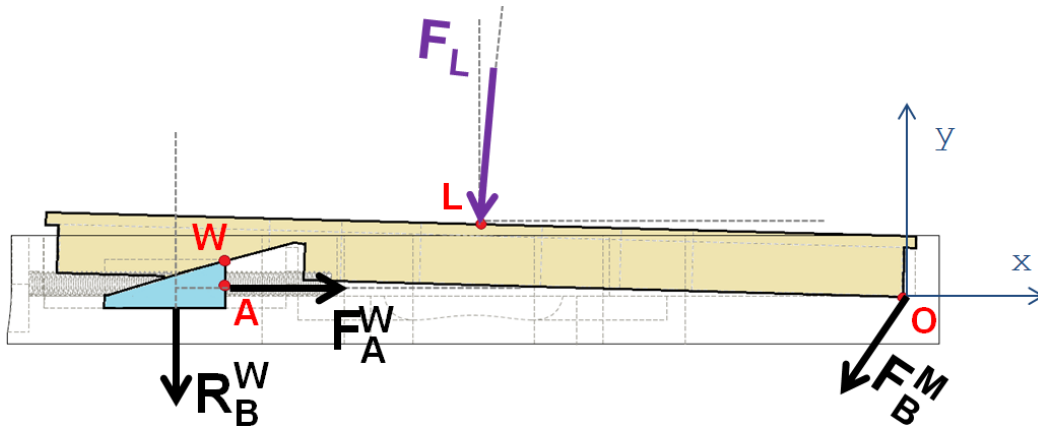


Figure 4.18 – the locking system copes with three main forces (black)

ACTUATION PROCESS	LOCKING SYSTEM
$F_L = 300 \text{ N}$	$F_L = 2600 \text{ N}$
$\ F_B\ \approx 124 \text{ N}$	$\ F_B^M\ \approx 1075 \text{ N}$
$\ R\ \approx 190 \text{ N}$	$\ R_B^W\ \approx 1647 \text{ N}$
$\ F_A\ \approx 57 \text{ N}$	$\ F_A^W\ \approx 494 \text{ N}$

Table 4.6 – the locking system experiences higher reaction forces

The terms F_B^M and R_B^W represent two compression forces that get transmitted to the tibial baseplate, which is rigidly fixed onto the tibial bone; considering the great robustness properties of the selected Titanium Vanadium Alloy, namely its bearing and compressive yield strengths (respectively 1790 and 1070 MPa [121]), no material deformation should take place. On the other hand, the horizontal force F_A^W is the term that most should be given consideration while discussing the locking issue; the compression loads that get transmitted via the inclined mobile tray to the wedge try to push the latter back to its starting position. Because of the threaded profile, the force F_A^W acts along the leadscrew axis and pushes the whole WL system towards the center of the tibial baseplate. As already discussed in chapter 4.2.1, the leadscrew is held in place by specific supports and the WL system is designed to be mechanically irreversible: the wedge translation cannot produce the leadscrew revolution (which, indeed, can take place in both senses of rotation when driven by the microactuator). Moreover, the motor stall torque contributes to preventing any undesired motion. It follows that impeding any leadscrew axial translation movement should be enough to maintain the actuated wedge position and, consequently, the corresponding tibial tray lateral uplift.

In addition to the considerations made above, a further constraint is imposed by the necessity not to damage the micromotor responsible for the actuation: its shaft, which is rigidly fixed to the leadscrew, can bear axial loads only up to 5 N [120]. It is therefore evident that the force F_A^W must be neutralized in order not to put the microactuator out of order. To this purpose, two miniature thrust ball bearings can be embedded in both the supports that hold the two leadscrew ends, as depicted in Fig. 4.19; besides allowing free and practically frictionless leadscrew revolution movements, the combined action of the two bearings would essentially absorb any axial load experienced by the WL system.

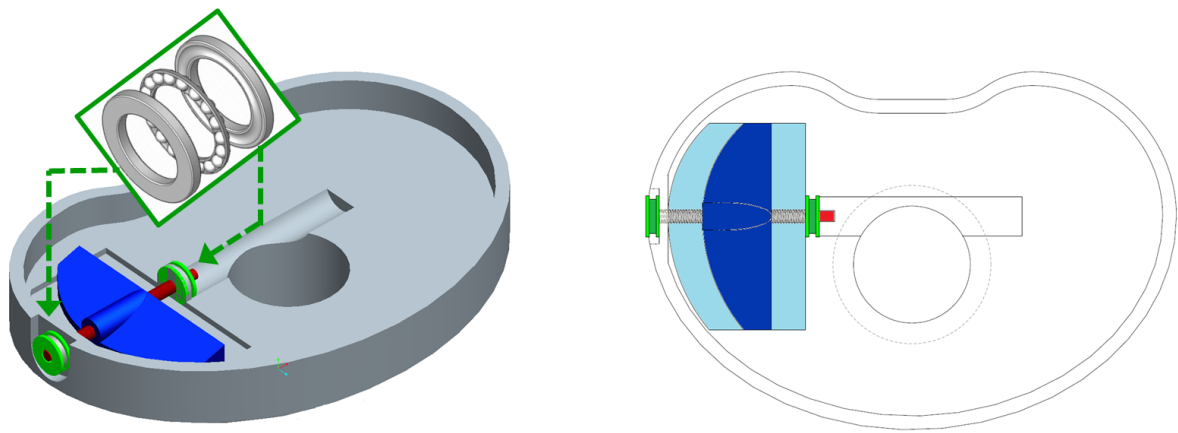


Figure 4.19 – two miniature thrust ball bearings (green) support the two leadscrew ends

If properly assembled, the two miniature bearings would protect the microactuator shaft from any damage. Browsing the currently available off-the-shelf products, it turns out that F2-6M [122] and F3-8M [123] thrust steel ball bearings can bear respectively 117 and 993 N dynamic loads; in this current application, a custom-designed version (intermediate between the two aforementioned models) will have to be manufactured so as to join a tiny size (6 mm maximum outer diameter) to a load rating at least equal to the force $F_A^W = 494$ N previously estimated. Also in this case, over-dimensioning is recommended and the use of ceramic balls instead of steel ones should be considered to further improve the system robustness properties.

In terms of solidity of the WL system threaded profile, there is no risk of failure: the ultimate yielding loads of a standard M2x0.4 steel thread (property class 8.8) are 1330 and 800 N respectively for axial and shear stresses [124, 125], two values which provide a considerably large margin of safety with respect to the axial force F_A^W considered above. Furthermore, titanium (and titanium alloy) threads are even stronger and lighter than steel ones [121, 126, 127], thus ensuring better robustness properties.

In the final analysis, the proposed design provides a passive locking system a priori reliable and very robust. Once the actuation has been completed, the corresponding profiles of the mobile tibial tray and the baseplate prevent any undesired relative movement between the two components; the tray stability is guaranteed by its contact line with the actuated wedge and its support point on the non-actuated side. A key role is played by the two miniature thrust ball bearings embedded in the leadscrew supports: thanks to them, as discussed above, the microactuator does not undergo the strong tibiofemoral efforts and is not involved in locking the mobile platform in the desired uplifted position. This aspect should also guarantee great lifespan conditions of the whole actuation system.

4.5.2 Fine-Tuning Actuation

The mobile tibial tray lateral uplift ranges between 0 and 3.6 mm; the wedge translation inside the tibial baseplate has a total stroke of 10 mm. These two quantities are related by the linear relationship described below and depicted in Fig. 4.20:

$$\text{Tray Uplift} = \frac{3.6}{10} \cdot \text{Wedge Translation}$$

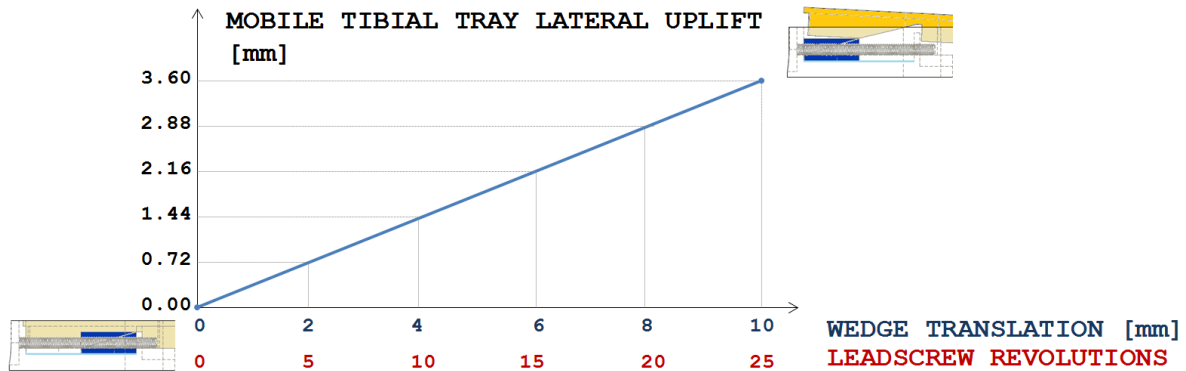


Figure 4.20 – the mobile tibial tray lateral uplift linearly depends on the wedge translation

As already mentioned in chapter 4.3.3, 25 leadscrew revolutions are needed to entirely cover the 10 mm wedge stroke and achieve a condition of full actuation; one complete leadscrew revolution makes the wedge laterally translate of 0.4 mm (the thread pitch) and results in a corresponding mobile tibial tray uplift of $\frac{3.6}{25} = 0.144$ mm. All these values have been verified on the 3D CAD model of the proposed instrumented tibial component. Considering that the selected rotary stepper micromotor [119] provides 20 steps per revolution, the actuation process proposed in chapter 3.1

can be actually carried out with submillimetre accuracy. This achievement satisfies the accuracy requirement defined in chapter 3.3.2.

4.5.3 Materials and Sealing

In the previous chapters, all the prosthetic components and the actuation system mechanical parts have been assumed to be made of Titanium Vanadium Alloy (Ti-6Al-4V), a material that is commonly chosen nowadays for knee implants [5] because of its excellent biocompatibility “*especially when direct contact with tissue or bone is required. Ti-6Al-4V’s poor shear strength makes it undesirable for bone screws or plates. It also has poor surface wear properties and tends to seize when in sliding contact with itself and other metals. Surface treatments such as nitriding and oxidizing can improve the surface wear properties*” [121]. These last considerations further endorse the effectiveness of the anti-friction coating treatment already proposed in chapter 4.3.2.

The design must guarantee also the sealing of the embedded actuation system. The miniaturised mechanical and electronics components should be prevented from entering in contact with the physiological fluids that bath the knee articulation, which might fill the very thin spacing that generates between the mobile tibial tray and the baseplate during the actuation process. A possible solution to this problem could be represented by employing an elastic micro-membrane, properly folded in an accordion-like fashion between the mobile tibial tray lateral edges and the baseplate internal ones (Fig. 4.21). Such membrane could passively follow the mobile tray lateral uplift and create a sort of sealed volume for the embedded components. The membrane material has to be selected in order to ensure excellent biocompatibility and resistance properties, so as to minimize the risk of failure. Additionally, as a precautionary measure, the microactuators and their related electronics could be properly arranged in specific casings treated with a biocompatible coating material.



Figure 4.21 – the elastic micro-membrane employed for the actuation system components sealing

4.5.4 Actuation System Scaling

The tibial baseplate actually embeds two identical actuation systems, each one responsible for the mobile tibial tray lateral uplift on one side; as shown in Fig. 4.22, two symmetrical WL systems can be positioned at the same time inside the baseplate if a 6 mm distance is kept between the two leadscrews axes. With respect to the design presented in chapter 4.2.1, the presence of two wedges at the same time implies for each of them a 3 mm shift of the threaded hole in the AP direction; this change does not affect neither the actuation system operating conditions, nor the validity of all the explanations and analyses discussed so far.

A more delicate issue concerns the actuation system scaling for knee implants of different size. As mentioned in chapter 3.2, the actuation system presented here has been dimensioned for a Size 6 knee prosthesis [86]. In the case of smaller or bigger tibial components, besides scaling each system component down or up, the mechanical analysis presented in chapter 4.3 should be entirely carried out again so as to discuss and assess the overall system feasibility in each specific case. A priori, a major limitation might be represented by the microactuator selection: contrarily to the mechanical components dimensions, which can be customised according to the design needs, micro-motors of different size might not meet the torque requirements or, even worse, might not be available on the market. In these terms, the overall system feasibility goes along with and depends on technological advancements.

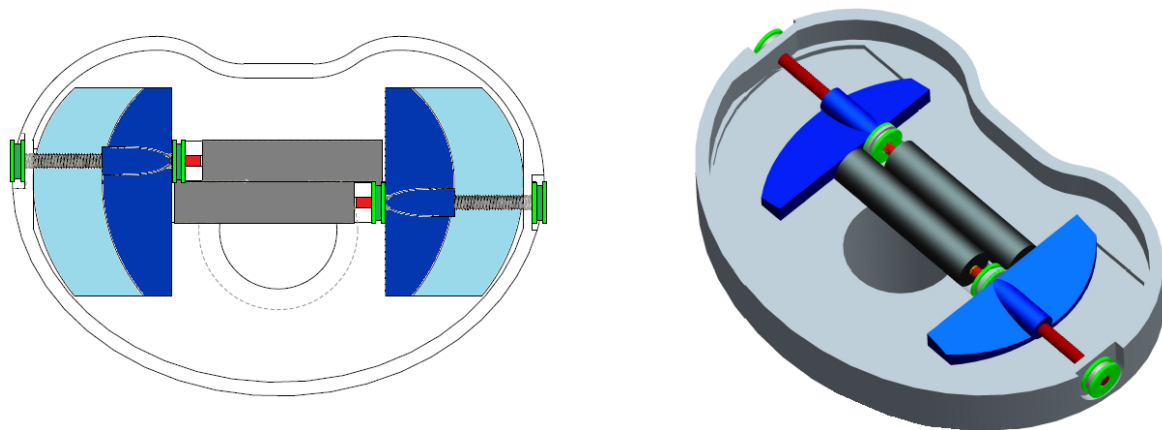


Figure 4.22 – two identical actuation systems are embedded inside the tibial baseplate

Experimental validation is a key step to assess the validity of the mechanical analysis results (chapter 4.3) and of the considerations relating thereto. In this work, at an early stage, simulations carried out on the 3D model of the proposed implant allowed to detect potential design flaws, perform useful optimisations and evaluate the components robustness properties. In order to test the actuation system performances under normal working conditions, the successive step consisted in fabricating a full-scale prototype of the instrumented tibial component and testing it on a knee simulator. As discussed in the following, the very promising results of the experimental validation stage also provided precious indications for future studies and improvements.

5.1 3D Model Simulations

5.1.1 Static Analyses

The 3D model of the proposed tibial implant was evaluated by means of static analyses. The system was considered in a configuration of full actuation on one side of the tibial baseplate (10 mm wedge translation, 3.6 mm mobile tibial tray lateral uplift). A compression load $L = 2600$ N was defined perpendicularly to the mobile tibial tray upper surface, reproducing the peak tibiofemoral force acting inside the prosthetic KJ during normal gait cycle [90]. The selected components material was Titanium Vanadium Alloy (Ti-6Al-4V, mesh elements parameters: max aspect ratio = 5, allowable angles range = 15–165 degrees). The following two measures were considered to evaluate the results of the static analyses:

- the distribution of Von Mises Stress (VMS), a scalar value (unit: MPa) commonly used to predict yielding of materials under any user-defined loading condition [128];

- the deformation of the mobile tibial tray (unit: mm) under the effect of the aforementioned compression load L .

Fig. 5.1 shows the distribution of VMS computed by the first static analysis carried out on the proposed instrumented tibial component. As expected, VMS were more concentrated in the regions where the mobile tibial tray thickness is reduced by the different cuts made to fit the presence of the two actuation systems. In particular, higher VMS occurred along the sharp edges of the ML cut necessary to host the two microactuators embedded in the tibial baseplate (red-coloured in Fig. 5.1).

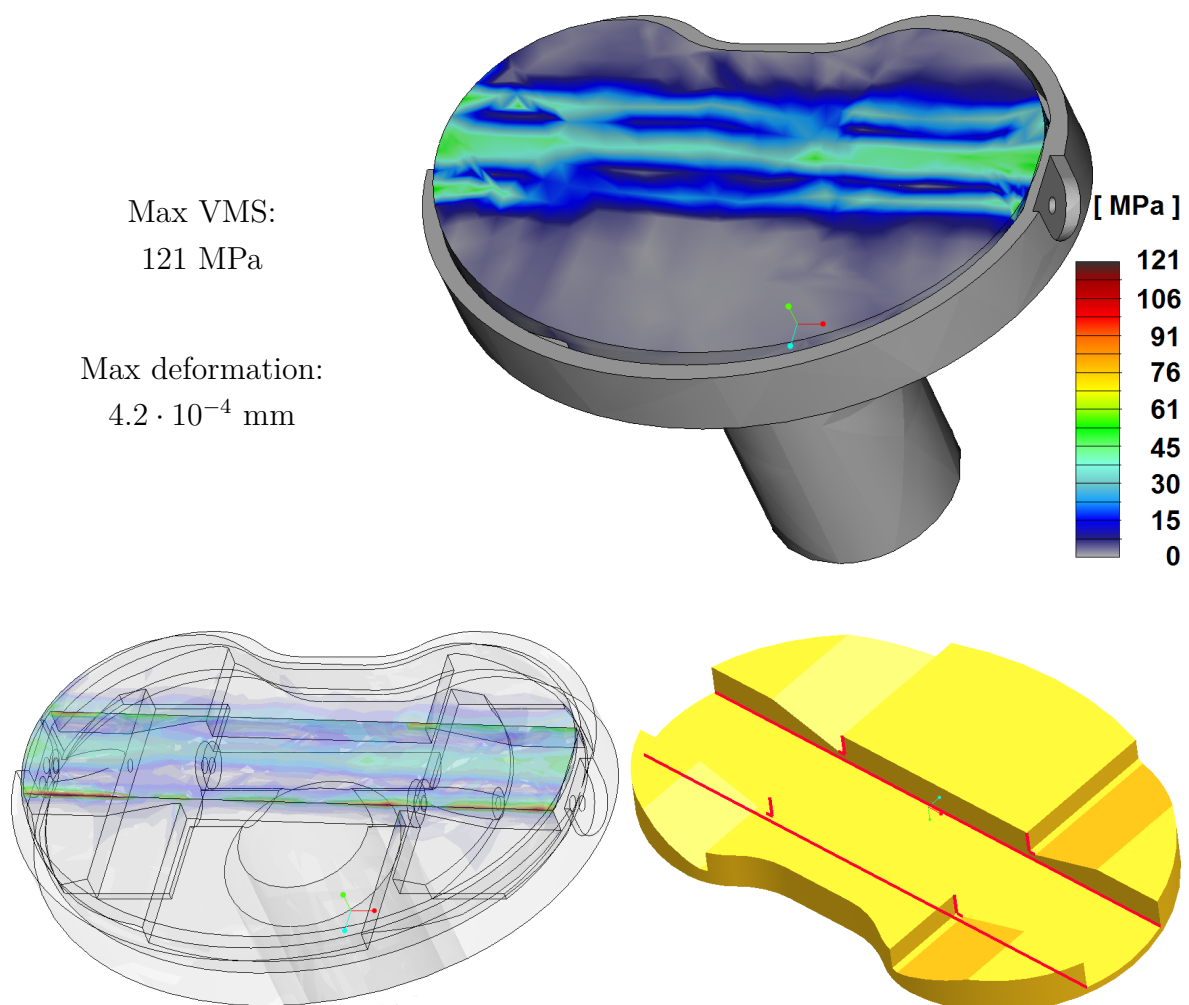


Figure 5.1 – the first static analysis results

As previously mentioned, the selected Titanium Vanadium Alloy offers a compressive yield strength of 1070 MPa [121]. Such value, being almost nine time greater than the maximum VMS computed by the static analysis (121 MPa), was considered to give a very reliable margin of safety; furthermore, since the maximum material deformation

was estimated to be on the order of half a micrometre, it was concluded that the risk of failure of the mobile tibial tray was not a major concern. However, the stress distribution can be further improved by means of the two expedients proposed hereafter and depicted in Fig. 5.2 ; due to the volume constraint (chapter 3.3.1), the necessity not to further increase the tibial platform overall thickness and the presence of the actuation system embedded components, any design adjustment can be applied only locally.

Thickness Increase - The quantity of volume removed by the cuts can be minimized by locally increasing the mobile tibial tray thickness where possible. The medial and lateral edges of the tray can be thickened by 1 mm (green-coloured in Fig. 5.2) while still fitting the presence of the leadscrews. This should strengthen the tray borders and reduce the risk of deformation.

Filleted Edges - The sharp edges of the mobile tibial tray bottom surface, along which VMS concentration is expected to be higher, can be smoothed by means of a fillet (pink-coloured in Fig. 5.2). The choice between a rounded and a chamfer profile is arbitrary, but the former normally gives lower concentration factors and improves the quality of stress distribution [128]. Due to the presence of the two micromotors, the maximum radius applicable to round the ML cut edges is 3 mm; on the other hand, the edges of the two AP cuts made to host the two wedges can be rounded off at most up to 1 mm.

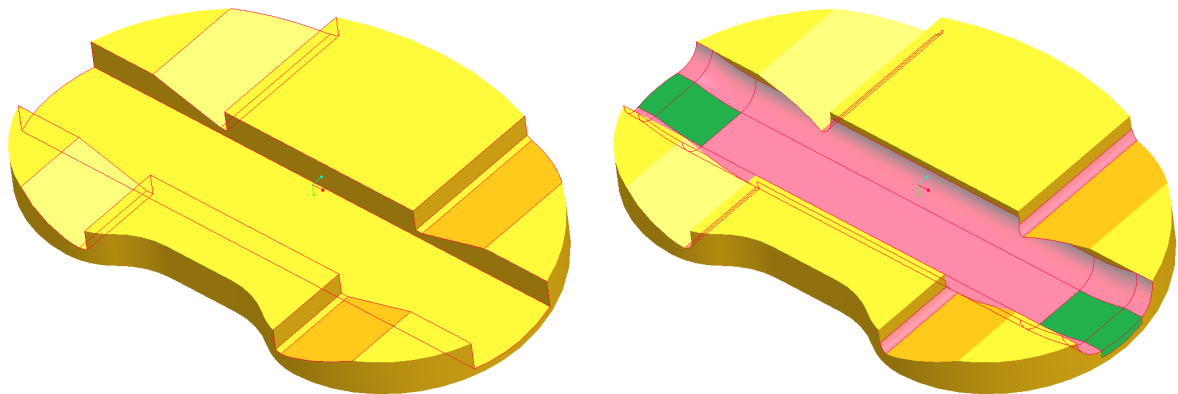


Figure 5.2 – the stress distribution on the mobile tibial tray can be improved by means of smart design adjustments

The optimal rounding radii to be applied to the considered sharp edges were determined by means of an optimisation study. It turned out that, in order for the maximum VMS value to be minimized, the filleting should be as much significant as possible: the sharp edges should be rounded off by 3 and 1 mm respectively for the ML cut and the wedges AP grooves. Such result was accepted as consistent with the criterion of

reinforcing the mobile tibial tray as much as possible; the opportunity to round off other minor edges was considered and quickly explored, but turned out not to give any significant improvement in the distribution of the VMS experienced by the implant. Thereafter, the static analysis previously defined was carried out again, with the mobile tibial tray optimised according to the considerations made above; results are shown in Fig. 5.3, while the main optimisation steps are summarized in Table 5.1.

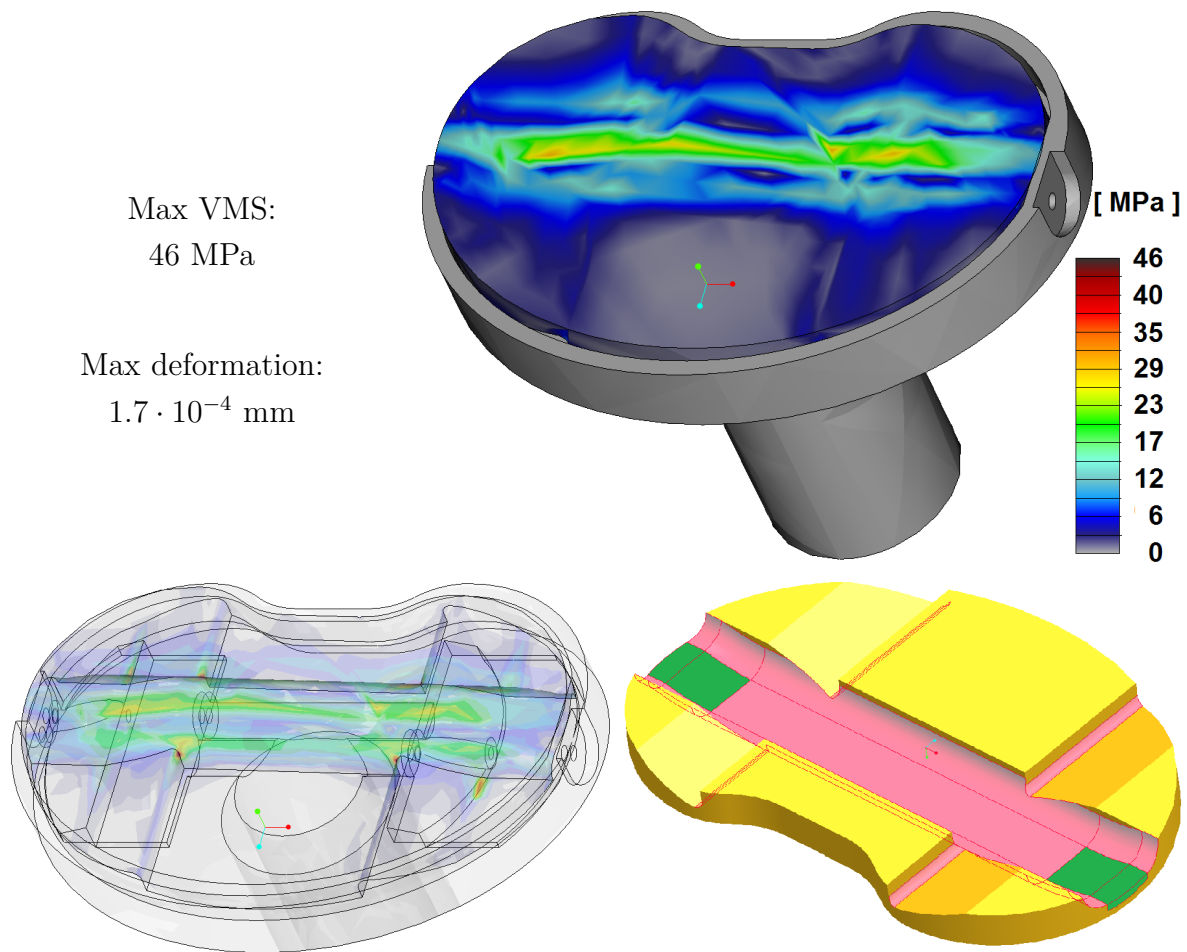


Figure 5.3 – the static analysis results after the optimisation study

measure	1 st static analysis	increased thickness	1 mm fillet (ML)	2 mm fillet (ML)	3 mm fillet (ML)
Max VMS [MPa]	121	98	71	81	46
Max deformation [mm]	$4.2 \cdot 10^{-4}$	$5.2 \cdot 10^{-4}$	$3.6 \cdot 10^{-4}$	$2.8 \cdot 10^{-4}$	$1.7 \cdot 10^{-4}$

Table 5.1 – the main optimisation steps

The design changes introduced by the optimisation study further improved the margin of safety in terms of material robustness. With respect to the first static analysis, besides a more uniform stress distribution of the load $L = 2600$ N onto the mobile tibial tray, the computed values of the maximum VMS and deformation were both reduced by a factor of 2.5. A particularly interesting achievement was the fact that, after the design optimisation, the estimated maximum VMS (46 MPa) turned out to be more than 23 times lower than the limit represented by the Titanium Vanadium Alloy compressive yield strength (1070 MPa [121]). The implant great robustness properties got further endorsed by means of buckling and fatigue analyses.

Buckling Analysis - The mobile tibial tray, laterally uplifted after full actuation, was estimated to be capable of withstanding a maximum load of $1.976 \cdot 10^6$ N (uniformly distributed on its surface) before experiencing any permanent deformation. By way of illustration, such tibiofemoral force would be produced by a person weighing about 200000 kg, which is a rather implausible circumstance.

Fatigue Analysis - In order to consider the worst-case postoperative scenario, the force $L = 2600$ N was simulated as an intermittent tibiofemoral load repeatedly exerted onto the mobile tibial tray (1 hertz frequency [90]). The number of repeated loads (cycles) that the implant was able to bear before failure was then studied by means of fatigue analysis; the minimum lifespan of the implant (in fully actuated configuration) was estimated as $1.3 \cdot 10^{18}$ cycles. Taking into account a previous study [129], it had been estimated that “*the number of gait cycles performed by an active patient during 15 years after primary TKA is about $4.7 \cdot 10^7$* ” [81, p. 152]; with respect to such reference value, thus, the instrumented knee implant proposed in this work should offer a $2.7 \cdot 10^{10}$ times longer lifespan.

5.1.2 Remarks

In light of all the considerations made above, it was concluded that no mechanical failure of the mobile tibial tray was likely to occur under normal conditions of use. Concerning the components embedded in the tibial baseplate, which underlie the actuation system working principle, the relative motions among the leadscrew, the wedge and the mobile tibial tray were carefully defined and allowed to assess the validity of the theoretical computations discussed in chapter 4.3.1.

At an early design stage, simulations are commonly accepted as useful tools to quickly compare alternatives, detect potential design flaws and discuss proposed changes. In general terms, results from static analyses should always be integrated by

more exhaustive studies, taking into account, for instance, time-varying loads and less idealised constraints among the system components. In the case of a knee prosthesis, dynamic analyses should therefore be preferred to static ones for the evaluation of the implant behaviour under realistic conditions of use. A major limitation consists in the fact that the KJ dynamics (briefly discussed in chapter 1.1.2) is extremely complex to be finely reproduced in a virtual environment as that of 3D simulations. Since the KJ biomechanics is highly variable among individuals, defining accurately all the prosthetic components interactions in terms of standardised dynamic analysis parameters is a really challenging task; however reliable a knee model may be, it generally includes only the articulation key components (major ligaments, soft tissues and bony structures) and, consequently, offers limited application possibilities [130]. For such reasons, in this work it was established to carry out dynamic analyses by means of a knee simulator rather than resorting to 3D simulations. A knee simulator is a machine especially designed to replicate the KJ motions and physiological environment during simulated daily life activities; orthopaedic implants can therefore be accurately evaluated under conditions that truly replicate those experienced in situ. To this purpose, as presented hereafter, a prototype of the proposed tibial component was manufactured in two successive fabrication steps.

5.2 Prototyping

As already discussed, the proposed instrumented tibial component is meant to include two sub-parts:

- the first one for the evaluation of knee collateral ligaments postoperative laxity conditions, by exploiting four PC elements embedded in the tibial baseplate as both force sensors and energy harvesters [81];
- the second one for restoring optimal balance conditions, by means of a miniaturised actuation system able to laterally lift the tibial tray up on the side corresponding to the lax collateral ligament [106].

It has been clarified that the main goal of this current work consists in proposing and testing the actuation system sub-part; consequently, the fabrication of a prototype did not concern the PC elements sub-part (already extensively discussed in previous studies [75, 76, 77, 80, 104, 105]) but focused on manufacturing the mechanical components that have been described throughout chapter 4.

A first full-scale prototype of the proposed tibial component was initially manufactured by means of a 3D printer, as a simple proof-of-concept of the actuation system working principle. The tibial baseplate, the mobile tray and the wedge were all fabricated as plastic components and assembled together (Fig. 5.4). The actuation, performed manually, allowed to assess the effectiveness of the proposed design and confirmed the 3.6 mm tray lateral uplift corresponding to the maximum wedge translation (10 mm).



Figure 5.4 – the 3D-printed plastic prototype

Thereafter, the components of the proposed implant were manufactured as full-scale steel mechanical parts (Fig. 5.5) and assembled (Fig. 5.6). The design guidelines and components dimensions presented in chapter 4.2 were followed; for ease of manufacture, a few minor design changes were adopted (summarized in Table 5.2).

component	fabrication changes
Wedge	<ul style="list-style-type: none"> • absence of the ball bearings proposed in chapter 4.3.2
Tibial Baseplate	<ul style="list-style-type: none"> • rail for wedge translation grooved only on one side • longer groove for micromotor (for further development)
Mobile Tray	<ul style="list-style-type: none"> • additional cuts on the non-actuated side

Table 5.2 – the minor design changes considered for the components manufacturing

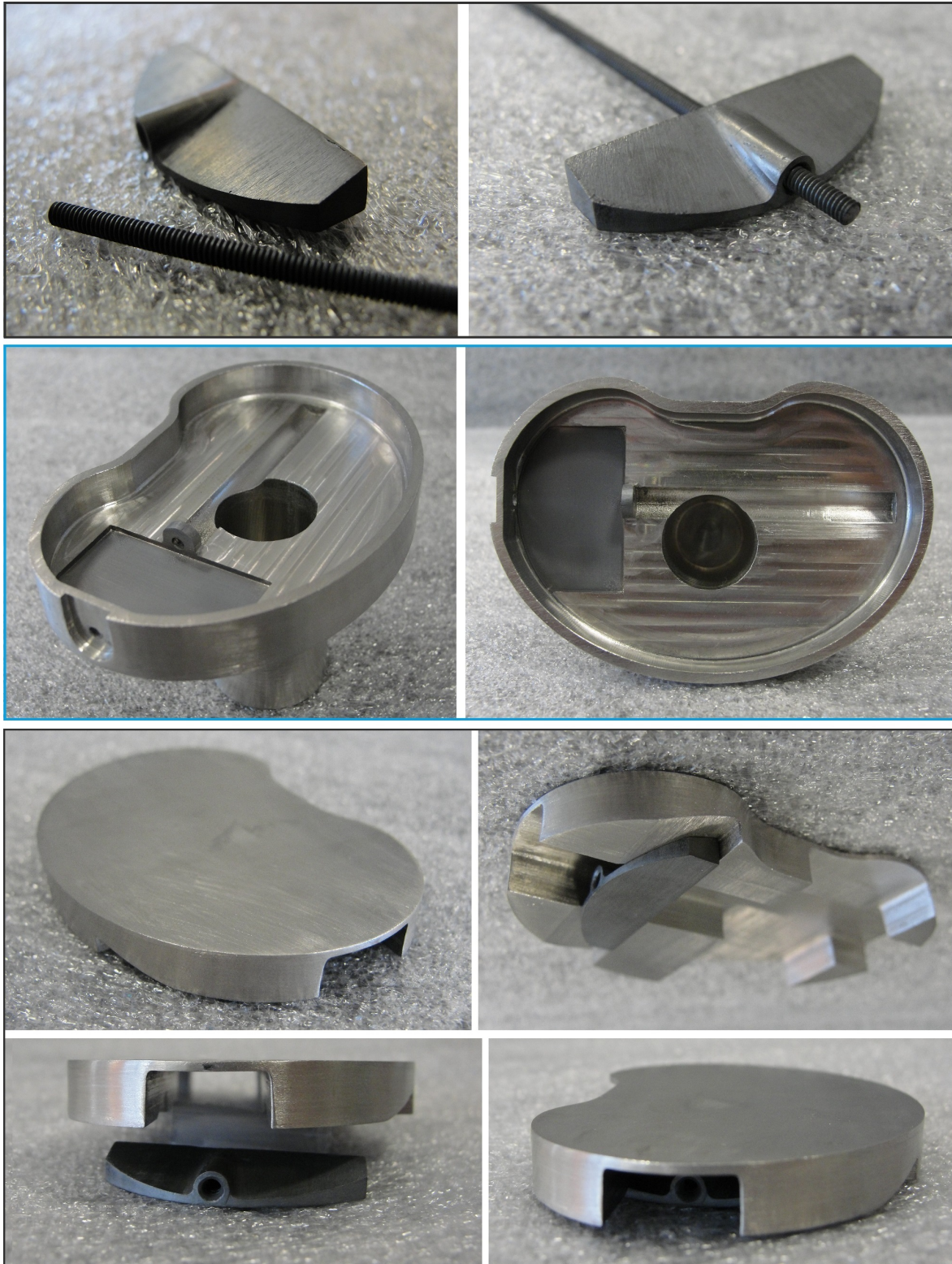


Figure 5.5 – the steel components of the proposed implant



Figure 5.6 – the manufactured components assembled all together

According to the locking issue considerations made in chapter 4.5.1, two miniature thrust steel ball bearings (F2-6M [122]) were positioned at the two leadscrew ends. The WL system was properly fastened by means of thin hexagonal M2 nuts, which in the final design of the proposed knee implant are supposed to be replaced by less bulky supports, specifically manufactured to be compact and sound at the same time. Due to the absence of the wedge ball bearings (proposed in chapter 4.3.2 so as to minimize friction losses), the steel prototype was intended to be manually actuated, thus deferring the implementation of the selected microactuator (chapter 4.4) to a later stage. A PE insert of the proper size was centred onto the mobile tibial tray upper surface and stuck to it by means of a very strong double-sided adhesive tape.

5.3 Knee Simulator

The knee simulator employed in this work is the ADL-Force 5 Simulator, “a servo-hydraulic machine with four independent actuators. It provides a vertical tension and compression axis with rotation about the same axis, and a horizontal axis with translation and rotation. With these actuators the machine can be used for many different independent or combined motions. The Force 5 is supplied with an easily adjustable load frame crosshead making it suitable for a variety of single and multi-axis materials testing applications” [131, p. 5].

As anticipated, the KJ motions and physiological environment associated with daily life activities can be accurately replicated for the evaluation of orthopaedic implants; the wide variety of experimental tests that can be run with such machine faces with the fact that, in this work, the prototype parts are all made of steel. The material choice, made for ease of manufacture, affects the experimental validation stage in the sense that it obliges to select those tests which can give significant results and to discard the less appreciable ones; by way of illustration, it would be of little significance to carry out fatigue tests on components which are not made of the same titanium alloy that will be used for the final version of the knee implant.

5.4 Stability Tests

In view of the considerations made in the previous chapter, specific tests were defined in order to evaluate the stability of the mobile tibial tray during repeated gait cycles and under different conditions of use. Such kind of analysis is independent of the prototype material and is critical for the definitive validation of the proposed actuation system working principle.

5.4.1 Experimental Protocol

The knee simulator features a wide range of motion and can accurately reproduce the four main DoF of the KJ, already discussed in chapter 1.1.2 and briefly reported hereafter for sake of clarity [11]:

FE: the characterizing movement during gait dynamics, the rotation of the tibia with respect to the femur about the knee ML axis, from 0 degrees (complete extension, aligned femur and tibia) to 135 degrees (complete flexion);

IER: rotation of the tibia with respect to the femur about the tibial axis, free during FE movements (except for the cases of complete flexion and complete extension) in the ranges 0-20 and 0-30 degrees respectively for internal and external rotation;

APD: slight translation (2-3 mm) of the tibia with respect to the femur along the knee AP axis;

VVR: rotation of the leg segments about the knee AP axis, it strictly depends on the laxity and passive stiffness properties of the two collateral ligaments.

By default, the whole FE RoM is fully taken into account by the knee simulator while replicating gait cycles. Regarding variations in VVR, it was planned to address the issue of KJ balance conditions more specifically at a subsequent experimental stage. Therefore, for the evaluation of the mobile tibial tray stability, it was decided to study the variations in IER and APD values according to the following steps:

- (i) Before starting any test, the knee simulator was calibrated following the instructions provided by the manufacturer.
- (ii) The instrumented tibial component was manually set in its starting position (null actuation: 0 mm mobile tibial tray lateral uplift).
- (iii) The orientation of the implant on the machine was set in order to have full contact between the PE insert and the femoral component (fixed above the tibial baseplate, onto a dedicated holding arm): such position was saved as Zero Position (ZP) and considered as a reference configuration.
- (iv) The knee simulator was put into operation to simulate 500 successive gait cycles.
- (v) Via the knee simulator control panel, the IER value was manually changed to 15 degrees internal rotation and 500 gait cycles were reproduced.
- (vi) The IER value was set to 15 degrees external rotation and 500 gait cycles were replicated.
- (vii) The tibial component was oriented again in ZP and subjected to 500 gait cycles.
- (viii) The APD value was manually changed to 2 mm anterior translation and 500 gait cycles were simulated.
- (ix) The APD value was manually changed to 2 mm posterior translation and 500 gait cycles were reproduced.
- (x) The instrumented tibial component was manually actuated so as to produce a mobile tibial tray lateral uplift of 1.8 mm. Steps (iii) to (ix) were repeated.
- (xi) The mobile tibial tray lateral uplift was manually set to 3.6 mm (full actuation condition). Steps (iii) to (ix) were repeated.

Table 5.3 summarizes the steps of the stability tests. Fig. 5.7 depicts the variations in the IER and APD settings. The starting ZP configuration of the prosthesis on the knee simulator (step (iii)) is shown in Fig. 5.8.

(step)	IER ref.: 0-20 deg I, 0-30 deg E			APD ref.: 2-3 mm AP		
	ZP (iii , iv)	15 deg I (v)	15 deg E (vi)	ZP (vii)	2 mm A (viii)	2 mm P (ix)
0 mm tray uplift	✓	✓	✓	✓	✓	✓
1.8 mm tray uplift	✓	✓	✓	✓	✓	✓
3.6 mm tray uplift	✓	✓	✓	✓	✓	✓

Table 5.3 – the mobile tibial tray was assessed as stable (✓) in 15 different configurations

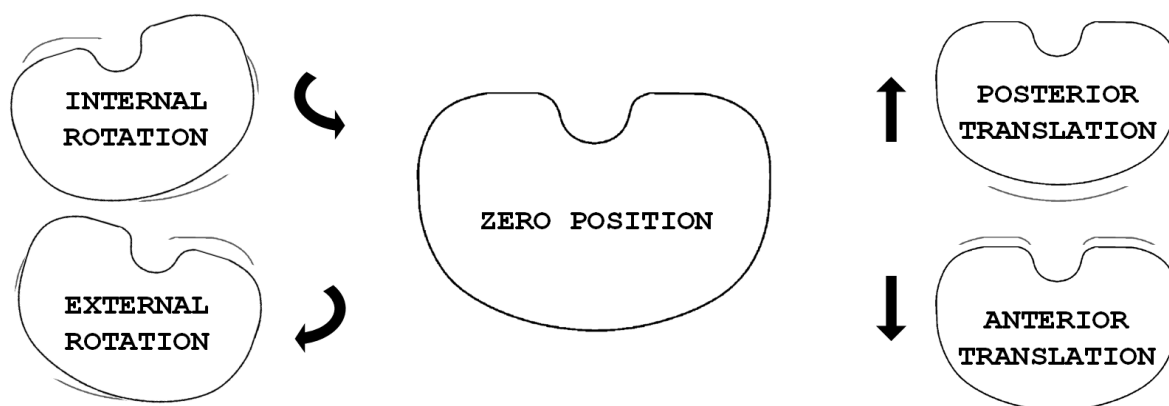


Figure 5.7 – the variations in the IER and APD settings

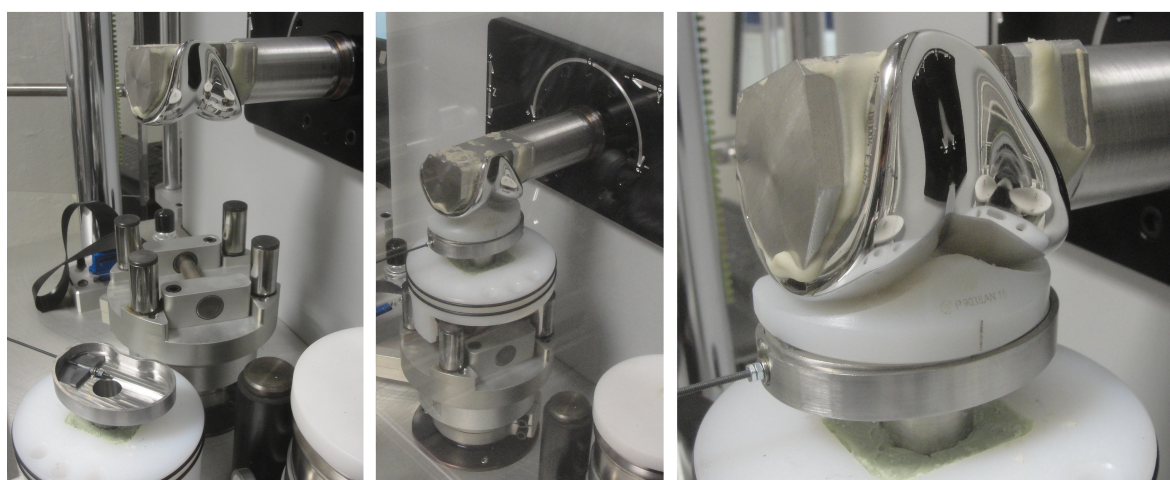


Figure 5.8 – the prototype installed on the knee simulator in ZP configuration

5.4.2 Results

During the experimental stage described above, the prototype underwent a total of $9 \cdot 10^3$ gait cycles (2600 N peak tibiofemoral load, 1 s walking cycle [90]) equally distributed among three distinct actuation cases (null, intermediate and full mobile tibial tray lateral uplift). Concerning the configuration of the knee simulator in terms of IER and APD settings, the selected values were specifically chosen (coherently with the standards defined by [132]) to give rise to impaired contact conditions among the prosthetic components: with respect to the current ZP, any IER and APD change turned out to compromise the full contact experienced at the PE insert-femoral component interface. This allowed to simulate walking conditions slightly different from the standard ones [132], but all related to possible scenarios during walking, with respect to which the stability of the mobile tibial tray could be evaluated and discussed.

Not surprisingly, in each of the fifteen different configurations that were studied no uncontrolled movement of the actuated tray took place; in chapter 4.5.1 it was already anticipated that the corresponding profiles of the mobile tibial tray and the baseplate would prevent any undesired relative movement between the two components. Such design choice proved to be really effective, since the tray did not experience neither undesired vibrations nor unexpected oscillations throughout the multiple gait cycles replicated by the knee simulator.

In addition to this, the full KJ motions experienced by the implant did not produce any change in the wedge position, thus confirming the soundness of the considerations made in chapter 4.5.1 about the passive locking system provided by the design. Contextually, the contact line between the tray and the actuated wedge together with the support point on the baseplate non-actuated side were definitively validated as sufficient conditions for the tray stability.

Due to the experimental settings and to the absence of a measurement system associated to the tibial component or to the knee simulator, the aforementioned results were all inferred from visual evaluations. Hereupon, in order to integrate the stability tests outcomes with more consistent and arguable experimental data, two force sensors were implemented in the prototype, as discussed in the following.

5.5 Force Sensors

Considering the complexity of the KJ kinematics, the implementation of any sensor in the prototype should be defined very accurately in order not to disturb the test

dynamics replicated by the knee simulator. Such requirement was met by positioning two FlexiForce B201 sensing devices [133] onto the mobile tibial tray upper surface, as depicted in Fig. 5.9. Symmetrically aligned with respect to the tray geometric center, the two contact piezoresistive force sensors, which easily fit the thin spacing between the tray and the PE insert, “can be used to measure both static and dynamic forces and are thin enough (0.208 mm thickness) to enable non-intrusive measurement. The sensors use a resistive-based technology; the application of a force to the active sensing area of the sensor results in a change in the resistance of the sensing element in inverse proportion to the force applied” [133, p. 6]. Connected to a computer via Universal Serial Bus (USB) handles, the data acquisition system allows to display a real-time graphical representation of the sensed forces and to collect data for further processing. The great measurement system linearity and accuracy ($\pm 3\%$), as well as the great flexibility in use, make the FlexiForce sensors the ideal solution for this work.

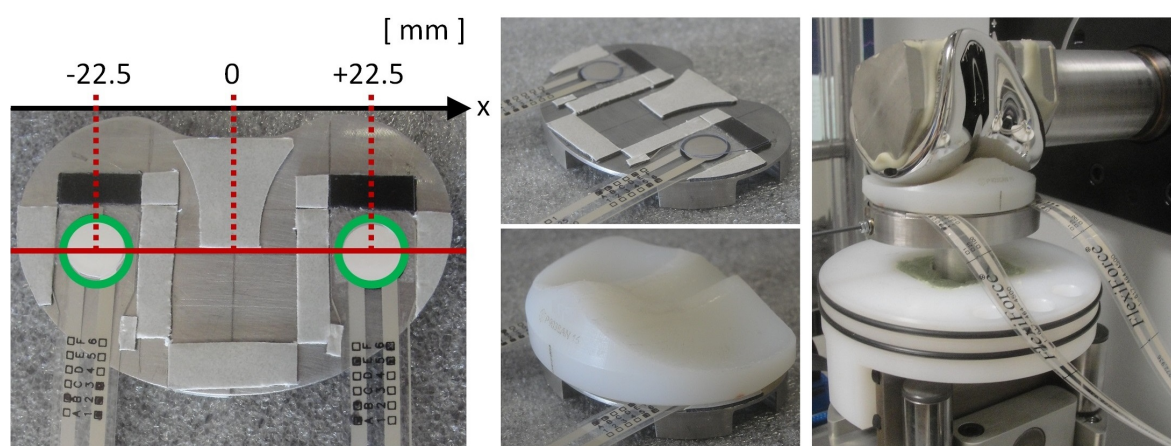


Figure 5.9 – the positioning of the two force sensors (green-coloured circular sensing areas)

5.5.1 Experimental Protocol

The goal of this experimental stage consisted in employing the two force sensors to evaluate the variations in the distribution of tibiofemoral loads on the mobile tibial tray under different actuation system configurations. In line with the considerations made in chapter 3.1, any collateral ligament laxity condition leads to a non-homogeneous loads distribution between the two mobile tibial tray compartments; given the experimental environment, this corresponds to an uneven solicitation of the two sensors during simulated gait cycles.

Once completed the individual calibration of the two sensing devices via the graphical interface, the PE insert was positioned onto the mobile tibial tray upper surface in the same position previously adopted for the stability tests (chapter 5.4). The ADL-Force 5 Simulator does not provide the possibility to replicate specific knee collateral ligaments laxity conditions: the VVR value, which sets the rotation about the knee AP axis of the tibial component with respect to the femoral one, cannot be customised and is automatically determined by the machine as a function of the IER and APD settings [131]. In order to reproduce realistic imbalance conditions, it was therefore deemed appropriate to take into account the IER and APD values already considered in chapter 5.4: the tibial component was oriented at 15 degrees internal rotation and 2 mm anterior translation, so as to impair the full contact normally experienced at the PE insert-femoral component interface. Such configuration allowed to simulate the laxity of the lateral collateral ligament.

In order to allow for a more immediate interpretation of the tibiofemoral loads distribution, the unit chosen for displaying the data collected by the two force sensors was the solicitation percentage with respect to their total measurement range (0–4448 N [133]). Herein, such values will be addressed as $M\%$ and $L\%$ respectively for the medial and the lateral force sensors.

With the actuation system in its starting position (null wedge translation, null mobile tibial tray lateral uplift), the implant was subjected to 50 successive gait cycles (2600 N peak tibiofemoral load, 1 s walking cycle [90]). As expected, the simulated laxity of the lateral collateral ligament resulted in an overload of the tibial platform medial compartment: Fig. 5.10 clearly shows the non-homogeneous solicitation of the two force sensors (for sake of clarity, $M\%$ and $L\%$ data are shown only for the last 25 simulated gait cycles).

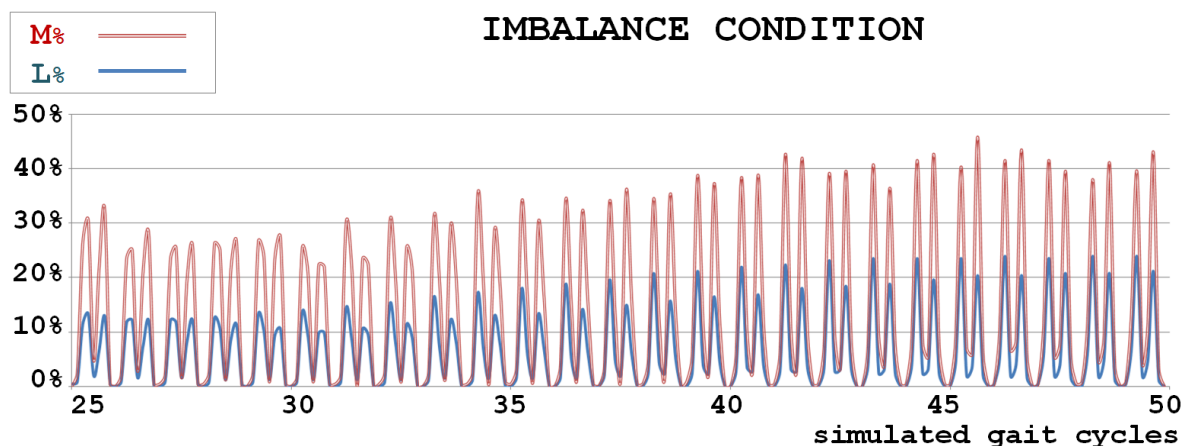


Figure 5.10 – $M\%$ and $L\%$ data at the simulated imbalance condition

To compensate for the simulated imbalance condition, the progressive correction procedure defined in chapter 3.1 was followed. The criterion for considering balance conditions as optimally restored consisted in visually matching the recorded graphical representations of $M\%$ and $L\%$. Due to the constraints imposed by the experimental settings, each successive system actuation step (manually performed) was alternated to a series of 50 simulated gait cycles, necessary to update the data collected by the force sensors.

The first actuation consisted in 10 complete leadscrew revolutions; as depicted in Fig. 5.11, this was not sufficient to fully restore the homogeneous distribution of the tibiofemoral efforts onto the tibial platform. However, as a consequence of the corresponding tibial tray lateral uplift, the difference between $M\%$ and $L\%$ was reduced.

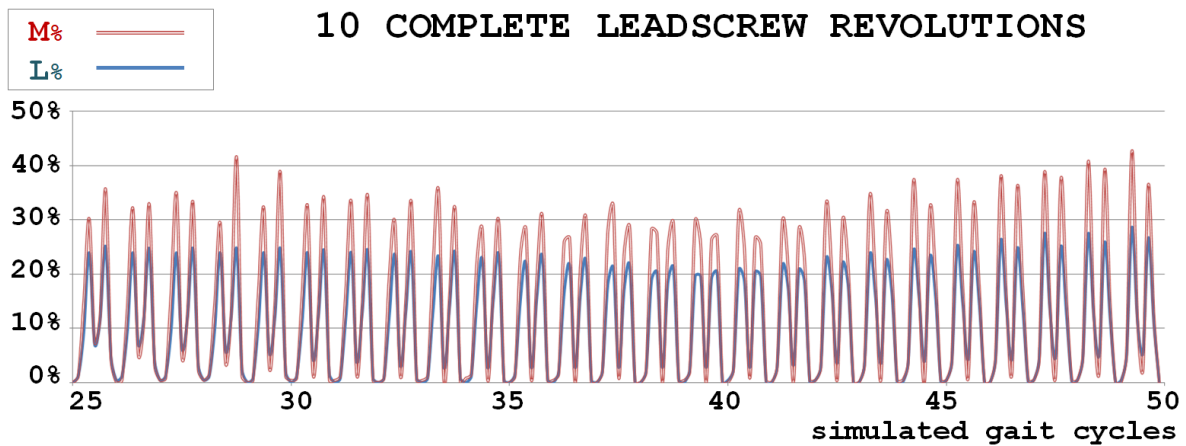
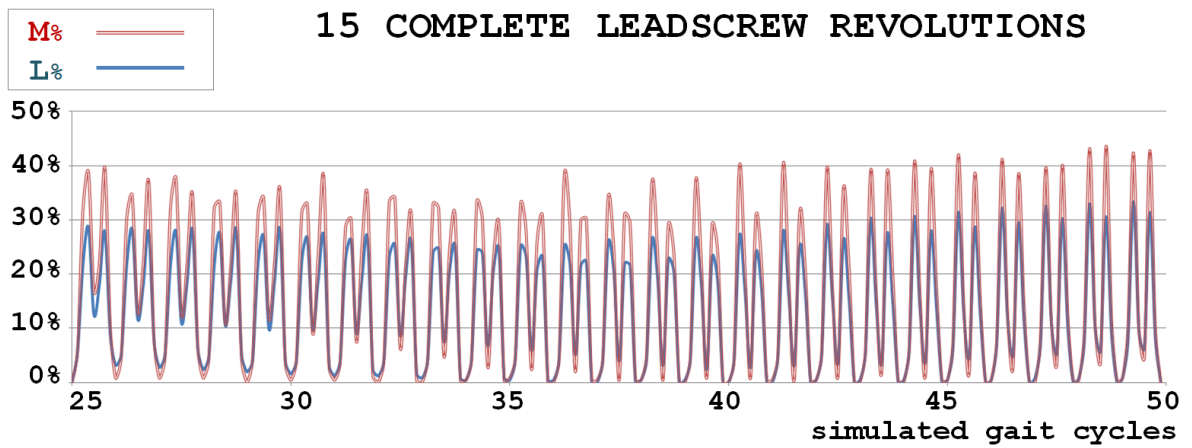
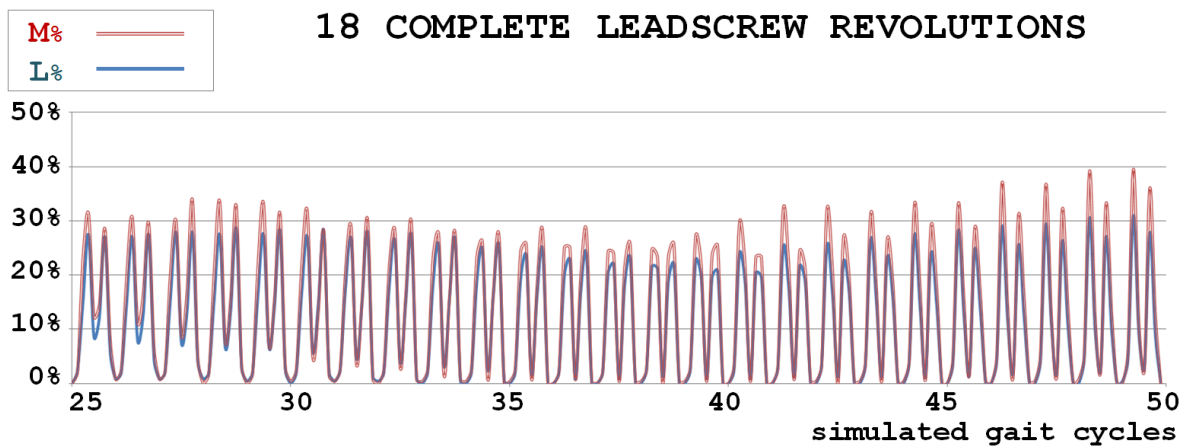
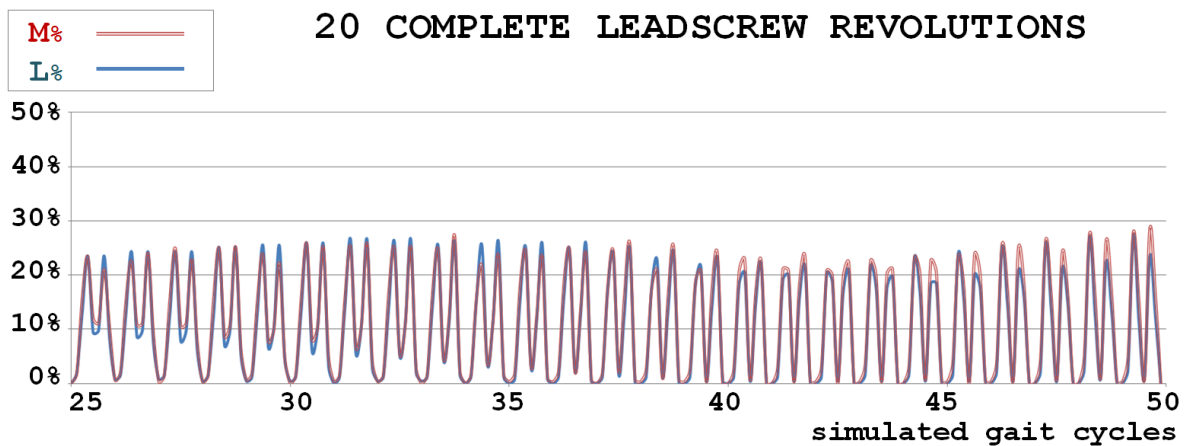


Figure 5.11 – $M\%$ and $L\%$ data after ten complete leadscrew revolutions

The actuation was carried out again, by means of 5 additional complete leadscrew revolutions (total: 15); once again, the tray uplift resulted in a more homogeneous solicitation of the two tibial platform compartments during the simulated gait cycles, but still not sufficient to make the recorded $M\%$ and $L\%$ data equal (Fig. 5.12).

Accordingly, the actuation was carried out a third time by adding 3 complete leadscrew revolutions (total: 18), as shown in Fig. 5.13. A good visual matching of the two graphical representations of $M\%$ and $L\%$, depicted in Fig. 5.14, was obtained after a fourth and last actuation process, by means of 2 complete leadscrew revolutions (total: 20). As previously mentioned, optimal knee balance conditions were considered as restored according to the equal solicitation of the two force sensors.

Figure 5.12 – $M\%$ and $L\%$ data after fifteen complete leadscrew revolutionsFigure 5.13 – $M\%$ and $L\%$ data after eighteen complete leadscrew revolutionsFigure 5.14 – $M\%$ and $L\%$ data after twenty complete leadscrew revolutions

5.5.2 Results

Table 5.4 summarizes the results of the force sensors tests:

- the terms $\overline{M\%}$ and $\overline{L\%}$ denote respectively the medial and lateral force sensors data averaged over the 50 gait cycles simulated after each actuation step;
- the term x_{CoP} is a qualitative evaluation of the tibiofemoral loads CoP position. Due to the experimental settings, the CoP lies on the line connecting the two force sensors. With respect to the simple reference system illustrated in Fig. 5.15, the CoP coordinate x_{CoP} (unit: mm) can be computed from the sensors location on the tibial tray according to the following equation:

$$x_{CoP} = \frac{\overline{M\%} \cdot (+22.5) + \overline{L\%} \cdot (-22.5)}{\overline{M\%} + \overline{L\%}}$$

- the mobile tibial tray lateral uplift was computed from the number of complete leadscrew revolutions (linear relationship previously discussed in chapter 4.5.2).

leadscrew revolutions	$\overline{M\%}$ [%]	$\overline{L\%}$ [%]	x_{CoP} [mm]	tray uplift [mm]
0	16.00	6.00	10.23	0.00
10	13.50	10.50	2.81	1.44
15	16.00	13.00	2.33	2.16
18	13.00	11.50	1.38	2.59
20	11.00	10.50	0.52	2.88

Table 5.4 – the results of the force sensors tests

The key achievement of this experimental stage consisted in assessing the effectiveness of the actuation protocol proposed in chapter 4.5.2. The gradual mobile tibial tray lateral uplift was proved to actually affect the distribution of tibiofemoral loads under normal KJ kinematics conditions (accurately replicated by the knee simulator). According to the considerations made in chapter 4, the 20 complete leadscrew revolutions produced a 8 mm wedge translation and a 2.88 mm tray lateral uplift: such values were both verified after the experimental phase, as a further assessment of the actuation system accuracy.

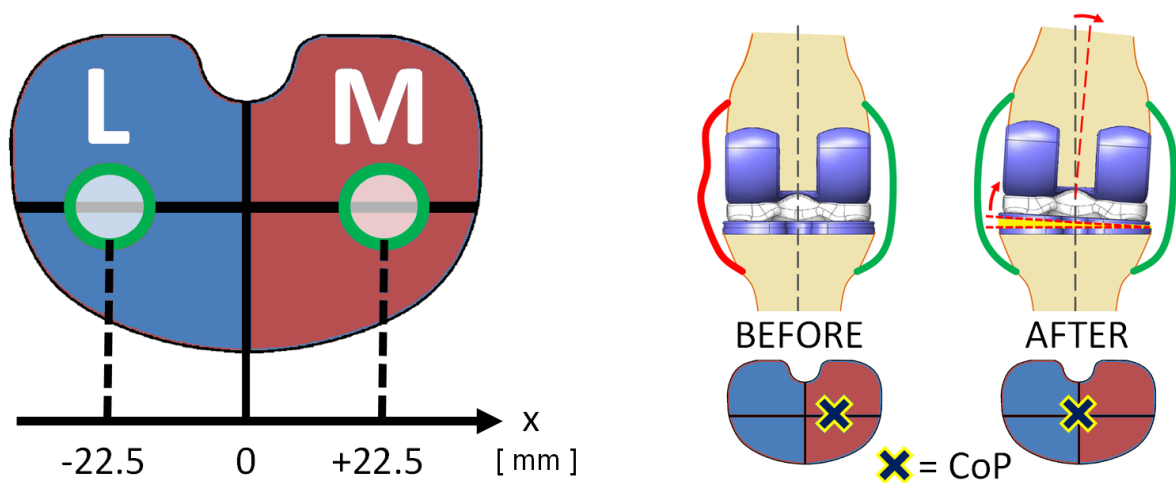


Figure 5.15 – the tibiofemoral loads CoP position before and after actuation

Before actuation, the simulated laxity of the lateral collateral ligament resulted in an overload of the tibial platform medial compartment ($\overline{M}_{\%} = 16\%$) with respect to the lateral one ($\overline{L}_{\%} = 6\%$). Throughout the four actuation steps, the progressive mobile tibial tray lateral uplift led to a more homogeneous distribution of the simulated tibiofemoral loads; this was clearly shown by the $M_{\%}$ and $L_{\%}$ data graphical representations, which gradually reduced their distance. The actuation was considered complete after 20 complete leadscrew revolutions, when the two tibial platform compartments were equally solicited ($\overline{M}_{\%} = 11\%$ and $\overline{L}_{\%} = 10.50\%$). However, the criterion of considering knee balance conditions as optimally restored according to the visual matching of the two sensors data should limit any interpretation of the experimental outcomes to a qualitative level.

With respect to the starting configuration of the prosthetic components, the progressive correction process carried out by the manual actuation of the proposed tibial component re-established proper full contact conditions at the PE insert-femoral component interface. Accordingly, the simulated KJ dynamics affected more homogeneously the whole PE insert surface, without overloading only one tibial tray compartment.

The mobile tibial tray lateral uplift varied from 0 to 2.88 mm and effectively allowed to compensate for the simulated ligament imbalance condition; such achievement was confirmed by the value of x_{CoP} , which throughout the actuation process gradually translated from the tibial tray medial compartment (10.23 mm) towards the platform geometric center (0.52 mm). Considering the variations in the CoP position, the greatest distance was covered after the first 10 complete leadscrew revolutions with a translation from 10.23 mm to 2.81 mm. The remaining actuation steps apparently

had a smaller impact on the CoP position; this aspect, as well as the total travelled distance (9.71 mm), should be object of further investigations.

5.6 Comments

The outcomes of the experimental validation stage globally met the expectations and were therefore judged satisfactory and promising. The stability and force sensors tests were defined specifically to evaluate in a realistic KJ physiological environment the actuation system working principle (chapter 4.1) and to assess the effectiveness of the proposed design choices (chapters 4.3 and 4.5) under normal conditions of use. The actuation procedure proposed in chapter 3.1 allowed to achieve the gradual homogenisation of the tibiofemoral loads distribution on the two tibial platform compartments.

This experimental validation stage was considered essential for planning further investigation, namely based on the fabrication of a fully functional instrumented tibial component including both the PC elements and the actuation system sub-parts; in particular, the possibility to carry out experimental tests on a titanium alloy prototype would allow to collect more reliable data about the robustness properties and the overall functioning of the proposed implant.

6.1 Conclusions

Over the last fifty years, the development of CAMI techniques has led to more and more accurate and patient-specific medical interventions [1]. Concerning TKA surgery, the design of instrumented knee prostheses has been definitively accepted as a way forward to provide the surgeon with further useful pre- and intraoperative knowledge: the data collected by smart knee implants during and after surgery, besides improving the quality of the surgical procedure itself, have turned out to be very helpful for both clinicians and prosthesis designers.

A key achievement of TKA consists in intraoperatively setting up proper tension conditions of the two knee collateral ligaments: this stage, which directly determines the postoperative KJ function and the implant lifespan, cannot be standardised for all patients and is generally carried out by evaluating variable and user-dependent loads [72]. Despite the use of the assistive tools that can be found in the literature, nowadays the surgeon's experience and perception are still of paramount importance during the delicate knee stabilisation process, which inevitably leads to intraoperative inaccuracies [8, 74]. Moreover, the morphofunctional evolution that the prosthetic KJ normally undergoes during the rehabilitation period and in its aftermath may alter the collateral ligaments tension values set during surgery; suboptimal balance conditions might lead to postoperative complications and, in the worst-case scenario, to the need for revision surgery already a few years after primary TKA [6, 7]. These considerations suggest therefore to take into account the possibility to compensate for intraoperative inaccuracies in the postoperative period. In such framework, this work aims to propose a novel instrumented knee implant able to detect collateral ligaments laxity conditions right after primary TKA and, if needed, restore optimal balance conditions before the occurrence of more severe complications. In the long term, such achievement is intended to strongly reduce the need for revision surgery.

The instrumented tibial component presented in this work, which further develops the smart knee implant proposed by our research team [81], includes two sub-parts:

Imbalance Detection - Four PC elements embedded in the tibial baseplate to be employed as both force sensors [80] and energy harvesters for the evaluation of collateral ligaments laxity conditions [77]. Upon further validation (ongoing research work), the collected data are processed and wirelessly transmitted to the clinician's computer, in order to define a proper correcting action for restoring optimal balance conditions.

Imbalance Correction - A miniaturised actuation system embedded in the tibial baseplate [106] is used to re-tighten the detected lax collateral ligament by adjusting the height and inclination of the tibial tray on the corresponding side. Such correcting action, which must be performed without impairing the prosthesis alignment to the LLMA achieved during TKA, is meant to be able to compensate for any collateral ligament laxity condition detected in the aftermath of the rehabilitation period.

To our knowledge, no other ongoing study copes with the problem of postoperative knee ligament imbalance with the same approach proposed in this work. The idea of embedding a miniaturised actuation system inside a knee prosthesis is no doubt ambitious and, as previously mentioned, requires a strongly multidisciplinary research work that must be supported by experimental data.

The actuation system was dimensioned so as to fulfil the clinical requirements while facing with technical and technological limitations. The severe constraints imposed by a biocompatible environment were met by means of smart design choices: the combined use of a wedge and a screw resulted in an efficient mechanism able to develop great output forces in face of reduced input efforts. Efficiency was deemed a key aspect of the miniaturised actuation system, which must be sufficiently small in order to be embedded in the tibial component and, at the same time, robust enough to face with the strong KJ cyclic efforts during everyday life activities. The mechanical model of the proposed actuation system was accurately studied by means of static force analysis and different design expedients were discussed for the minimization of friction losses. All the microelectronics components necessary for the implant functioning (power conditioning and telemetry system, microactuators integrated circuitry) were assumed to be hosted inside the hollow tibial stem, in the form of an integrated low-power consumption system whose design is currently investigated.

The creation of an accurate 3D model of the proposed implant allowed to carry out simulated static force analyses, to perform useful design optimisations and to esti-

mate the components robustness properties. Afterwards, in order to test the actuation system performances under normal working conditions, a full-scale prototype of the instrumented tibial component was fabricated and tested on a knee simulator. Stability and force sensors tests were defined specifically to evaluate the actuation system working principle in a realistic KJ physiological environment, as well as to assess the effectiveness of the proposed design choices under normal conditions of use; the very promising results of such experimental validation stage globally met the expectations and provided precious indications for future studies and improvements.

The proposed actuation system has been designed taking into consideration the presence of the four PC elements employed for the detection of collateral ligament imbalance conditions. The WL system does not entail any change in the tibiofemoral loads transmission to the PC elements: all forces acting on the inclined mobile tibial tray get distributed onto the baseplate via the actuated wedge and the contact point on the non-actuated side. It is therefore sufficient to position the PC elements under the actuation system part, as shown in Fig. 6.1, in order to make them experience any tibiofemoral load acting inside the KJ during daily life activities.

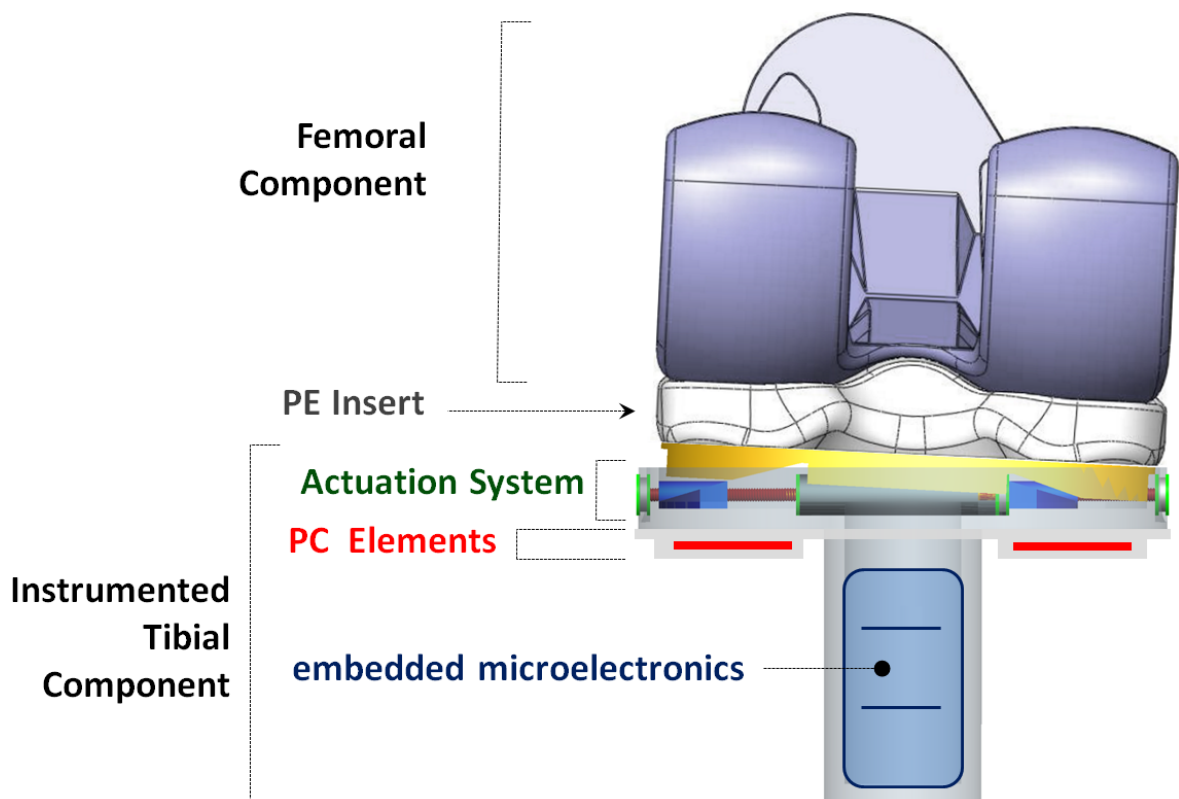


Figure 6.1 – a simplified representation of the instrumented tibial component and its embedded sub-parts

Considering the integration of the PC part and the actuation system into a single instrumented tibial component, the baseplate overall thickness should be reduced as much as possible in order to limit the implant invasiveness, namely the amount of tibial bone that needs to be resected during TKA surgery. Taken singularly, the PC part and the actuation system require a tibial platform respectively 4.5 and 9 mm thick; by properly joining the common contact surfaces of the two sub-parts, their assembly could lead to a 12 mm thick baseplate, that is practically two and a half times the thickness of conventional implants. This result is objectively acceptable, considering that the presence of embedded components inevitably results in bulkier prosthetic parts; if necessary, a possible expedient to further reduce the tibial platform thickness is the possibility to perform extra drillings in the resected tibial surface in order to gain available volume. The PC elements could be contained, at least partially, inside dedicated grooves specifically drilled around the tibial stem; such opportunity is completely at the surgeon's discretion and the choice of whether or not to consider it clearly depends on the patient's knee bony structures conditions.

6.2 Perspectives

The encouraging outcomes of the stability and force sensors tests presented in the previous chapters were considered essential before proceeding with further investigation. Hereafter, a few suggestions are made about possible future work.

Titanium Alloy Prototype - The fabrication of a titanium alloy prototype would allow to carry out fatigue tests, as well as vibration analyses, studied over several million simulated gait cycles; this would allow to evaluate more realistically the robustness properties and the overall functioning of the proposed implant. The obtained results would integrate those of the stability tests, for the definitive validation of the design choices and the actuation system working principle.

Micromotor and Actuation Force - It would be very interesting to implement the selected rotary stepper micromotor [119, 120] on the prototype. Upon fabrication of a fully functional wedge (including the presence of the embedded miniaturised balls suggested in chapter 4.3.2), it would be possible to drive the actuation system under more realistic conditions. Contextually, a force sensor could be positioned on the mobile tibial tray upper surface and employed during the lateral uplift process: such experimental test would allow to evaluate the total actuation force actually developed by the WL system and compare it to the computed theoretical value.

Wireless Power Supply and Control - As already discussed in chapter 3.3.4, in the case of instrumented prosthetic implants the most reliable and widely documented power supply technique is represented by inductive coupling. Ongoing research is currently carried out to evaluate different solutions concerning the wireless power supply and control issues; the two approaches currently investigated are introduced and briefly discussed here.

Two identical microactuators will be embedded in the tibial baseplate, one per side, but only one of them will need to be powered to perform the actuation; because of the very limited available volume, the motor wireless power supply and control should be managed by a centralized unit. One receiving coil, positioned inside the tibial stem, is supposed to be connected to both motors via one control circuit; a simple switch, integrated to the already present microelectronics, could be controlled from an external base station by means of radiofrequency techniques. Such architecture would allow to power only the required microactuator wirelessly and in a perfectly biocompatible way, with the external coil positioned around the patient's knee throughout the whole actuation process.

Alternatively, inductive coupling could be employed only for the time necessary to recharge a dedicated microbattery connected to the control unit, with the external coil successively removed; this second approach is slightly less invasive than the first one, but may require more time to complete the battery charge process. In both cases, the two coupled coils have to be properly dimensioned so as to guarantee a sufficient amount of energy transferred through the biological tissues and the metal prosthetic components.

Fully Integrated Prototype - A fully functional instrumented tibial component including both the PC elements and the actuation system sub-parts could be manufactured so as to evaluate the performances of the proposed implant as a whole. Along the lines of the force sensors tests (chapter 5.5), the use of the four PC elements for the estimation of the tibiofemoral loads CoP displacements during simulated gait cycles would provide much more accurate and reliable data. In vivo experiments could be planned to test the fully functional prototype and collect more consistent and arguable experimental data.

In principle, all the considerations made above, which concern the WL model [106], could be considered valid also for the alternative actuation system design [107] presented in the Appendix. However, upon further development, the adaptive and autonomous instrumented knee implant presented in this work is meant to be capable, at the same time, to:

- intraoperatively assist the surgeon to achieve optimal knee balance conditions during TKA soft tissues release procedure;
- monitor the prosthetic patient's KJ evolution after surgery and detect any instability;
- if needed, compensate for the detected imbalances and restore optimal balance conditions without the need for revision TKA.

In the long term, if successfully achieved and upon acceptance by the orthopaedic community, the proposed smart knee prosthesis could strongly reduce the need for revision surgery.

Actuated Screws Model

A.1 Introduction

The WL actuation system [106] is presented as the main contribution of this work. As introduced in chapter 4, an alternative solution has been fully developed, discussed [107] and eventually set aside because of its higher invasiveness. This Appendix provides the description of a second actuation system, based on the use of four actuated screws for the realisation of the required tibial tray lateral uplift. Coherently with the considerations made in chapter 6.1, also this model is intended to be integrated to the PC part into a single instrumented tibial component.

A.2 Actuation System Design

The miniaturised actuation system presented here is based on two main sub-parts which, for sake of clarity, are described hereafter separately:

Screw-nut Mechanism - Fig. A.1 shows a customised screw-nut mechanism assembled in the tibial baseplate. The screw body is 16 mm long and is positioned perpendicularly to the baseplate surface. The screw head, on the lower side of the baseplate, is a geared wheel that can only rotate without translating. The nut has a total thickness of 5 mm: 3 mm with a square section (10 mm side length) and 2 mm with a rounded profile, as depicted in Fig. A.1. The square section part of the nut is contained in the baseplate and prevents the nut from rotating with the screw body. The two components share a standard M5x0.8 thread (5 mm nominal outer diameter, 0.8 mm pitch [108]), because of which any screw rotation produces a corresponding nut translation along a direction that is perpendicular to the tibial baseplate. The free rotation of each screw head with respect to the baseplate is allowed by two thrust ball bearings, fastened to each other by means of a thin

hexagonal nut. The tibial baseplate embeds a total of four screw-nut mechanisms of this kind, two per each side (medial and lateral).

Gear Train - The lower part of the tibial baseplate partially embeds two gear trains, one per side. Each single train (Fig. A.2) has one input gear (named G1) and two output gears (G4 and G5). The latter are the geared wheels that, as previously mentioned, form the screw heads of the screw-nut mechanisms. G2 is a large internal gear, on whose upper surface a smaller gear (G3 identical to G1) is rigidly fixed. When G1 is driven by a rotary stepper micromotor, the train transmits the rotation to G4 and G5, thus making the two screws rotate together at the same speed. Table A.1 summarizes the gear train parameters, that were selected so as to maximize the overall gear ratio in compliance with the tibial baseplate dimensions.

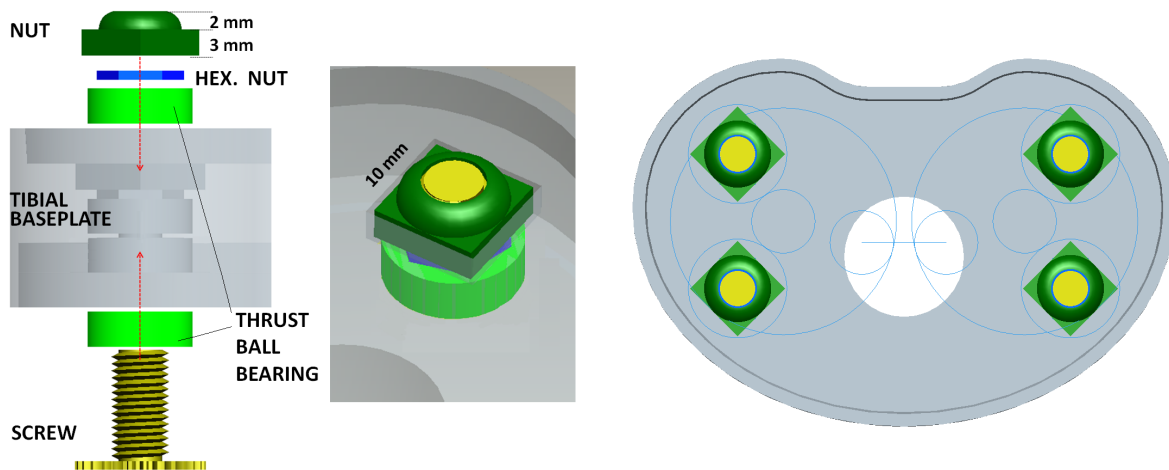


Figure A.1 – the tibial baseplate embeds four customised screw-nut mechanisms

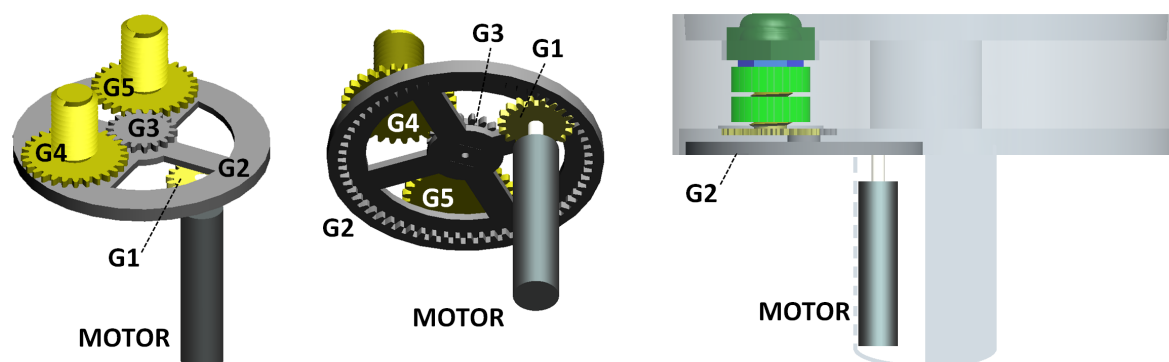


Figure A.2 – the bottom part of the tibial baseplate partially embeds two gear trains, one per side

	G1 = G3	G2	G4 = G5
Nominal Outer Diameter [mm]	9	32	14
Number of Teeth	18	64	28
all spur gears	module = 0.5	pressure angle = 20 deg	

Table A.1 – the gear train parameters

Considering the presence of the aforementioned components, the instrumented tibial baseplate in the starting position (null actuation) has an overall thickness of 18 mm, which is twice that of the WL model. Simulations carried out on a detailed 3D CAD model of the proposed model showed that a 2 mm unscrewing of the actuated nuts produces a 3 mm mobile tibial tray lateral uplift. For these two main reasons, this actuation system was considered as a less promising model than the WL one and set aside for the fabrication of a steel prototype.

Concerning the actuation procedure, once detected the collateral ligament laxity condition (chapter 3.1), the clinician wirelessly activates the micromotor on the corresponding side; via the gear train, the two screws start rotating together. This produces the simultaneous translation of the two nuts, which get unscrewed out of the baseplate. The mobile tibial tray, which as for the WL model is initially contained in the baseplate but not constrained inside it (chapter 4.2.2), gets laterally pushed upwards by the two nuts and pivots on the non-actuated side, without changing its orientation on the AP plane. An example of the system working principle is given in Fig. A.3, where, for sake of clarity, the actuation system is represented on only one side of the tibial component. Once the actuation procedure is completed, the mobile tray is still partially contained in the baseplate with which it shares three contact points: the two actuated nuts and the pivot point on the opposite side.

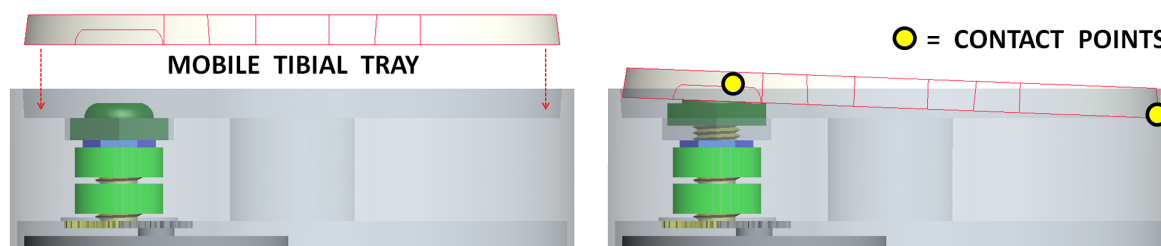


Figure A.3 – the proposed tibial component before (left) and after (right) actuation

A.3 Mechanical Analysis

In order to lift the mobile tibial tray up, the two actuated nuts together must be able to overcome the knee collateral ligaments passive force (150 N [47]). The force produced by the translation of each nut can be computed by applying the screw equation already mentioned in chapter 4.3.3 and reported below:

$$T = L \cdot r \cdot \frac{\tan \alpha + f \cdot \lambda}{1 - f \cdot \lambda \cdot \tan \alpha} \quad \text{with:} \quad \lambda = \sqrt{1 + \tan^2(\theta/2) \cdot \cos^2(\alpha)}$$

$$\alpha = \arctan\left(\frac{p}{2 \cdot \pi \cdot r}\right)$$

It is possible to compute the torque $T_{OUT} = T$ to be applied to each output gear in order to overcome the load $L = 75$ N (each nut experiences half of the total collateral ligaments passive force). Table A.2 defines the equation terms; concerning the thread friction coefficient, the worst-case scenario is considered by assuming the screw-nut system as made of Titanium Vanadium Alloy (Ti-6Al-4V).

term	value	unit	description
$T_{OUT} = T$	unknown	mNm	torque applied to the screw
L	75	N	axial load applied onto the screw
r	2.24 [108]	mm	M5x0.8 screw thread mean radius
p	0.8 [108]	mm	M5x0.8 screw thread pitch
f	0.36	-	friction coefficient inside the thread
α	3.25 [118]	deg	thread helix angle
θ	60 [118]	deg	thread profile angle

Table A.2 – definition of the screw-nut equation terms

The equation gives the value $T_{OUT} = 81.26$ mNm, which is the torque to be provided to each actuated screw. According to the parameters summarized in Table A.1), the gear train MA is 5.53 : this means that each output gear (G4 and G5) rotates 5.53 times slower than the input gear (G1), but provides a torque which is 5.53 times higher than the input one. Thanks to the great efficiency provided by gear trains (95-97 % [134]), at an early design stage it can be assumed that the torque transmission takes place without any power loss; by defining as P_1 , P_4 and P_5 the power transferred by respectively G1, G4 and G5, the following equations hold:

$$\begin{cases} P_{IN} = P_1 \\ P_{OUT} = P_4 + P_5 \end{cases} \Rightarrow P_{IN} = P_{OUT} \Rightarrow P_1 = P_4 + P_5$$

The power P_i transferred by any generic gear can be defined as the product of the gear torque T_i and its angular velocity ω_i . Thus, the previous equation can be expressed as follows:

$$T_1 \cdot \omega_1 = T_4 \cdot \omega_4 + T_5 \cdot \omega_5$$

As previously mentioned, the gear train design guarantees that the two output gears rotate together simultaneously 5.53 times slower than the input gear; this means that:

$$\omega_4 = \omega_5 = \frac{\omega_1}{5.53}$$

which leads to:

$$5.53 \cdot T_1 = T_4 + T_5$$

The last equation confirms that the input torque $T_{IN} = T_1$ is amplified by the gear train and equally distributed between the two output gears. According to the chosen notation, $T_{OUT} = T_4 = T_5$. Therefore, the relation between T_{IN} and T_{OUT} becomes:

$$5.53 \cdot T_{IN} = 2 \cdot T_{OUT} \quad \Rightarrow \quad T_{IN} = \frac{2}{5.53} \cdot T_{OUT}$$

In conclusion, considering the value $T_{OUT} = 81.26$ mNm previously computed, the rotary stepper micromotor must provide a torque $T_{IN} = 29.39$ mNm to G1. As already suggested in chapter 4.3.2, the operating conditions could be greatly improved by taking in consideration the use of specific anti-friction coating materials to minimize the friction losses occurring inside the screw-nut mechanism thread.

A.4 Microactuator Selection

The same rotary stepper micromotor (Faulhaber ADM0620-2R-V2-05 [119]) already selected for the WL model can be employed also for the actuated screws system: combined to its integrated planetary gearhead (06/1 K 1024:1 [120]), this microactuator can provide up to 35 mNm intermittent torque, which theoretically results in a total actuation force (considering both the actuated nuts) of about 180 N. Thanks to its compact dimensions (cylindrical volume of 29.6 mm height and 6 mm diameter), this motor perfectly fits half the volume offered by the hollow tibial stem and can easily

be arranged in order to drive the gear train on the corresponding side. Unlike the WL model, the microelectronics components necessary for the implant functioning (the power conditioning system to cope with the energy harvested by the PC elements, the telemetry system responsible for wireless data transmission and the integrated circuit for the microactuator power supply and control) should mainly be embedded inside the thicker tibial baseplate.

A.5 Discussion

The considerations made in this section are organised as in chapter 4.5, to which the reader is referred in order to draw a parallel between the two proposed actuation systems. The contents presented in the following are summarized so as to prevent redundancies.

A.5.1 Locking Issue

The tibial platform is the load-bearing surface of the prosthetic articulation and, as such, it continuously undergoes repeated vibrations, compression loads and shear forces. Such cyclic efforts are transmitted to the two actuated nuts that, constrained inside their square holes, cannot produce any screw rotation; thus the nuts keep their lifted position and, consequently, also the corresponding mobile tibial tray lateral uplift. In addition to this, the motor stall torque, amplified by the gear train, contributes to blocking the rotation of the output gears. The corresponding profiles of the mobile tibial tray and the baseplate prevent any undesired relative movement between the two components; the tray stability is guaranteed by its two contact points with the actuated nuts and the pivot point on the non-actuated side.

The axial efforts experienced by the two actuated nuts get transmitted via the threaded profiles to the screw bodies; for each screw, the presence of the thin hexagonal nut and the two miniature thrust ball bearings is necessary to prevent force transmission to the gear train and to the micromotor shaft, which is rigidly fixed to G1 and can bear axial loads only up to 5 N [120]. The thrust ball bearings must be dimensioned taking into account the 2600 N peak tibiofemoral force acting inside the prosthetic knee during normal gait cycle [90]. Theoretically, the maximum load experienced by each actuated nut is 650 N and, as in the case of the WL model, over-dimensioning is recommended as a precautionary measure; browsing the currently available off-the-shelf products, it turns out that F5-12M thrust steel ball bearings [135] can bear up to 942 and 1056

N respectively static and dynamic loads. The system robustness properties could be further improved by considering the use of ceramic balls instead of steel ones.

According to the considerations made above, the proposed design provides a passive locking system a priori reliable and robust. A key role is played by the two miniature thrust ball bearings positioned along the screw bodies, thanks to which the microactuator does not undergo the strong tibiofemoral efforts and is not involved in locking the mobile platform in the desired uplifted position. This aspect also guarantees great lifespan conditions of the whole actuation system.

A.5.2 Fine-Tuning Actuation

The mobile tibial tray lateral uplift ranges between 0 and 3 mm, with the condition of full actuation corresponding to a 2 mm nut translation. Considering the 0.8 mm thread pitch, the actuation process ranges:

- between 0 and 2.5 complete screw (G4 and G5) revolutions;
- due to the gear train MA (5.53), between 0 and 13.825 complete G1 revolutions.

Since the selected rotary stepper micromotor [119] provides 20 steps per revolution, about 277 steps are required to cover the entire actuation range; the procedure proposed in chapter 3.1 can therefore be carried out with submillimetre accuracy, according to the requirement defined in chapter 3.3.2.

A.5.3 Materials and Sealing

All the prosthetic components and the actuation system mechanical parts are assumed to be made of Titanium Vanadium Alloy (Ti-6Al-4V), a biocompatible material commonly chosen nowadays for knee implants [5]. The actuation system miniaturised mechanical and electronics components must be properly sealed in order not to enter in contact with the physiological fluids that bath the knee articulation, which might fill the very thin spacing that generates between the mobile tibial tray and the baseplate during the actuation process. As already proposed for the WL model in chapter 4.5.3, an elastic micro-membrane could be properly fixed between the mobile tibial tray lateral edges and the baseplate internal ones, so as to create a sealed volume for the embedded components. Biocompatible casings could also be employed to host the microactuators and their related electronics.

A.5.4 Actuation System Scaling and Integration with the Piezoceramics Elements

The tibial baseplate embeds two identical actuation systems, positioned symmetrically with respect to the stem hole, each one responsible for the tray lateral uplift on one side. The design presented here has been dimensioned for a Size 6 knee prosthesis; as for the WL model, the actuation system scaling for knee implants of different size must be performed very carefully, with particular focus on the gear train dimensioning (which the system MA depends on). Concerning the actuated screws size, the M5x0.8 standard was deemed a reasonable compromise between robustness and compactness. The four PC elements employed for the detection of collateral ligament imbalance conditions could be positioned under the actuation system part, as shown in Fig. A.4. With respect to the WL model, the integration of the PC part (4.5 mm thick) and the actuation system (18 mm thick) into a single instrumented tibial component considerably increases the implant invasiveness.

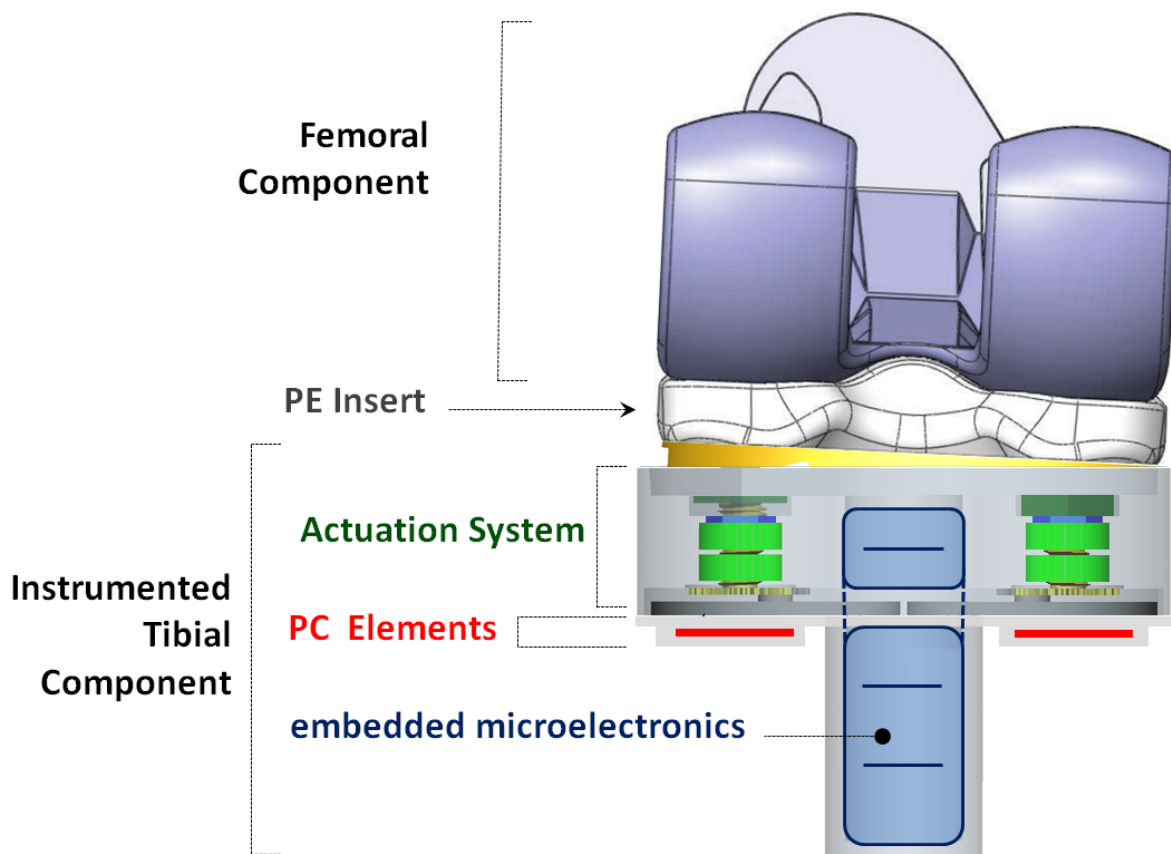


Figure A.4 – a simplified representation of the instrumented tibial component and its embedded sub-parts

A.6 Experimental Stage

Even if the actuated screws model was eventually set aside because of its higher invasiveness in favour of the WL actuation system, an early stage experimental phase was carried out to further investigate the mechanical analysis theoretical results.

A.6.1 3D Model Simulations

Forces distribution and components deformation were evaluated by means of static analyses simulated on the 3D model of the proposed implant. The mobile tibial tray was blocked in fully actuated configuration (3 mm uplift) and subjected to a distributed force of 2600 N [90]. As expected, VMS concentration occurred around the three contact points (the two actuated nuts and the pivot point on the opposite side). Neither uncontrolled movements nor relevant deformation were detected. As for the WL model, smart design adjustments such as thickness increase and filleted edges turned out to further improve the robustness and stress distribution properties of the implant.

Concerning the efforts experienced by the screw-nut mechanism threaded profile, by way of illustration, a standard steel M5x0.8 screw (property class 8.8) withstands more than 2500 N tensile loads [124, 125]. Titanium (and titanium alloy) threads are much stronger and lighter than steel ones [121, 126, 127], thus ensuring better robustness properties; considering also the selected Titanium Vanadium Alloy compressive and tensile yield strengths (respectively 1070 and 1100 MPa [121]), it was concluded that no mechanical failure of the actuation system components should take place.

A.6.2 Prototyping

A full-scale prototype of the proposed tibial component was manufactured by means of a 3D printer, in order to evaluate the actuation system working principle on one side of the prosthesis. The tibial baseplate, the mobile tray and two actuated nuts were all fabricated as plastic components and assembled together (Fig. A.5). In order to facilitate parts assembly and handling, a thicker baseplate was employed. Standard steel screws and spur gears were used for the realisation of the gear train. The aforementioned miniature thrust ball bearings were properly embedded in the baseplate, so as to allow free screw revolutions. The manual actuation of the gear train allowed to assess the effectiveness of the proposed design and confirmed the 3 mm tray lateral uplift corresponding to a 2 mm nuts translation (2.5 complete screws revolutions). The stability of the mobile tibial tray was assessed both during and after the actuation process: no

uncontrolled rotation of the tray took place with respect to the baseplate. As expected, thanks to the thrust ball bearings, compressive forces manually applied onto the tray surface did not get transmitted to the gear train. This prototype was intended as a simple proof-of-concept of the proposed actuation system for further development.

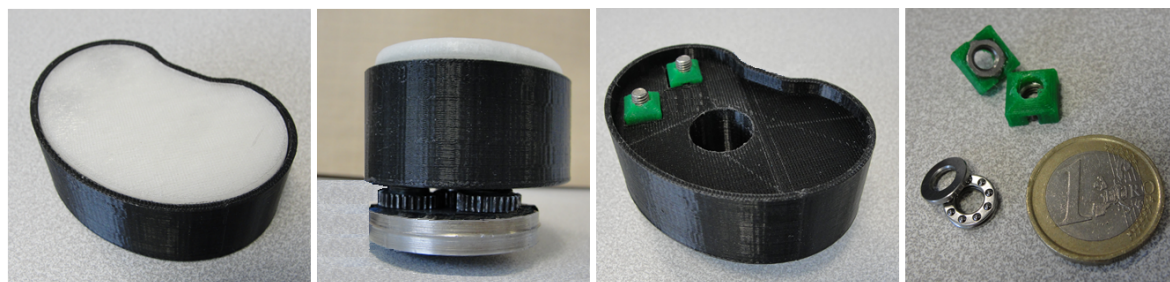


Figure A.5 – the 3D-printed plastic prototype of the actuated screws model

A.7 Conclusions and Perspectives

The actuated screws model is an alternative to the WL actuation system, which is presented as the main contribution of this work. Table A.3 offers a qualitative comparison between the two models and explains why the design presented in this Appendix was set aside and considered as an alternative solution. First, considering the tibial baseplate thickness required by the presence of the embedded actuation system, the actuated screws model is twice more invasive than the WL one. Second, the maximum mobile tibial tray lateral uplift produced by the actuated nuts is 3 mm, against the 3.6 mm offered by the WL mechanism. Third, any miniaturised mechanical structure based on the use of a gear train inevitably copes with the problem of backlash (*“the clearance or lost motion in a mechanism caused by gaps between the parts”*[136]); thus, in terms of accuracy, the linear relationship relating the wedge translation to the tray lateral uplift in the WL model (chapter 4.5.2) is a priori much more reliable and should therefore be preferred. Fourth, the two proposed implants provide both a passive locking system to keep the mobile tibial tray in the desired uplifted position; also in this case, the WL model is favoured by its design simplicity, with contact surfaces among more compact mechanical components.

In the final analysis, the actuated screws model relies on a working principle which, upon further development, could effectively restore optimal knee balance conditions in the postoperative period. The actuation system design could be greatly improved by drawing on the fields of mechanical watchmaking and biomedical instrumentation, two research areas close to each other, both technologically (millimetre scale) and in their

industrial fabric. For instance, a proper dimensioning and assembling of the gear train (gears thickness, module, pressure angle) would improve the actuation system overall efficiency. In such framework, the theoretical computations considered throughout the mechanical analysis phase should be further discussed and assessed by means of experimental validation, upon the fabrication of a full-scale prototype of the instrumented tibial component.

	Actuated Screws Model	WL Model
tibial platform thickness	18 mm	9 mm
max tray lateral uplift	3 mm	3.6 mm
actuation process accuracy	backlash \rightarrow less reliable	linear relationship \rightarrow more reliable
passive locking system robustness	threaded profiles (nuts)	threaded profile (leadscrew) + wedge surfaces

Table A.3 – qualitative comparison between the two proposed actuation systems

Bibliography

- [1] E. Dombre, M. DeMathelin, and J. Troccaz, “Medical robotics: Characteristics and state of the art,” in *Medical Robotics* (J. Troccaz, ed.), London, United Kingdom: ISTE Ltd., 2012.
- [2] L. M. Specht and K. J. Koval, “Robotics and computer-assisted orthopaedic surgery,” *Bulletin of the NYU Hospital for Joint Diseases*, vol. 60(3 and 4), pp. 168–172, 2001.
- [3] L. P. Nolte and T. Beutler, “Basic principles of caos,” *Injury - International Journal of the Care of the Injured*, vol. 35, pp. SA6–SA16, 2004.
- [4] G. R. Scuderi and A. J. Tria, *Knee Arthroplasty Handbook: Techniques in Total Knee and Revision Arthroplasty*. New York, NY: Springer, 2006.
- [5] T. P. Vail and J. E. Lang, “Surgical techniques and instrumentation in total knee arthroplasty,” in *Surgery of The Knee* (W. N. Scott, ed.), Philadelphia, MS: Churchill Livingstone, 2006.
- [6] C. Lavernia, D. J. Lee, and V. H. Hernandez, “The increasing financial burden of knee revision surgery in the united states,” *Clinical Orthopaedics and Related Research*, vol. 446, pp. 221–226, 2006.
- [7] S. Kurtz, K. Ong, E. Lau, F. Mowat, and M. Halpern, “Projections of primary and revision hip and knee arthroplasty in the united states from 2005 to 2030,” *Journal of Bone and Joint Surgery*, vol. 89(4), pp. 780–785, 2007.
- [8] M. J. Winemaker, “Perfect balance in total knee arthroplasty: the elusive compromise,” *Journal of Arthroplasty*, vol. 17(1), pp. 2–10, 2002.
- [9] J. Kulowski, “Flexion contracture of the knee: The mechanics of the muscular contracture and the turnbuckle cast method of treatment; with a review of fifty-five cases,” *Journal of Bone and Joint Surgery*, vol. 14(3), pp. 618–630, 1932.

- [10] A. Faller and M. Schuenke, *The Human Body: an Introduction to Structure and Function*. New York, NY: Thieme, 2004.
- [11] W. Platzer, *Color Atlas of Human Anatomy: Locomotor System*. New Delhi, India: Thieme, 2004.
- [12] M. Bonnin and P. Chambat, *Osteoarthritis of the Knee*. Paris, France: Springer, 2008.
- [13] J. A. Buckwalter and J. A. Martin, "Osteoarthritis," *Advanced Drug Delivery Reviews*, vol. 58, pp. 150–167, 2006.
- [14] R. E. Booth, "Joint arthroplasty in the 21st century," *Journal of Orthopaedics*, vol. 22, pp. 793–795, 1999.
- [15] A. S. Verneuil, "Affection articular du genou," *Arch Med*, 1863.
- [16] W. S. Baer, "Arthroplasty with the aid of animal membrane," *Americal Journal of Orthopedic Surgery*, vol. 16, pp. 1–29 and 171–199, 1918.
- [17] W. C. Campbell, "Arthroplasty of the knee: Report of cases," *Americal Journal of Orthopedic Surgery*, vol. 19, pp. 430–434, 1921.
- [18] J. E. Brown, W. H. McGaw, and D. T. Shaw, "Use of cutis as an interposing membrane in arthroplasty of the knee," *Journal of Bone and Joint Surgery*, vol. 40, pp. 1003–1018, 1958.
- [19] F. B. Mazas, "Guepar total knee prosthesis," *Clinical Orthopaedics and Related Research*, vol. 94, pp. 211–221, 1973.
- [20] J. Charnley, "The reaction of bone to self-curing acrylic cement: a long-term histological study in man," *Journal of Bone and Joint Surgery*, vol. 52B, pp. 340–353, 1970.
- [21] S. D. Cook, K. A. Thomas, and R. J. Haddad, "Histologic analysis of retrieved human porous-coated total joint components," *Clinical Orthopaedics and Related Research*, vol. 237, pp. 90–101, 1988.
- [22] J. M. Viton, L. Atlani, S. Mesure, J. Massion, J. P. Franceschi, A. Delarque, and A. Bardot, "Reorganization of equilibrium and movement control strategies after total knee arthroplasty," *Journal of Rehabilitation Medicine*, vol. 34(1), pp. 12–19, 2002.
- [23] S. S. Leopold, "Minimally invasive total knee arthroplasty for osteoarthritis," *The New England Journal of Medicine*, vol. 360, pp. 1749–1758, 2009.

- [24] P. Brooks, "Seven cuts to the perfect total knee," *Orthopedics*, vol. 32(9), 2009.
- [25] R. D. Scott and R. F. Santore, "Unicompartmental replacement for osteoarthritis of the knee," *Journal of Bone and Joint Surgery*, vol. 63A, pp. 536–544, 1981.
- [26] S. Breeman, M. Campbell, H. Dakin, N. Fiddian, R. Fitzpatrick, A. Grant, A. Gray, L. Johnston, G. Maclellan, R. Morris, and D. Murray, "Patellar resurfacing in total knee replacement: five-year clinical and economic results of a large randomized controlled trial," *Journal of Bone and Joint Surgery*, vol. 93(16), pp. 1473–1481, 2011.
- [27] E. T. Habermann and M. Kerner, "Patella resurfacing in total knee replacement: Is it an option?," *FLEXION - Newsletter for Orthopaedic Surgeons*, vol. 2(3), 2001.
- [28] J. N. Insall, "Total knee replacement," in *Surgery of The Knee* (J. N. Insall, ed.), Philadelphia, MS: Churchill Livingstone, 1984.
- [29] D. Hansen and J. S. Jensen, "Prechilling and vacuum mixing not suitable for all bone cements," *Journal of Arthroplasty*, vol. 5, pp. 287–290, 1990.
- [30] B. Bloch, J. K. Haken, and G. W. Hastings, "Evaluation of cold curing acrylic cement for prosthesis stabilization," *Clinical Orthopaedics and Related Research*, vol. 72, p. 239, 1970.
- [31] G. R. Scuderi, J. N. Insall, and R. E. Windsor, "Survivorship of cemented knee replacements," *Journal of Bone and Joint Surgery*, vol. 71, pp. 798–803, 1989.
- [32] L. A. Whiteside, "Cementless total knee replacement. nine to eleven year results and ten years survivorship analysis," *Clinical Orthopaedics and Related Research*, vol. 309, pp. 185–192, 1994.
- [33] F. F. Buechel, M. J. Pappas, and M. D'Alessio, "Twenty year evaluation of meniscal bearing and rotating platform knee replacements," *Clinical Orthopaedics and Related Research*, vol. 388, pp. 41–50, 2001.
- [34] K. Vince, "Revision knee arthroplasty," in *Operative Orthopedics* (J. B. Lippincott, ed.), Philadelphia, MS: Churchill Livingstone, 1993.
- [35] K. Vince, "Planning revision total knee arthroplasty." *Seminars in Arthroplasty*, 1996.

- [36] W. D. Bugbee, D. J. Ammeen, and G. A. Engh, "Does implant selection affect outcome of revision knee arthroplasty?," *Journal of Arthroplasty*, vol. 16(5), pp. 581–585, 2001.
- [37] S. C. Hwang, J. Y. Kong, D. C. Nam, D. H. Kim, H. B. Park, S. T. Jeong, and S. H. Cho, "Revision total knee arthroplasty with a cemented posterior stabilized, condylar constrained or fully constrained prosthesis: A minimum 2-year follow-up analysis," *Clinics in Orthopedic Surgery*, vol. 2(2), pp. 112–120, 2010.
- [38] S. M. Mortazavi, J. Schwartzenberger, M. S. Austin, J. J. Purtill, and J. Parvizi, "Revision total knee arthroplasty infection: incidence and predictors," *Clinical Orthopaedics and Related Research*, vol. 468(8), pp. 2052–2059, 2010.
- [39] S. E. Sydney, S. A. Pickering, C. Bell, and R. Crawford, "Reducing metal debris generation during total knee arthroplasty," *Orthopedics*, vol. 30(12), 2007.
- [40] T. P. James, O. P. McGonigle, I. S. Hasan, and E. L. Smith, "Adjustable slot cutting guide for improved accuracy during bone resection in total knee arthroplasty," *Journal of Medical Devices*, vol. 7(4), 2013.
- [41] K. Chareancholvanich, R. Narkbunnam, and C. Pornrattanamaneewong, "A prospective randomised controlled study of patient-specific cutting guides compared with conventional instrumentation in total knee replacement," *The Bone and Joint Journal*, vol. 95-B(3), pp. 354–359, 2013.
- [42] V. Y. Ng, J. H. DeClaire, K. R. Berend, B. C. Gulick, and A. V. Lombardi, "Improved accuracy of alignment with patient-specific positioning guides compared with manual instrumentation in tka," *Clinical Orthopaedics and Related Research*, vol. 470(1), pp. 99–107, 2012.
- [43] T. J. Heyse and C. O. Tibesku, "Improved femoral component rotation in tka using patient-specific instrumentation," *The Knee*, vol. 21(1), pp. 268–271, 2014.
- [44] M. Swank, J. R. Romanowski, L. L. Korbee, and S. Bignozzi, "Ligament balancing in computer-assisted total knee arthroplasty: improved clinical results with a spring-loaded tensioning device," *Proceedings of the Institution of Mechanical Engineers - part H - Journal of Engineering in Medicine*, vol. 221(7), pp. 755–761, 2007.
- [45] K. Tanaka, H. Muratsu, K. Mizuno, R. Kuroda, S. Yoshiya, and M. Kurosaka, "Soft tissue balance measurement in anterior cruciate ligament-resected knee joint: cadaveric study as a model for cruciate-retaining total knee arthroplasty," *Journal of Orthopaedic Science*, vol. 12, pp. 149–153, 2007.

- [46] Y. H. Kim, K. S. Sohn, and J. S. Kim, "Range of motion of standard and high-flexion posterior stabilized total knee prostheses. a prospective, randomized study," *Journal of Bone and Joint Surgery*, vol. 87(A), pp. 1470–1475, 2005.
- [47] C. Marmignon, *Modeles et instruments robotises pour l etude biomecanique per-operatoire de l equilibre ligamentaire du genou*. PhD thesis, Universite Joseph Fourier, Grenoble, France, december 2004.
- [48] S. M. Kim, Y. S. Park, C. W. Ha, S. J. Lim, and Y. W. Moon, "Robot-assisted implantation improves the precision of component position in minimally invasive tka," *Orthopedics*, vol. 35(9), pp. e1334–e1339, 2012.
- [49] T. Matsumoto, H. Muratsu, N. Tsumura, K. Mizuno, R. Kuroda, S. Yoshiya, and M. Kurosaka, "Joint gap kinematics in posterior-stabilized total knee arthroplasty measured by a new tensor with the navigation system," *Journal of Biomechanical Engineering*, vol. 128(6), pp. 867–871, 2006.
- [50] T. Matsumoto, K. Mizuno, H. Muratsu, N. Tsumura, N. Fukase, S. Kubo, S. Yoshiya, M. Kurosaka, and R. Kuroda, "influence of intra-operative joint gap on post-operative flexion angle in osteoarthritis patients undergoing posterior-stabilized total knee arthroplasty," *Knee Surgery, Sports Traumatology, Arthroscopy*, vol. 15, pp. 1013–1018, 2007.
- [51] E. Stindel, J. L. Briard, P. Merloz, S. Plaweski, F. Dubrana, C. Lefevre, and J. Troccaz, "Bone morphing: 3d morphological data for total knee arthroplasty," *Journal of Image Guided Surgery*, vol. 7(3), pp. 156–168, 2002.
- [52] J. Y. Jenny and C. Boeri, "Unicompartmental knee prosthesis implantation with a non-image based navigation system. a matched-paired comparative study of the quality of implantation with a conventional technique," *Techniques in Orthopaedics*, vol. 18(2), pp. 167–173, 2003.
- [53] L. Perlick, H. Bathis, C. Luring, M. Tingart, and J. Grifka, "Two-stage reimplantation for infected total knee arthroplasty - usability of a ct-based navigation system," in *Proceedings of Surgetica*, (Grenoble, France), pp. 36–42, september 2002.
- [54] P. Ritschl, F. Machacek, and R. Fuiko, "Computer assisted ligament balancing in tkr using the galileo system," in *Computer Assisted Orthopaedic Surgery* (F. Langlotz, B. L. Davies, and A. Bauer, eds.), Darmstadt, Germany: Steinkopff, 2003.

- [55] P. M. Bonutti, D. A. Dethmers, M. S. McGrath, S. D. Ulrich, and M. A. Mont, "Navigation did not improve the precision of minimally invasive knee arthroplasty," *Clinical Orthopaedics and Related Research*, vol. 466, pp. 2730–2735, 2008.
- [56] W. P. Yau, K. Y. Chiu, J. L. Zuo, W. M. Tang, and T. P. Ng, "Computer navigation did not improve alignment in a lower-volume total knee practice," *Clinical Orthopaedics and Related Research*, vol. 466, pp. 935–945, 2008.
- [57] P. S. John, "Navigating the future - surgery using computer," *Indian Journal of Orthopaedics*, vol. 39, pp. 1–3, 2005.
- [58] S. Bhandari, "Inertial sensor based surgical navigation system for knee replacement surgery." US patent US20110275957-A1, november 2011.
- [59] P. J. Sell, "Instrumented implants in orthopaedics," *Journal of Biomedical Engineering*, vol. 11(2), pp. 111–112, 1989.
- [60] S. Almouahed, C. Hamitouche, E. Stindel, and C. Roux, "New trends in instrumented knee prostheses," in *ICTTA 2008 - 3rd International conference on information and communication technologies : from theory to applications*, (Damascus, Syrian Arab Republic), pp. 1–6, april 2008.
- [61] C. Marmignon, A. Leimnei, and P. Cinquin, "Robotized distraction device for knee replacement surgery," *International Congress Series*, vol. 1268, pp. 638–643, 2004.
- [62] C. Marmignon, A. Leimnei, S. Lavallee, and P. Cinquin, "Automated hydraulic tensor for total knee arthroplasty," *International Journal of Medical Robotics and Computer Assisted Surgery*, vol. 1(4), pp. 51–57, 2005.
- [63] D. Crottet, T. Maeder, D. Fritschy, H. Bleuler, L. P. Nolte, and I. P. Pappas, "Development of a force amplitude- and location-sensing device designed to improve the ligament balancing procedure in tka," *IEEE Transactions on Biomedical Engineering*, vol. 52(9), pp. 1609–1611, 2005.
- [64] K. H. Bloemker, T. M. Guess, L. Maletsky, and K. Dodd, "Computational knee ligament modeling using experimentally determined zero-load lengths," *The Open Biomedical Engineering Journal*, vol. 6, pp. 33–41, 2012.
- [65] B. A. Morris, D. D. D'Lima, J. Slamin, N. Kovacevic, S. W. Arms, C. P. Townsend, and C. W. Colwell, "e-knee: Evolution of the electronic knee prosthesis : Telemetry technology development," *Journal of Bone and Joint Surgery*, vol. 83(2 suppl 1), pp. 62–66, 2001.

- [66] M. E. Hardwick, P. A. Pulido, D. D. D’Lima, and C. W. Colwell, “e-knee: the electronic knee prosthesis,” *Orthopaedic Nursing*, vol. 25(5), pp. 326–329, 2006.
- [67] F. Graichen, R. Arnold, A. Rohlmann, and G. Bergmann, “Implantable 9-channel telemetry system for in vivo load measurements with orthopedic implants,” *IEEE Transactions on Biomedical Engineering*, vol. 54(2), pp. 253–261, 2007.
- [68] A. Mundermann, C. O. Dyrby, D. D. D’Lima, C. W. Colwell, and T. P. Andriacchi, “In vivo knee loading characteristics during activities of daily living as measured by an instrumented total knee replacement,” *Journal of Orthopaedic Research*, vol. 26(9), pp. 1167–1172, 2008.
- [69] H. Chen, M. Liu, W. Wan, C. Jia, C. Zhang, and Z. Wang, “Low-power circuits design for the wireless force measurement system of the total knee arthroplasty,” in *2010 Annual International Conference of the IEEE Engineering in Medicine and Biology Society (EMBC)*, (Buenos Aires, Argentina), pp. 3539–3542, september 2010.
- [70] A. Arami, M. Simoncini, O. Atasoy, W. Hasenkamp, S. Ali, A. Bertsch, E. Meurville, S. Tanner, H. Dejnabadi, V. Leclercq, P. Renaud, C. Dehollain, P. A. Farine, B. M. Jolles, K. Aminian, and P. Ryser, “Instrumented prosthesis for knee implants monitoring,” in *2011 IEEE Conference on Automation Science and Engineering (CASE)*, (Trieste, Italy), pp. 828–835, august 2011.
- [71] A. Arami, M. Simoncini, O. Atasoy, W. Hasenkamp, A. Bertsch, E. Meurville, S. Tanner, P. Renaud, C. Dehollain, P. A. Farine, B. M. Jolles, K. Aminian, and P. Ryser, “Instrumented knee prosthesis for force and kinematics measurements,” *IEEE Transactions on Automation Science and Engineering*, vol. 10, pp. 615–624, 2013.
- [72] F. Zimmermann, C. Schwenninger, U. Nolten, F. P. Firmbach, R. Elfring, and K. Radermacher, “A new approach to implant alignment and ligament balancing in total knee arthroplasty focussing on joint loads,” *Biomedizinische Technik - Biomedical engineering*, vol. 57(4), pp. 283–291, 2012.
- [73] F. Schmidt, R. Elfring, U. Nolten, W. Mokwa, and K. Radermacher, “A new intra-articular load measuring device for ligament balancing and prosthesis alignment in total knee arthroplasty,” in *Proceedings of the International Federation for Medical and Biological Engineering (IFMBE)*, (Munich, Germany), pp. (25/VI) 331–332, september 2009.

- [74] F. Schmidt, F. Lampe, and R. Elfring, "Soft-tissue management in primary knee arthroplasty: common techniques, navigation and force-sensing devices," *Zeitschrift fur Orthopadie und Unfallchirurgie*, vol. 145(5), pp. 599–607, 2007.
- [75] S. Almouahed, M. Gouriou, C. Hamitouche, E. Stindel, and C. Roux, "Finite element study for intra and postarthroplastic evaluation of ligament balancing in standing position using instrumented tibial baseplate," in *WoWMoM 2009 - IEEE International Symposium on a World of Wireless, Mobile and Multimedia Networks and Workshops*, (Kos, Greece), pp. 1–6, june 2009.
- [76] C. Lahuec, S. Almouahed, M. Arzel, D. Gupta, C. Hamitouche, M. Jezequel, E. Stindel, and C. Roux, "A self-powered telemetry system to estimate the post-operative instability of a knee implant," *IEEE Transactions on Biomedical Engineering*, vol. 58(3), pp. 822–825, 2011.
- [77] S. Almouahed, M. Gouriou, C. Hamitouche, E. Stindel, and C. Roux, "Design and evaluation of instrumented smart knee implant," *IEEE Transactions on Biomedical Engineering*, vol. 58(4), pp. 971–982, 2011.
- [78] S. R. Platt, S. Farritor, and H. Haider, "On low-frequency electric power generation with pzt ceramics," *IEEE/ASME Transactions on Mechatronics*, vol. 10, pp. 240–252, 2005.
- [79] S. R. Platt, S. Farritor, K. Garvin, and H. Haider, "The use of piezoelectric ceramics for electric power generation within orthopedic implants," *IEEE/ASME Transactions on Mechatronics*, vol. 10, pp. 455–461, 2005.
- [80] S. Almouahed, M. Gouriou, C. Hamitouche, E. Stindel, and C. Roux, "The use of piezoceramics as electrical energy harvesters within instrumented knee implant during walking," *IEEE/ASME Transactions on Mechatronics*, vol. 16(5), pp. 799–807, 2011.
- [81] S. Almouahed, *Study, implementation and evaluation of a prototype of self-powered diagnostic knee implant*. PhD thesis, Telecom Bretagne, Brest, june 2011.
- [82] J. M. Wright, H. C. Crockett, D. P. Slawski, M. W. Madsen, and R. E. Windsor, "High tibial osteotomy," *Journal of the American Academy of Orthopaedic Surgeons*, vol. 13, pp. 279–289, 2005.
- [83] G. Puddu, M. Cipolla, G. Cerullo, V. Franco, and E. Gianni, "Which osteotomy for a valgus knee?," *International Orthopaedics*, vol. 34(2), pp. 239–247, 2009.

- [84] T. Koshino, T. Murase, and T. Saito, "Medial opening-wedge high tibial osteotomy with use of porous hydroxyapatite to treat medial compartment osteoarthritis of the knee," *Journal of Bone and Joint Surgery*, vol. 85A(1), pp. 78–85, 2003.
- [85] C. Sherman and M. E. Cabanela, "Closing wedge osteotomy of the tibia and the femur in the treatment of gonarthrosis," *International Orthopaedics*, vol. 34(2), pp. 173–184, 2010.
- [86] "Genesis 2 system versatility." Smith and Nephew Richards Inc. - Genesis 2 Total Knee System, april 1997.
- [87] R. F. LaPrade, A. H. Engebretsenand, T. V. Ly, S. Johansen, F. A. Wentorf, and L. Engebretsen, "The anatomy of the medial part of the knee," *Journal of Bone and Joint Surgery*, vol. 89(9), pp. 2000–2010, 2007.
- [88] D. D. D'Lima, B. J. Fregly, S. Patil, N. Steklov, and C. W. Colwell, "Knee joint forces: prediction, measurement, and significance," *Proceedings of the Institution of Mechanical Engineers, Part H: Journal of Engineering in Medicine*, vol. 226(2), pp. 95–102, 2012.
- [89] D. D. D'Lima, N. Steklov, S. Patil, and C. W. Colwell, "The mark coventry award: in vivo knee forces during recreation and exercise after knee arthroplasty," *Clinical Orthopaedics and Related Research*, vol. 466(11), pp. 2605–2611, 2008.
- [90] "Iso standard 14243-1, implants for surgery - wear of total knee-joint prostheses - part 1: Loading and displacement parameters for wear-testing machines with load control and corresponding environmental conditions for test." International Organisation for Standardization, 2009.
- [91] C. P. Townsend, S. W. Arms, and M. J. Hamel, "Remotely powered, multichannel, microprocessor based telemetry systems for smart implantable total knee implant," in *Proceedings of SPIE's 6th Annual International Conference on Smart Structures and Materials*, (Newport Beach, California, USA), march 1999.
- [92] S. W. Arms, M. J. Hamel, and C. P. Townsend, "Multi-channel structural health monitoring network, powered and interrogated using electromagnetic fields," in *International SAMPE Symposium and Exhibition - Society for the Advancement of Material and Process Engineering*, (Baltimore, Maryland, USA), june 2007.
- [93] D. Crescini, E. Sardini, and M. Serpelloni, "An autonomous sensor for force measurements in human knee implants," in *Proceedings of the Eurosensors XXIII Conference*, (Lausanne, Switzerland), pp. 718–721, september 2009.

- [94] D. Crescini, E. Sardini, and M. Serpelloni, "Design and test of an autonomous sensor for force measurements in human knee implants," *Sensors and Actuators A: Physical*, vol. 166(1), pp. 1–8, 2011.
- [95] O. Atasoy and C. Dehollain, "A study for remote powering of a knee prosthesis through inductive link," in *2010 Conference on Ph.D. Research in Microelectronics and Electronics (PRIME)*, (Berlin, Germany), pp. 1–4, august 2010.
- [96] J. Holmberg, L. Alexander, R. Rajamani, and J. E. Bechtold, "Battery-less wireless instrumented knee implant," *Journal of Medical Devices*, vol. 7(1), 2013.
- [97] F. Multon and P. Delamarche, "L'énergie chez l'homme." Colloque Energie Portable: autonomie et integration dans l'environnement humain, 2002.
- [98] S. Turri and G. Poulin, "Dispositifs electromecaniques permettant l'exploitation de l'énergie des mouvements humains." Colloque Energie Portable: autonomie et integration dans l'environnement humain, 2002.
- [99] D. Williams, "Revisiting the definition of biocompatibility," *Medical Device Technology*, vol. 14(8), pp. 10–13, 2003.
- [100] A. Collo, S. Almouahed, P. Poignet, C. Hamitouche, and E. Stindel, "Towards a dynamic tibial component for postoperative fine-tuning adjustment of knee ligament imbalance," in *Proceedings of the International Conference on Biomedical Electronics and Devices (Biodevices 2013)*, (Barcelona, Spain), pp. 95–102, february 2013.
- [101] A. Coty, "Alimentation électrique transdermique." Colloque Energie Portable: autonomie et integration dans l'environnement humain, 2002.
- [102] A. R. Paul, P. Roy, and S. Mukherjee, *Mechanical Sciences: Engineering Mechanics and Strength of Materials*. New York, NY: Prentice-Hall of India, 1914.
- [103] W. B. Anderson, *Physics for Technical Students: Mechanics and Heat*. New York, NY: McGraw Hill, 1914.
- [104] S. Almouahed, C. Hamitouche, E. Stindel, and C. Roux, "Finite element lifetime prediction of a miniature adjustable orthopedic device," in *2012 Annual International Conference of the IEEE Engineering in Medicine and Biology Society (EMBC)*, (San Diego, California, USA), pp. 4030–4033, august 2012.
- [105] S. Almouahed, C. Hamitouche, E. Stindel, and C. Roux, "Towards a fine-tunable tibial implant for the in-vivo correction of ligament imbalance resulting from

- patient morpho-functional evolution,” *Universal Journal of Medical Science*, vol. 1(2), pp. 56–63, 2013.
- [106] A. Collo, P. Poignet, C. Hamitouche, S. Almouahed, and E. Stindel, “A miniaturised actuation system embedded in an instrumented knee implant for postoperative ligament imbalance correction,” in *Proceedings of the 36th Annual International Conference of the IEEE Engineering in Medicine and Biology Society (EMBC 2014)*, (Chicago, Illinois, USA), pp. 6211–6214, august 2014.
- [107] A. Collo, P. Poignet, C. Hamitouche, S. Almouahed, and E. Stindel, “An active tibial component for postoperative fine-tuning adjustment of knee ligament imbalance,” in *Proceedings of the 5th IEEE/RAS-EMBS International Conference on Biomedical Robotics and Biomechatronics (BioRob 2014)*, (Sao Paulo, Brasil), pp. 126–131, august 2014.
- [108] “Iso standard 68-1, iso general purpose screw threads - basic profile - part 1: Metric screw threads.” International Organisation for Standardization, 1998.
- [109] S. P. Parker, *McGraw-Hill Concise Encyclopedia of Science and Technology*. New York, NY: McGraw Hill, 1992.
- [110] P. Agati, G. Delville, and Y. Bremont, *Mecanique du solide - Applications industrielles*. Paris, France: Dunod, Sciences Sup., 2003.
- [111] J. L. Fanchon, *Guide de Mecanique : Sciences et Technologies Industrielles*. Paris, France: Nathan, 2001.
- [112] T. Bartels, “Lubricants and lubrication,” in *Ullmann’s Encyclopedia of Industrial Chemistry* (Wiley-VCH, ed.), Weinheim, Germany: Wiley-VCH, 2005.
- [113] “Minilub - revetement lubrifiant.” Metallisation Nord Industrie - <http://www.mni-hi-tech.com>, 2014.
- [114] T. A. Harris, *Rolling Bearing Analysis*. New York, NY: Wiley-Interscience, 2001.
- [115] Wikipedia, “Ceramic — wikipedia, the free encyclopedia.” <http://en.wikipedia.org/w/index.php?title=Ceramic&oldid=600596241>, 2014. [Online; accessed 7-May-2014].
- [116] Boca-Bearings, “Ceramic bearings.” <http://www.bocabearings.com/bearing-info/frequently-asked-questions>, 2014. [Online; accessed 7-May-2014].

- [117] Lily-Bearings, “F3-8m si3n4 silicon nitride full ceramic thrust ball bearings.” <http://www.lily-bearing.com/en/cp/si3n4-Full-Ceramic-Thrust-Bal-bearings-F3-8m.htm>, 2014. [Online; accessed 8-May-2014].
- [118] “Iso standard 261, iso general purpose metric screw threads - general plan.” International Organisation for Standardization, 1998.
- [119] Faulhaber, “Miniature drive systems - adm0620-2r-v2-05.” <http://www.micromo.com/ecatalog/page245.html>, 2014. [Online; accessed 12-May-2014].
- [120] Faulhaber, “Miniature drive systems - precision gearheads - 06/1 k 1024:1.” <http://www.micromo.com/ecatalog/page294.html>, 2014. [Online; accessed 12-May-2014].
- [121] Matweb, “Titanium vanadium alloy properties.” <http://www.matweb.com/search/DataSheet>, 2014. [Online; accessed 13-May-2014].
- [122] Lily-Bearings, “F2-6m thrust ball bearings.” <http://www.lily-bearing.com/en/miniature/f2-6m.htm>, 2014. [Online; accessed 12-May-2014].
- [123] AST-Bearings, “F3-8m thrust ball bearings.” <http://www.astbearings.com/product.html?product=F3-8M>, 2014. [Online; accessed 12-May-2014].
- [124] Engineering-abc, “Maximum tensile loading.” http://www.tribology-abc.com/calculators/e3_6d.htm, 2014. [Online; accessed 14-May-2014].
- [125] Plymouth-University, “Bolt ultimate strength calculator.” <http://www.tech.plymouth.ac.uk/sme/desnotes/boltb.htm>, 2014. [Online; accessed 14-May-2014].
- [126] Azom.com, “Titanium alloys - ti6al4v grade 5.” <http://www.azom.com/article.aspx?ArticleID=1547>, 2014. [Online; accessed 14-May-2014].
- [127] Supra-Alloys, “Titanium grade overview.” <http://www.supraalloys.com/titanium-grades.php>, 2014. [Online; accessed 14-May-2014].
- [128] H. Ford and J. M. Alexander, *Advanced Mechanics of Materials*. London, United Kingdom: Longmans, 1963.
- [129] T. P. Schmalzried, E. S. Szuszczewicz, M. R. Northfield, K. H. Akizuki, R. E. Frankel, G. Belcher, and H. C. Amstutz, “Quantitative assessment of walking activity after total hip or knee replacement,” *Journal of Bone and Joint Surgery*, vol. 80, pp. 54–59, 1998.

- [130] M. Barink, A. V. Kampen, M. D. W. Malefijt, and N. Verdonschot, “A three-dimensional dynamic finite element model of the prosthetic knee joint: simulation of joint laxity and kinematics,” *Proceedings of the Institution of Mechanical Engineers, Part H: Journal of Engineering in Medicine*, vol. 219(6), pp. 415–424, 205.
- [131] “Adl-force 5 simulator user manual.” AMTI Force and Motion, november 2010.
- [132] “Iso standard 14243-3, implants for surgery - wear of total knee-joint prostheses - part 3: Loading and displacement parameters for wear-testing machines with displacement control and corresponding environmental conditions for test.” International Organisation for Standardization, 2004.
- [133] Tekscan, “Flexiforce elf user manual.” <http://www.tekscan.com/flexible-force-sensors>, august 2013.
- [134] RoyMech, “Gear efficiency.” http://www.roymech.co.uk/Useful_Tables/Drive/Gear_Efficiency.html, 2013. [Online; accessed 14-May-2014].
- [135] AST-Bearings, “F5-12m thrust ball bearings.” <http://www.astbearings.com/product.html?product=F5-12M>, 2014. [Online; accessed 12-June-2014].
- [136] V. S. Bagad, *Mechatronics*. Pune, India: Pune, Technical Publications, 2009.

Publications

International Conference Articles

- A. Collo, S. Almouahed, P. Poignet, C. Hamitouche, and E. Stindel, "Towards a Dynamic Tibial Component for Postoperative Fine-tuning Adjustment of Knee Ligament Imbalance," in *Proceedings of the International Conference on Biomedical Electronics and Devices (Biodevices 2013)*, (Barcelona, Spain), pp. 95-102, february 2013.
- A. Collo, P. Poignet, C. Hamitouche, S. Almouahed, and E. Stindel, "An Active Tibial Component for Postoperative Fine-tuning Adjustment of Knee Ligament Imbalance," in *Proceedings of the 5th IEEE/RAS-EMBS International Conference on Biomedical Robotics and Biomechatronics (BioRob 2014)*, (Sao Paulo, Brasil), pp. 126-131, august 2014.
- A. Collo, P. Poignet, C. Hamitouche, S. Almouahed, and E. Stindel, "A Miniaturised Actuation System Embedded in an Instrumented Knee Implant for Postoperative Ligament Imbalance Correction," in *Proceedings of the 36th Annual International Conference of the IEEE Engineering in Medicine and Biology Society (EMBC 2014)*, (Chicago, Illinois, USA), pp. 6211-6214, august 2014.

International Journal Articles

SUBMITTED:

- A. Collo, S. Almouahed, C. Hamitouche, P. Poignet, and E. Stindel, "Design and Evaluation of an Actuated Knee Implant for Postoperative Ligament Imbalance Correction," submitted to *IEEE Transactions on Biomedical Engineering*, september 2014.

List of Figures

1.1	the human Knee Joint (source: unknown)	5
1.2	the Lower Limb Mechanical Axis [4]	6
1.3	the anatomical planes of the human body (source: unknown)	7
1.4	the concept of body midline (source: unknown)	8
1.5	the four degrees of freedom of the human Knee Joint (source: unknown)	9
1.6	comparison between normal and osteoarthritis conditions in human knee (source: unknown)	10
1.7	examples of hinge knee prosthesis [4]	11
1.8	current model of total knee prosthesis before and after primary TKA surgery www.yoursurgery.com	12
1.9	TKA surgery restores full KJ function www.jcl.com	12
1.10	bone resection in TKA surgery includes seven different bone cuts www.orthopaedics.co.uk	13
1.11	optimal flexion and extension gaps are rectangular and same size [4]	15
1.12	example of revision TKA procedure www.gocomplexjoint.com	16
1.13	comparison of two failed primary TKA implants (left) and their corre- sponding revisions (right) [37]	18
2.1	example of a cutting tool for TKA, with details on two different types of oscillating blades, employed with cutting slots during primary TKA [39], www.wheelessonline.com	20
2.2	examples of standard frame (left) and customizable frame (center and right) for femur resection [4, 40]	21

2.3	example of use of knee spreaders for bone resection during primary TKA www.innomed.net	21
2.4	example of combined use of a navigation system and a knee spacer equipped with reflecting marks during TKA www.brainlab.com, [58]	22
2.5	a simplified representation of the robotized spacer employed with a nav- igation system [61]	23
2.6	the second version of the robotized spacer [62]	24
2.7	the small force-sensing device and the forces it can measure [63]	25
2.8	the electronic knee prosthesis e-Knee [65]	25
2.9	the proposed instrumented tibial component (right) compared to a con- ventional one (left) [67]	26
2.10	the position of the four load cells embedded in the tibial tray (left) and the analysis of compression loads for the seven considered activities (right) [68]	27
2.11	design details and working principle of the smart knee prosthesis [70]	28
2.12	the genALIGN system with the instrumented tibial inlay (left), the femoral instrument (center) and an example of intraoperative use (right)[72]	29
2.13	three strain gauges are embedded in the instrumented tibial baseplate for the computation of the CoP of the total axial tibiofemoral load [75]	31
2.14	four PC elements are embedded in the instrumented tibial component for the computation of the net tibiofemoral force CoP trajectory [77]	33
2.15	a lax collateral ligament (left) can be properly re-tightened by laterally uplifting the tibial tray on the corresponding side (right)	35
3.1	flowchart of the envisaged protocol to restore optimal knee balance con- ditions	38
3.2	osteotomy results in adjusting tibiofemoral alignment conditions [82], www.orthopale.com	39
3.3	simplified representation of the prosthetic KJ during the proposed actu- ation	40
3.4	the total available volume offered by the tibial component to embed the actuation system	41

3.5	some examples of lower limb prosthetic implants	44
3.6	example of wireless interaction between the proposed instrumented knee implant and the clinician's computer during a follow-up visit	45
4.1	the leadscrew (red) drives the wedge (blue) inside its rail (cyan)	50
4.2	without any actuation, the mobile tibial tray (light brown) is fully contained inside the baseplate	51
4.3	the wedge translation laterally lifts the mobile tray up	52
4.4	the wedge dimensions (in mm)	53
4.5	dimensions and assembly of the tibial baseplate and the mobile tibial tray	54
4.6	comparison between a standard wedge (yellow, left) and the custom-designed wedge proposed in this work (pink, right)	55
4.7	the actuation system configuration selected for the static force analysis	56
4.8	during actuation, the full surface contact between the wedge and the mobile tibial tray becomes a line contact	56
4.9	free-body force diagram of the mobile tibial tray	58
4.10	free-body force diagram of the wedge	60
4.11	the contact areas (green) among system components during actuation .	61
4.12	conventional use of a wedge (blue) to lift up an object (brown) [111] . .	62
4.13	the lifting wedge model (left) approximates the proposed actuation system (right)	63
4.14	miniaturised balls can be embedded in the wedge in order to minimize friction losses	65
4.15	the wedge translation is driven by the leadscrew rotation	66
4.16	a standard screw-nut system [111]	66
4.17	the micromotor (grey) is embedded in the tibial baseplate [119, 120] . . .	68
4.18	the locking system copes with three main forces (black)	70
4.19	two miniature thrust ball bearings (green) support the two leadscrew ends	71
4.20	the mobile tibial tray lateral uplift linearly depends on the wedge translation	72

4.21	the elastic micro-membrane employed for the actuation system components sealing	73
4.22	two identical actuation systems are embedded inside the tibial baseplate	74
5.1	the first static analysis results	76
5.2	the stress distribution on the mobile tibial tray can be improved by means of smart design adjustments	77
5.3	the static analysis results after the optimisation study	78
5.4	the 3D-printed plastic prototype	81
5.5	the steel components of the proposed implant	82
5.6	the manufactured components assembled all together	83
5.7	the variations in the IER and APD settings	86
5.8	the prototype installed on the knee simulator in ZP configuration	86
5.9	the positioning of the two force sensors (green-coloured circular sensing areas)	88
5.10	$M_{\%}$ and $L_{\%}$ data at the simulated imbalance condition	89
5.11	$M_{\%}$ and $L_{\%}$ data after ten complete leadscrew revolutions	90
5.12	$M_{\%}$ and $L_{\%}$ data after fifteen complete leadscrew revolutions	91
5.13	$M_{\%}$ and $L_{\%}$ data after eighteen complete leadscrew revolutions	91
5.14	$M_{\%}$ and $L_{\%}$ data after twenty complete leadscrew revolutions	91
5.15	the tibiofemoral loads CoP position before and after actuation	93
6.1	a simplified representation of the instrumented tibial component and its embedded sub-parts	97
A.1	the tibial baseplate embeds four customised screw-nut mechanisms	104
A.2	the bottom part of the tibial baseplate partially embeds two gear trains, one per side	104
A.3	the proposed tibial component before (left) and after (right) actuation	105
A.4	a simplified representation of the instrumented tibial component and its embedded sub-parts	110

A.5 the 3D-printed plastic prototype of the actuated screws model 112

List of Tables

3.1	average peak tibiofemoral forces during common daily life activities, expressed as multiples of BW [88]	43
3.2	comparison of the three considered approaches for the realization of the actuation system embedded in the tibial tray	48
4.1	terms notation for the static force analysis	57
4.2	terms notation for the lifting wedge equation	62
4.3	corresponding terms between the lifting wedge model and the proposed actuation system	63
4.4	terms notation for the standard screw-nut system equation	66
4.5	corresponding terms between the screw-nut system and the proposed WL system	67
4.6	the locking system experiences higher reaction forces	70
5.1	the main optimisation steps	78
5.2	the minor design changes considered for the components manufacturing	81
5.3	the mobile tibial tray was assessed as stable (✓) in 15 different configurations	86
5.4	the results of the force sensors tests	92
A.1	the gear train parameters	105
A.2	definition of the screw-nut equation terms	106
A.3	qualitative comparison between the two proposed actuation systems . .	113

**Étude, Mise en Œuvre et
Évaluation d'une Prothèse
Instrumentée de Genou pour la
Correction du Déséquilibre
Ligamentaire Postopératoire**

synthèse en français du manuscrit de thèse

Abréviations

AP	AntéroPostérieur
ATG	Arthroplastie Totale de Genou
EPE	Éléments PiézoÉlectriques
ML	MédioLatéral
PTG	Prothèse Totale de Genou
RIE	Rotation Interne-Externe
TAP	Translation Antéro-Postérieure
3D	TriDimensionnel

Table des matières

1	Introduction	1
1.1	Contexte Clinique	1
1.2	Prothèse Totale de Genou	2
2	État de l'Art	5
2.1	Outils d'Assistance au Chirurgien	5
2.2	Un Composant Tibial Original	6
2.3	Objectifs de cette Thèse	7
3	Besoins Cliniques	9
3.1	Protocole Envisagé	9
3.2	Contraintes	10
4	Système d'Actionnement	11
4.1	Principe de Fonctionnement	11
4.2	Analyse Mécanique	12
4.3	Discussion	14
5	Validation Expérimentale	17
5.1	Simulations 3D	17
5.2	Prototypage	18
5.3	Tests de Stabilité	18

5.4 Capteurs de Force	19
6 Conclusion	21
Bibliographie	23

1.1 Contexte Clinique

Au cours des dernières décennies, l'amélioration des techniques associées aux Gestes Médico-Chirurgicaux Assistés par Ordinateur (GMCAO) a permis le développement d'un ensemble d'outils aidant le praticien dans la préparation et la réalisation de leurs gestes diagnostiques et thérapeutiques. Grâce à l'assistance fournie par ces systèmes, les praticiens ont désormais la possibilité d'opérer avec une précision et une efficacité plus élevées, tout en minimisant l'invasivité du geste réalisé [1]. En ayant comme objectif principal l'évaluation et le traitement de données médicales multimodales, la conception d'outils originaux s'appuie sur plusieurs domaines de recherche tels que l'ingénierie, la robotique, la biomécanique et le traitement de l'information. Il est désormais possible de définir pour chaque patient un traitement de plus en plus personnalisé et efficace, ce qui apporte des avantages aussi pour les praticiens. Pour cette raison, les GMCAO sont considérés aujourd'hui comme l'avenir de la chirurgie et la recherche dans cette direction vise à la fois à l'amélioration des systèmes déjà existants et au développement de nouvelles techniques.

L'Arthroplastie Totale de Genou (ATG) consiste à remplacer les structures osseuses blessées ou endommagées de l'articulation par une prothèse [2]. Le chirurgien orthopédique doit réussir à mettre en place un compromis optimal entre stabilité et mobilité [3], de façon à rétablir une fonctionnalité postopératoire appropriée de l'articulation opérée [4]. En termes généraux, l'application de techniques GMCAO à cette chirurgie permet au chirurgien :

- en préopératoire, de planifier de manière très précise les coupes osseuses le moins invasives possible et la taille optimale de l'implant à installer ;
- pendant la chirurgie (phase peropératoire), de vérifier en temps réel le positionnement approprié des composants prothétiques, suivant ce qui a été planifié.

Une phase clé de l'ATG consiste à mettre en place des conditions de tension appropriées au niveau des deux ligaments collatéraux du genou. Cette opération d'équilibrage ligamentaire est très délicate et directement liée à la durée de vie postopératoire de la prothèse implantée. Toute imprécision peropératoire, en fait, risque de compromettre l'alignement des composants prothétiques par rapport à l'axe mécanique du membre inférieur, en limitant ainsi la mobilité de l'articulation. Malheureusement, aucun outil n'a encore été développé pour garantir une parfaite réussite de cette opération, qui reste entièrement à la charge du chirurgien [3, 5, 6]. Dans le cas de complications postopératoires beaucoup trop graves, la seule solution existante à l'heure actuelle est la chirurgie de reprise. Lors d'une seconde opération, une nouvelle prothèse de genou remplace la précédente pour rétablir encore une fois des conditions d'équilibre optimales et, par conséquent, la fonctionnalité de l'articulation [2].

Lors de son fonctionnement, une prothèse de genou est soumise à des contraintes qui évoluent au fil du temps suivant l'évolution morpho-fonctionnelle de l'individu. Le nombre des ATG augmente chaque année [7, 8], ainsi que celui des chirurgies de reprise (environ un dixième des ATG [1]). Par ailleurs, les imprécisions peropératoires sont presque inévitables. *“En conséquence, il est difficile d'imaginer que le positionnement choisi en peropératoire, sur la base d'informations multimodales, puisse être optimal et définitif en l'absence de réglages fins postopératoires”* [9].

Dans ce contexte, cette thèse s'inscrit dans un projet plus global qui a pour objectif le développement d'une prothèse instrumentée de genou qui soit capable de suivre l'évolution des conditions d'équilibre ligamentaire de l'articulation en postopératoire. L'implant doit être à même de détecter toute condition de laxité au niveau des ligaments collatéraux et, si nécessaire, de la compenser en modifiant la position relative entre les composants prothétiques. Cette action est censée être suffisante pour rétablir des conditions d'équilibre optimales sans besoin d'une chirurgie de reprise. Comme discuté plus loin dans le présent manuscrit, ce projet ambitieux et fortement pluridisciplinaire fait face à de nombreux verrous technologiques et contraintes.

1.2 Prothèse Totale de Genou

Le genou est une articulation très complexe du corps humain [10]. Trois os (le fémur, le tibia et la rotule) sont mis en jeu par le biais d'un ensemble de surfaces articulaires et cartilages, qui assurent la fluidité des mouvements du genou. L'usure des cartilages peut survenir au fil des ans et limiter la mobilité de l'articulation. Lorsque cette usure donne lieu à des instabilités et de la douleur qui ne peuvent pas être soignées au moyen

de traitements médicaux spécifiques, une chirurgie (ATG) devient nécessaire pour la mise en place d'une Prothèse Totale de Genou (PTG).

Pendant l'ATG, une procédure de coupes osseuses permet la mise en place d'un composant fémoral et d'un composant tibial. Entre les deux, un insert souvent en polyéthylène est positionné de façon à rétablir la présence des cartilages endommagés qui ont été enlevés (Fig. 1.1). Les composants prothétiques remplacent la totalité des surfaces articulaires et leur positionnement lors de l'ATG doit être effectué de manière très précise. La PTG doit être alignée par rapport à l'axe mécanique du membre inférieur du patient et orientée de façon à garantir des conditions de tension appropriées au niveau des deux ligaments collatéraux du genou, qui sont les seuls tissus mous de l'articulation à ne pas être enlevés lors de la chirurgie [4]. La durée de vie d'une PTG se situe entre 15 et 20 ans.

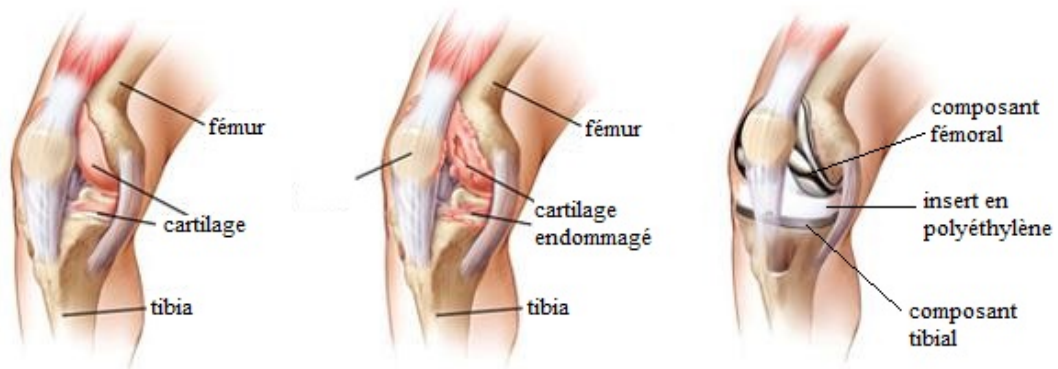


FIGURE 1.1 – l'articulation du genou avant et après l'ATG www.jcl.com

2.1 Outils d'Assistance au Chirurgien

Au cours des dernières décennies, différents outils ont été développés pour assister le chirurgien orthopédique au cours de l'ATG [11].

Quelques exemples d'écarteur instrumenté de genou peuvent être trouvés dans la littérature [12, 13, 14, 15]. En contrôlant des structures mécaniques miniaturisés, le chirurgien peut effectuer des mesures d'importants paramètres peropératoires et en monitorer l'évolution au cours de la chirurgie [16, 17].

Un autre type d'outils d'assistance est représenté par les plateformes tibiales instrumentées [18] : positionnées dans l'articulation après la phase des coupes osseuses et avant la mise en place des composants prothétiques, ces plateformes exploitent la présence de plusieurs capteurs embarqués pour effectuer des réglages fins en termes de tension ligamentaire. Malheureusement, ces ajustements ne sont optimaux que provisoirement : le remplacement des plateformes de mesure par les composants prothétiques introduit inévitablement des imprécisions peropératoires.

Dans ce contexte, le développement de prothèses instrumentées de genou est désormais considéré comme une voie très prometteuse vers des actes chirurgicaux de plus en plus précis et spécifiques au patient. Des PTG classiques ont commencé à être équipées avec des composants mécatroniques dédiés [19, 20], de manière à recueillir des données per- et postopératoires auparavant inaccessibles [21, 6, 22]. Outre l'amélioration de la qualité de l'opération chirurgicale elle-même, les prothèses instrumentées de genou s'avèrent être très utiles aussi pour les praticiens et les fabricants de prothèses [23].

2.2 Un Composant Tibial Original

Pour aborder le problème du déséquilibre ligamentaire du genou suite à l'ATG, notre équipe de recherche a proposé un modèle original de composant tibial de PTG [9]. Quatre Éléments PiézoÉlectriques (EPE) embarqués dans l'embase tibiale sont utilisés en tant que capteurs de force pour la mesure postopératoire de la répartition MédioLatérale (ML) et AntéroPostérieure (AP) des efforts tibiofémoraux lors de la marche [24] (Fig. 2.1). Les données recueillies par les EPE peuvent être traitées et transmises à l'extérieur de la prothèse grâce à un système de télémétrie miniaturisé [25]; ce dernier est censée être alimenté par les EPE mêmes, employés aussi comme générateurs d'énergie électrique [26]. Concernant le stockage de l'énergie et la communication sans fil opérés par la prothèse, un système à ultra-faible consommation d'énergie est actuellement en cours de développement.

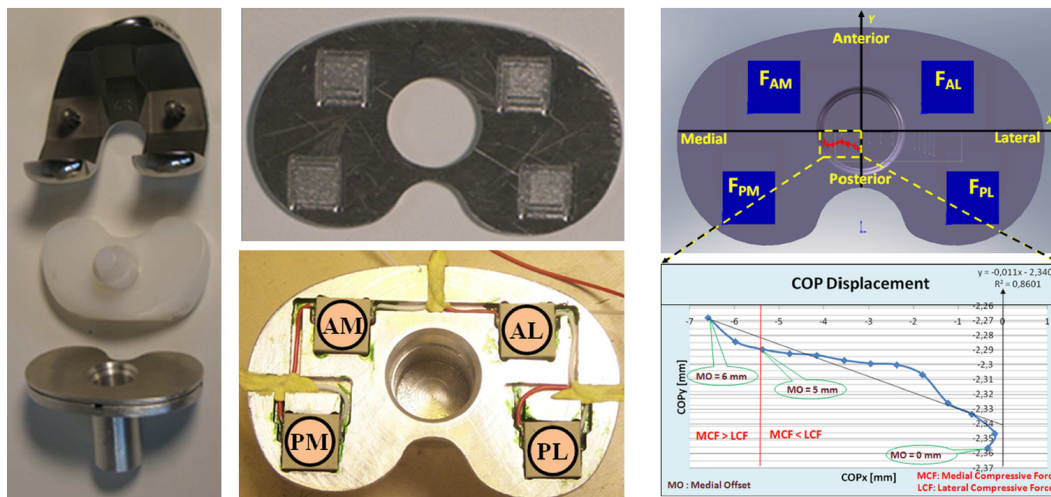


FIGURE 2.1 – quatre EPE sont embarqués dans l'embase tibiale [24]

Le composant tibial instrumenté proposé par notre équipe de recherche peut donc être utilisé comme suit :

En peropératoire - Après la mise en place des composants prothétiques, le genou opéré est manipulé par le chirurgien. Les EPE mesurent les forces tibiofémorales produites par les mouvements passifs de l'articulation, en donnant ainsi des indications précieuses pour achever une orientation optimale des composants prothétiques.

En postopératoire - Des visites médicales régulières sont programmées après la période de réhabilitation, afin de monitorer l'évolution des conditions d'équilibre de l'articulation. Lors de chaque visite, l'ensemble des données provenant des EPE

est utilisé pour créer une base de données spécifique au patient. Ce suivi postopératoire permet de détecter toute condition de déséquilibre ligamentaire qui peut se générer suite à l'évolution morpho-fonctionnelle du patient après l'ATG. Le chirurgien peut donc planifier des traitements appropriés pour prévenir de complications postopératoires plus graves.

2.3 Objectifs de cette Thèse

Ce travail de thèse s'inscrit dans la continuité logique de ces réalisations. Sur la base des informations issues des EPE, le chirurgien est à même de quantifier les conditions de laxité du ligament collatéral à l'origine du déséquilibre détecté. La tension du ligament relâché peut être rétablie de manière appropriée en ajustant l'inclinaison du plateau tibial de la prothèse (Fig. 2.2). Cette opération, réalisée avant la survenue de complications plus graves, est suffisante pour rétablir des conditions d'équilibre optimales sans besoin d'une seconde intervention chirurgicale.

Le soulèvement latéral du plateau tibial doit être réalisé par un système d'actionnement miniaturisé ; ce dernier doit être conçu et dimensionné de façon à répondre aux besoins cliniques tout en faisant face aux contraintes de biocompatibilité imposées par un milieu biologique tel que celui du genou. En termes généraux, le développement d'une telle prothèse de nouvelle génération devrait permettre, à long terme, de réduire le nombre des ATG de reprise.

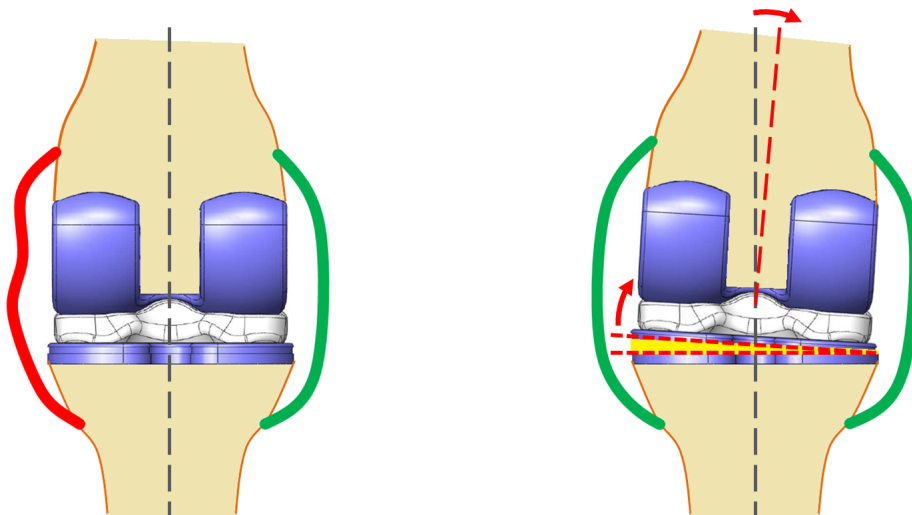


FIGURE 2.2 – un ligament collatéral relâché peut être retendu en postopératoire

3.1 Protocole Envisagé

Les données recueillies par les EPE permettent au chirurgien de quantifier les conditions de laxité du ligament collatéral à l'origine du déséquilibre détecté. Le soulèvement latéral du plateau tibial du côté correspondant au ligament relâché est effectué pour retendre ce dernier de façon optimale. Cette action stabilisatrice correspond à celle réalisée par les cales osseuses (ou coins) lors d'une ostéotomie du genou (Fig. 3.1) [27, 28, 29, 30] et ne doit pas compromettre l'alignement de la PTG par rapport à l'axe mécanique du membre inférieur [2, 4].

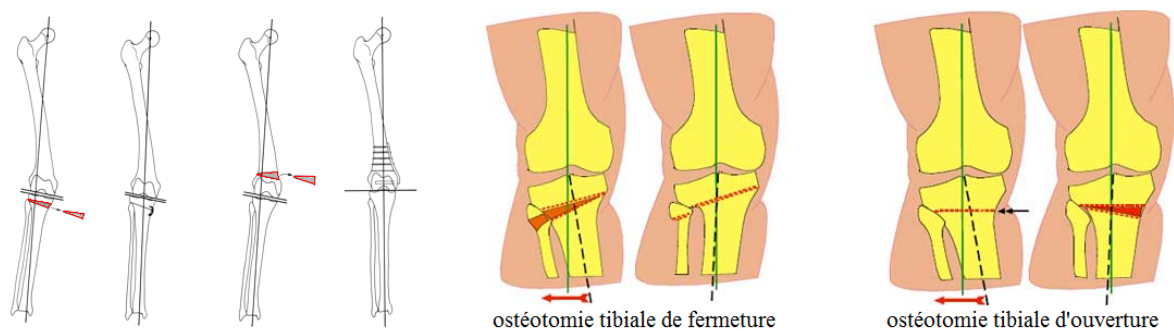


FIGURE 3.1 – exemples d'ostéotomie du genou [28], www.orthopale.com

L'inclinaison du plateau tibial est réglée par étapes successives. L'actionnement est réalisé une première fois et le plateau est verrouillé dans sa nouvelle position ; le patient est ensuite invité à marcher, de façon à vérifier, à l'aide des EPE, les nouvelles conditions de laxité ligamentaire. Si nécessaire, l'actionnement peut être effectué de nouveau en ajustant l'inclinaison du plateau tibial jusqu'à rétablir des conditions d'équilibre optimales.

3.2 Contraintes

Le système d'actionnement consiste en une structure mécanique miniaturisée contrôlée par un micromoteur [31]. Le tout doit être dimensionné de façon à pouvoir être embarqué dans le composant tibial d'une PTG. Outre l'épaisseur de la plateforme, la quille du composant tibial peut être aussi exploitée pour héberger le système d'actionnement et l'électronique nécessaire à son fonctionnement. En considérant les dimensions de la PTG prise en considération [32], le volume disponible est d'environ 50 cm³.

Le soulèvement latéral du plateau tibial doit pouvoir être effectué de façon très précise, en suivant le protocole envisagé présenté au chapitre précédent. Une fois rétablies les conditions d'équilibre optimales, la plateforme doit être verrouillée dans sa position inclinée de manière solide et robuste. Un système de blocage doit donc être prévu pour faire face aux charges tibiofémorales liées aux activités de la vie quotidienne [33, 34, 35].

Pour des raisons de biocompatibilité, l'alimentation et le contrôle du système d'actionnement doivent être réalisés à distance, sans fil. L'utilisation de techniques d'induction magnétique [36, 37, 38, 39, 40] peut représenter une possibilité efficace pour l'alimentation sans contact du micromoteur embarqué dans la prothèse. Cette solution serait préférable à l'utilisation d'une batterie, qui une fois déchargée ne pourrait être remplacée que par une opération chirurgicale. Le contrôle des composants électroniques embarqués dans la prothèse peut être réalisé par radiofréquence.

En termes plus généraux, la contrainte de biocompatibilité restreint fortement le choix des composants du système d'actionnement et en conditionne aussi la conception.

4.1 Principe de Fonctionnement

Le système d'actionnement [41] repose sur l'utilisation combinée d'une cale et une vis (standard M2x0.4 [42]), couplées dans l'embase tibiale par le biais d'un profil taraudé en commun (Fig. 4.1). La vis est positionnée de façon à pouvoir seulement tourner autour de son axe ; toute rotation de la vis produit une translation de la cale suivant le pas de vis du filetage (0.4 mm). Le mouvement de translation de la cale est unidirectionnel, étant guidé dans un rail spécifiquement prévu dans l'embase tibiale ; la course de la cale varie entre 0 et 10 mm.

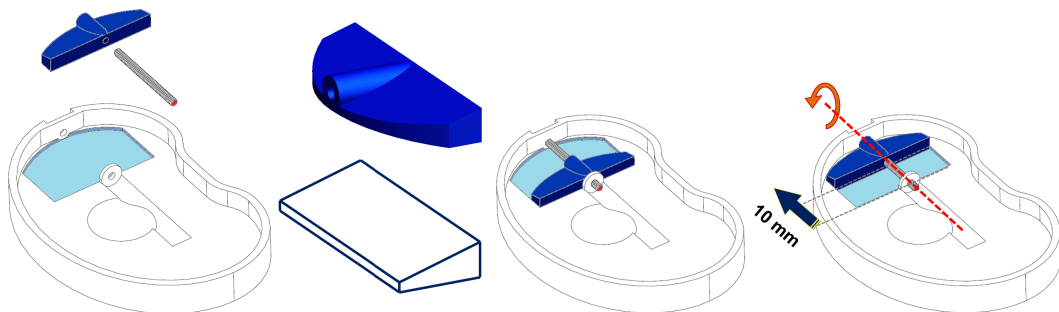


FIGURE 4.1 – la cale et la vis sont couplées dans l'embase tibiale

Les mouvements de rotation de la vis sont contrôlés par un micromoteur rotatif pas à pas rigidement fixé dans l'embase tibiale. Un plateau tibial mobile est positionné sur le système d'actionnement et, en position de départ (sans actionnement), est entièrement contenu dans l'embase tibiale. Lorsque la cale translate, elle glisse sous le plateau mobile en le soulevant latéralement (Fig. 4.2). La configuration d'actionnement complet correspond à une translation de la cale de 10 mm, ce qui produit un soulèvement latéral du plateau mobile de 3.6 mm.

L'embase tibiale contient deux systèmes d'actionnement identiques, un par côté, positionnés symétriquement par rapport à la quille du composant tibial. Chacune des

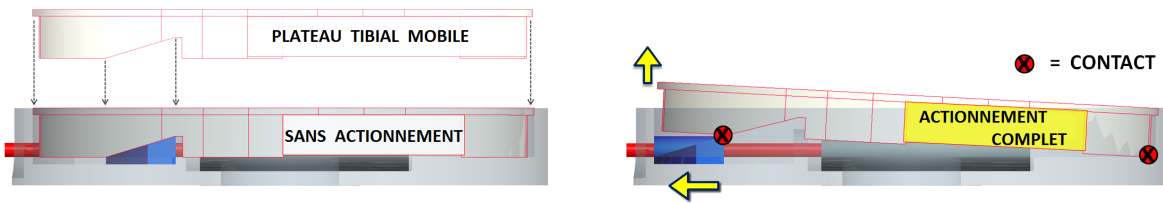


FIGURE 4.2 – le principe de fonctionnement du système d'actionnement

deux vis est contrôlée par un micromoteur rotatif pas à pas qui est responsable du soulèvement latéral du plateau tibial mobile.

4.2 Analyse Mécanique

Une cale est “*un organe simple permettant de transformer une charge appliquée en une autre, beaucoup plus grande, dans une direction approximativement perpendiculaire*” [43, p. 83]. Avec ses dimensions, la cale du système d'actionnement offre un avantage mécanique de $10/3$, ou 3.3 . Par conséquent, toute force d'entrée appliquée sur le plan de l'embase tibiale produit une force de sortie trois fois plus grande ; cette force de sortie est responsable du soulèvement du plateau tibial mobile.

L'actionnement est réalisé avec le patient en position allongée, de façon à éliminer la charge exercée par le poids corporel sur l'articulation. Pour réaliser le soulèvement latéral du plateau tibial, le système d'actionnement doit développer une force F_T capable de dépasser la résistance passive des deux ligaments collatéraux F_L . La valeur de F_L varie d'un individu à l'autre et a été estimée à 300 N de compression exercée par le fémur sur le tibia [11]. Cette force étant distribuée de manière uniforme sur le plateau tibial, chaque système d'actionnement fait face à 150 N de force de résistance.

Compte tenu de l'avantage mécanique de la cale, la force d'entrée minimum à fournir est $F_T = 50$ N. Les pertes dues au frottement entre les composants du système d'actionnement peuvent être minimisées en combinant les deux solutions de conception suivantes :

- la translation de la cale à l'intérieur du rail dans l'embase tibiale peut être réalisée par le biais de petites billes miniaturisées (comme dans le cas des butées à billes [44, 45, 46]) ;
- un traitement anti-frottement [47] peut être appliqué aux surfaces en contact (cale/embase, cale/plateau mobile) pour améliorer le glissement entre les composants.

Par précaution, la valeur de F_T peut être surdimensionnée à 65 N. Cette force doit être fournie à la cale par la translation de la vis, à laquelle le micromoteur rotatif pas à pas applique un couple T . La relation entre F_T et T est décrite par l'équation vis/cale suivante :

$$T = F_T \cdot r \cdot \frac{\tan \alpha + f \cdot \lambda}{1 - f \cdot \lambda \cdot \tan \alpha} \quad \text{avec :} \quad \lambda = \sqrt{1 + \tan^2(\theta/2) \cdot \cos^2(\alpha)}$$

$$\alpha = \arctan\left(\frac{p}{2 \cdot \pi \cdot r}\right)$$

terme	description	valeur	unité
T	couple appliqué à la vis	inconnu	mNm
F_T	force d'entrée à appliquer à la cale	65	N
r	rayon sur flancs de la vis	0.87 [42]	mm
p	pas de vis	0.4 [42]	mm
f	coefficient de frottement dans le filetage	0.36	-
α	angle d'hélice du filetage	4.18 [48]	deg
θ	angle du profil métrique du filetage	60 [48]	deg

TABLE 4.1 – termes de l'équation vis/cale

Le coefficient de frottement f est celui de l'alliage de titane (Ti-6Al-4V) choisi pour la réalisation du composant tibial et du système d'actionnement [4]. Le calcul de l'équation vis/cale avec les valeurs décrites dans le Tableau 4.1 donne la valeur $T = 28.6$ mNm. C'est le couple que le micromoteur doit fournir à la vis pour que la force de translation de la cale soit suffisante à soulever le plateau tibial mobile. Comme proposé précédemment, un traitement anti-frottement du filetage en commun entre la vis et la cale peut ultérieurement améliorer les conditions opérationnelles (voire diminuer la valeur de T nécessaire). De toute façon, toujours en considérant le principe de surdimensionnement, le micromoteur rotatif pas à pas qui a été sélectionné (Faulhaber ADM0620-2R-V2-05 [49]) avec son motoréducteur planétaire intégré (06/1 K 1024-1 [50]) est à même de fournir un couple intermittent maximal de 35 mNm. À titre d'exemple, l'équation vis/cale utilisée à l'inverse avec $T = 35$ mNm donne $F_T = 79.5$ N ; théoriquement, la force de sortie correspondante de la cale serait de 265 N, bien plus que les 150 N évoqués précédemment.

4.3 Discussion

Tous les composants électroniques nécessaires au fonctionnement du système d'actionnement (alimentation sans fil, contrôle à distance, système de télémétrie) devront être miniaturisés, de façon à être répartis entre l'embase tibiale et la quille du composant tibial. En considérant la présence du plateau mobile et des deux systèmes d'actionnement (un de chaque côté, Fig. 4.3), la plateforme tibiale a une épaisseur totale de 9 mm (environ deux fois plus épaisse que la PTG de départ [32]).

Après l'actionnement, le maintien en position inclinée du plateau tibial mobile est garanti par un système de blocage passif obtenu grâce aux deux choix de conception suivants :

- l'angle d'hélice du filetage en commun entre la cale et la vis est conçu de façon à être mécaniquement irréversible. Par conséquent, la translation de la cale (que les efforts cycliques tibiofémoraux repoussent vers sa position de départ) ne peut pas entraîner la vis en rotation et, donc, ne peut pas avoir lieu ;
- deux butées à billes miniaturisées sont fixées aux deux extrémités de la vis (de couleur verte sur la Fig. 4.3). En plus de permettre la rotation libre de la vis autour de son axe presque sans frottement, les deux butées absorbent toute charge axiale transmise à la vis [44, 45, 46]. Cela est fondamental pour éviter toute sollicitation de l'arbre du micromoteur, qui peut supporter une force axiale de 5 N maximum [50].

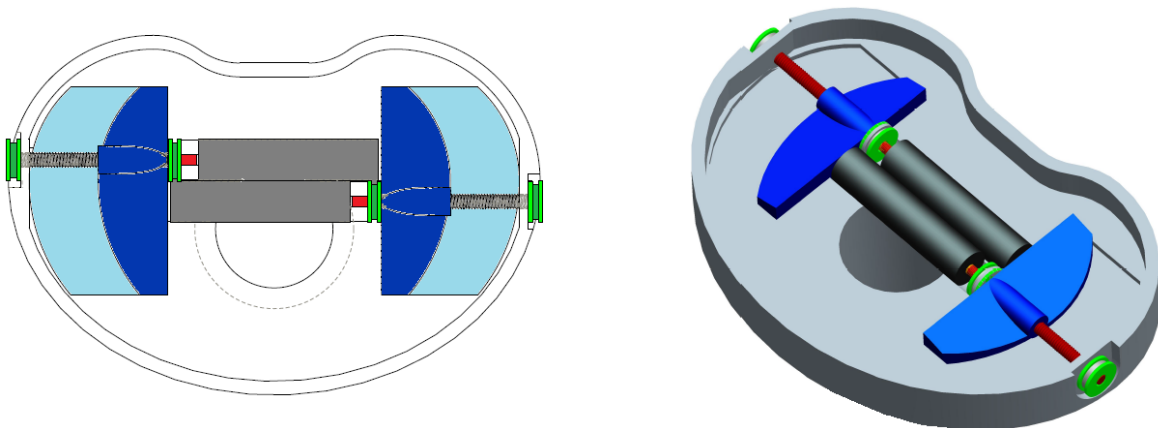


FIGURE 4.3 – l'embase tibiale contient deux systèmes d'actionnement identiques

Il existe une relation linéaire entre la translation de la cale (0–10 mm) et le soulèvement latéral du plateau tibial mobile (0–3.6 mm). Compte tenu du pas de vis (0.4 mm) et du pas angulaire du moteur (18 deg [49]), l'inclinaison du plateau mobile peut être estimée a priori et ajustée de façon très précise.

Les pièces mécaniques et les composants électroniques du système d'actionnement ne doivent pas être exposés au liquide synovial qui lubrifie l'articulation du genou. Des revêtements biocompatibles sont prévus à cet effet, ainsi que l'utilisation d'une micro-membrane élastique à fixer entre l'embase tibiale et le plateau tibial mobile : cette membrane est supposée s'adapter passivement au soulèvement latéral du plateau, de façon à créer un volume étanche à l'intérieur de l'embase tibiale.

À priori, le système d'actionnement peut être mis à l'échelle et embarqué dans des PTG de taille différente [32] ; par précaution, l'analyse mécanique devrait être conduite de nouveau au cas par cas. Des problèmes pourraient survenir lors de la recherche d'un actionneur adapté : un micromoteur autant puissant que celui sélectionné ([49, 50]) mais moins encombrant pourrait ne pas exister à l'heure actuelle. Ce verrou technologique doit être traité très attentivement.

5.1 Simulations 3D

Le composant tibial instrumenté a été d'abord défini à l'aide d'un logiciel de modélisation TriDimensionnel (3D). Une première phase de simulations 3D a permis d'évaluer l'efficacité des choix de conception, ainsi que la robustesse des pièces mécaniques du système d'actionnement.

Le plateau tibial mobile a été bloqué en position complètement actionnée (3.6 mm de soulèvement latéral) et soumis à une force statique de 2600 N, qui correspond à la charge tibiofémorale maximale agissant à l'intérieur du genou lors de la marche [33]. Les résultats des analyses statiques ont indiqué une bonne résistance du plateau mobile aux efforts simulés. Une étude d'optimisation a été également conduite pour optimiser la conception du plateau mobile de façon à en améliorer la robustesse, ainsi que la distribution des efforts sur sa surface inférieure.

Une analyse de flambage a permis d'estimer la déformation permanente du plateau tibial mobile lors d'une charge de $1.976 \cdot 10^6$ N (environ 200000 kg). En outre, une analyse en fatigue a été conduite pour estimer la durée de vie du plateau mobile en termes de cycles de marche : avec une charge maximale de 2600 N [33], le plateau mobile fixé en position inclinée est supposé casser après $1.3 \cdot 10^{18}$ cycles de marche. Un patient très actif, après l'ATG, effectue en moyenne $4.7 \cdot 10^7$ cycles de marche [51, 9] ; par rapport à cette valeur de référence, théoriquement, la PTG actionnée résiste à un nombre de cycles $2.7 \cdot 10^{10}$ fois supérieur.

Les résultats des simulations 3D ont permis de conclure qu'aucune défaillance mécanique des composants prothétiques ne devrait avoir lieu. L'étape suivante a consisté en la fabrication d'un prototype du composant tibial instrumenté.

5.2 Prototypage

Un premier prototype en plastique du composant tibial instrumenté a été réalisé à l'aide d'une imprimante 3D. Après avoir validé le principe de fonctionnement du système d'actionnement, un prototype à taille réelle de l'implant a été fabriqué en acier (Fig. 5.1). Le système d'actionnement a été assemblé dans l'embase tibiale et le composant tibial a été installé sur un simulateur du genou (ADL-Force 5 Simulator, AMTI Force and Motion [52]) pour procéder à la phase d'expérimentation.



FIGURE 5.1 – le prototype en acier du composant tibial instrumenté

Un simulateur du genou est une machine capable de reproduire les conditions in vivo de l'articulation du genou de façon très réaliste ; des essais fiables et reproductibles d'implants prothétiques peuvent donc être réalisés. Dans ce travail, des tests de stabilité et des essais à l'aide de deux capteurs de force ont été définis pour l'évaluation du prototype en acier du composant tibial instrumenté proposé.

5.3 Tests de Stabilité

Différentes configurations du composant tibial ont été considérées pour l'évaluation de la stabilité du plateau mobile lors de plusieurs cycles de marche simulés. Les paramètres de Rotation Interne-Externe (RIE) et de Translation Antéro-Postérieure (TAP)

du prototype par rapport au composant fémoral ont été modifiés manuellement par l'intermédiaire de l'interface du simulateur ; cela a permis de recréer 15 différents scénarios de marche, correspondant chacun à une condition de sous-optimalité en termes de position relative entre les composants prothétiques [53].

Un nombre total de $9 \cdot 10^3$ cycles de marche (force tibiofémorale maximale 2600 N, cycle de marche 1 s [33]), distribués entre trois conditions d'actionnement différentes (0, 1.8 et 3.6 mm de soulèvement latéral du plateau tibial mobile), a été simulé. Pour chacune des 15 configurations étudiées, aucun mouvement incontrôlé du plateau mobile incliné n'a eu lieu : sans présenter aucune vibration ni oscillation inattendues, le plateau a solidement conservé sa position au cours des essais. La stabilité de l'implant actionnée, ainsi que les choix de conception faits à cet effet, ont donc été validés.

5.4 Capteurs de Force

Deux capteurs de force Tekscan FlexiForce B201 [54] ont été employés pour la mesure des forces tibiofémorales agissant sur le prototype lors des cycles de marche simulés. Les deux capteurs ont été positionnés sur la surface supérieure du plateau tibial mobile, symétriquement par rapport au centre géométrique de ce dernier (Fig. 5.2) ; chacun des deux capteurs est ainsi responsable de la mesure des charges appliquées sur un seul compartiment de la prothèse.

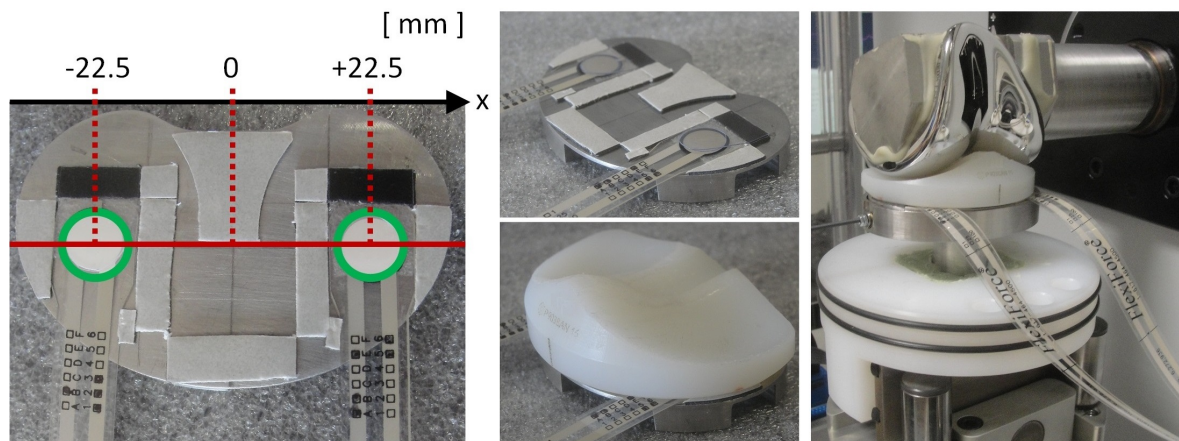


FIGURE 5.2 – les deux capteurs de force positionnés sur le plateau tibial mobile

La laxité du ligament collatéral latéral (externe) du genou a été recréée au simulateur en combinant les valeurs de RIE et TAP précédemment considérées pour les tests de stabilité. Cette condition de déséquilibre a compromis le contact uniforme entre les composants prothétiques, en donnant lieu ainsi à une distribution non homogène des

charges tibiofémorales entre les deux compartiments du plateau tibial mobile. Afin de permettre une interprétation plus immédiate des mesures expérimentales, la sollicitation pourcentage des capteurs de force par rapport à leur dynamique (0–4448 N [54]) a été choisie pour l’affichage des données recueillies. Dans les figures et tableaux qui suivent, les valeurs mesurées par les capteurs médial et latéral sont indiquées respectivement comme $M_{\%}$ et $L_{\%}$.

Le protocole d’actionnement proposé dans le chapitre 3.1 a été mis en œuvre. En amont de toute correction, les charges tibiofémorales étaient concentrées sur le compartiment médial du plateau tibial (Fig. 5.3). Quatre opérations d’actionnement successives (10, 15, 18 et 20 rotations totales de la vis) ont été nécessaires pour obtenir la superposition des données recueillies par les deux capteurs de force (Fig. 5.3) : cette condition a été supposée correspondre à l’optimalité des conditions d’équilibre, avec une sollicitation homogène des deux compartiments du plateau tibial.

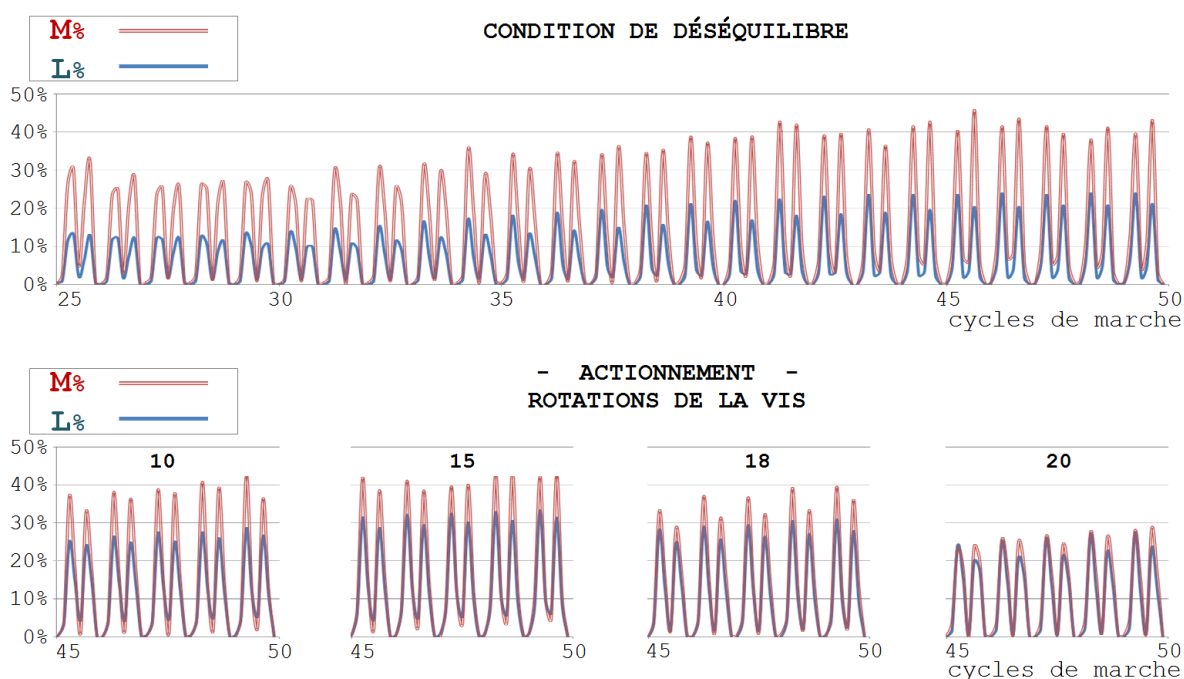


FIGURE 5.3 – les données $M_{\%}$ and $L_{\%}$ recueillies par les deux capteurs de force

Les essais expérimentaux à l’aide des capteurs de force ont permis d’évaluer l’efficacité du protocole d’actionnement envisagé pour rétablir des conditions d’équilibre optimales. Le soulèvement latéral du plateau tibial mobile obtenu par le biais du système d’actionnement a été validé donc comme voie prometteuse pour compenser en postopératoire des conditions de laxité des ligaments collatéraux du genou. Cette étape de validation expérimentale était considérée essentielle pour la planification de futurs travaux.

L'objectif de cette thèse est de proposer un modèle original de prothèse instrumentée de genou pour le suivi et l'évaluation des conditions d'équilibre ligamentaire de l'articulation après la chirurgie d'ATG. Le composant tibial de PTG proposé par notre équipe de recherche [9], déjà capable de détecter toute condition de laxité au niveau des deux ligaments collatéraux du genou, a été équipé d'un système d'actionnement miniaturisé [41]. Ce dernier, embarqué dans l'embase tibiale, a été dimensionné de façon à pouvoir soulever latéralement le plateau tibial de la prothèse du côté correspondant au ligament collatéral relâché; cette opération est suffisante pour rétablir des conditions d'équilibre optimales en postopératoire, sans passer par une chirurgie de reprise.

La conception du système d'actionnement a été réalisée en tenant compte de la présence de quatre EPE positionnés dans l'embase tibiale pour la détection de toute condition de déséquilibre ligamentaire (Fig. 6.1). La structure mécanique proposée repose sur la combinaison d'une cale et une vis; la rotation de cette dernière, contrôlée par un micromoteur rotatif pas à pas [49, 50], produit la translation de la cale. L'avantage mécanique de la cale permet de produire une force suffisante pour réaliser le soulèvement latéral du plateau tibial mobile [43]. Le maintien en position du plateau tibial après l'actionnement est garanti par l'irréversibilité du filetage en commun entre la cale et la vis; ce système de blocage passif est indispensable pour faire face aux efforts tibiofémoraux qui se produisent dans le genou lors de plusieurs activités de la vie quotidienne [33, 34, 35].

En répondant aux besoins cliniques et aux contraintes imposées par un milieu biocompatible tel que celui du genou, l'analyse mécanique du système d'actionnement a permis d'évaluer d'un point de vue théorique le bon rendement et l'efficacité des choix de conception. Un premier prototype à taille réelle du composant tibial a été réalisé à l'aide d'une imprimante 3D pour la validation du principe de fonctionnement du système proposé [41]. Dans un second temps, la fabrication d'un prototype en acier à taille réelle a permis de conduire des essais expérimentaux à l'aide d'un simulateur de genou. Globalement, les résultats très prometteurs de l'étape de validation expérimentale ont

donné des indications précieuses pour l'amélioration de la conception du système et pour la planification de futurs travaux.

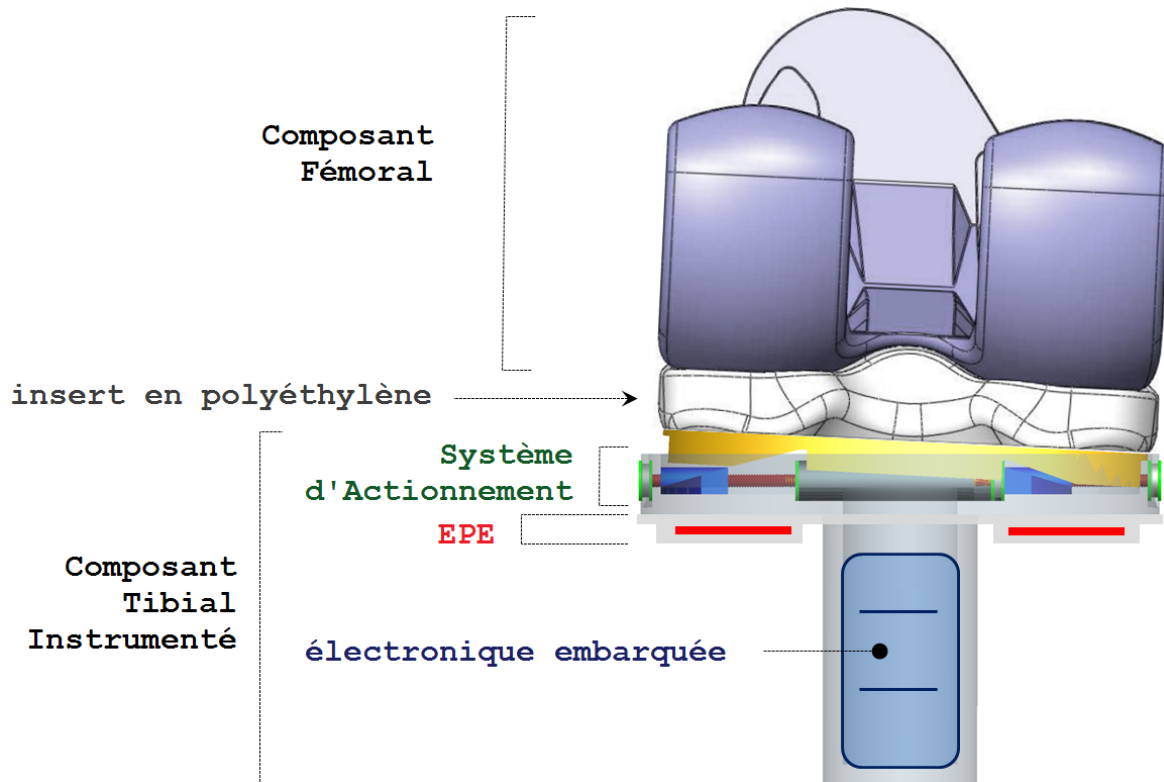


FIGURE 6.1 – le composant tibial instrumenté proposé

Bibliographie

- [1] E. Dombre, M. DeMathelin, and J. Troccaz, “Medical robotics : Characteristics and state of the art,” in *Medical Robotics* (J. Troccaz, ed.), London, United Kingdom : ISTE Ltd., 2012.
- [2] G. R. Scuderi and A. J. Tria, *Knee Arthroplasty Handbook : Techniques in Total Knee and Revision Arthroplasty*. New York, NY : Springer, 2006.
- [3] M. J. Winemaker, “Perfect balance in total knee arthroplasty : the elusive compromise,” *Journal of Arthroplasty*, vol. 17(1), pp. 2–10, 2002.
- [4] T. P. Vail and J. E. Lang, “Surgical techniques and instrumentation in total knee arthroplasty,” in *Surgery of The Knee* (W. N. Scott, ed.), Philadelphia, MS : Churchill Livingstone, 2006.
- [5] F. Schmidt, F. Lampe, and R. Elfring, “Soft-tissue management in primary knee arthroplasty : common techniques, navigation and force-sensing devices,” *Zeitschrift fur Orthopadie und Unfallchirurgie*, vol. 145(5), pp. 599–607, 2007.
- [6] F. Zimmermann, C. Schwenninger, U. Nolten, F. P. Firmbach, R. Elfring, and K. Radermacher, “A new approach to implant alignment and ligament balancing in total knee arthroplasty focussing on joint loads,” *Biomedizinische Technik - Biomedical engineering*, vol. 57(4), pp. 283–291, 2012.
- [7] C. Lavernia, D. J. Lee, and V. H. Hernandez, “The increasing financial burden of knee revision surgery in the united states,” *Clinical Orthopaedics and Related Research*, vol. 446, pp. 221–226, 2006.
- [8] S. Kurtz, K. Ong, E. Lau, F. Mowat, and M. Halpern, “Projections of primary and revision hip and knee arthroplasty in the united states from 2005 to 2030,” *Journal of Bone and Joint Surgery*, vol. 89(4), pp. 780–785, 2007.
- [9] S. Almouahed, *Study, implementation and evaluation of a prototype of self-powered diagnostic knee implant*. PhD thesis, Telecom Bretagne, Brest, june 2011.
- [10] A. Faller and M. Schuenke, *The Human Body : an Introduction to Structure and Function*. New York, NY : Thieme, 2004.

- [11] C. Marmignon, *Modeles et instruments robotises pour l etude biomecanique per-operatoire de l equilibre ligamentaire du genou*. PhD thesis, Universite Joseph Fourier, Grenoble, France, december 2004.
- [12] K. Tanaka, H. Muratsu, K. Mizuno, R. Kuroda, S. Yoshiya, and M. Kurosaka, “Soft tissue balance measurement in anterior cruciate ligament-resected knee joint : cadaveric study as a model for cruciate-retaining total knee arthroplasty,” *Journal of Orthopaedic Science*, vol. 12, pp. 149–153, 2007.
- [13] Y. H. Kim, K. S. Sohn, and J. S. Kim, “Range of motion of standard and high-flexion posterior stabilized total knee prostheses. a prospective, randomized study,” *Journal of Bone and Joint Surgery*, vol. 87(A), pp. 1470–1475, 2005.
- [14] C. Marmignon, A. Leimnei, and P. Cinquin, “Robotized distraction device for knee replacement surgery,” *International Congress Series*, vol. 1268, pp. 638–643, 2004.
- [15] C. Marmignon, A. Leimnei, S. Lavallee, and P. Cinquin, “Automated hydraulic tensor for total knee arthroplasty,” *International Journal of Medical Robotics and Computer Assisted Surgery*, vol. 1(4), pp. 51–57, 2005.
- [16] M. Swank, J. R. Romanowski, L. L. Korbee, and S. Bignozzi, “Ligament balancing in computer-assisted total knee arthroplasty : improved clinical results with a spring-loaded tensioning device,” *Proceedings of the Institution of Mechanical Engineers - part H - Journal of Engineering in Medicine*, vol. 221(7), pp. 755–761, 2007.
- [17] S. M. Kim, Y. S. Park, C. W. Ha, S. J. Lim, and Y. W. Moon, “Robot-assisted implantation improves the precision of component position in minimally invasive tka,” *Orthopedics*, vol. 35(9), pp. e1334–e1339, 2012.
- [18] D. Crottet, T. Maeder, D. Fritschy, H. Bleuler, L. P. Nolte, and I. P. Pappas, “Development of a force amplitude- and location-sensing device designed to improve the ligament balancing procedure in tka,” *IEEE Transactions on Biomedical Engineering*, vol. 52(9), pp. 1609–1611, 2005.
- [19] F. Graichen, R. Arnold, A. Rohlmann, and G. Bergmann, “Implantable 9-channel telemetry system for in vivo load measurements with orthopedic implants,” *IEEE Transactions on Biomedical Engineering*, vol. 54(2), pp. 253–261, 2007.
- [20] H. Chen, M. Liu, W. Wan, C. Jia, C. Zhang, and Z. Wang, “Low-power circuits design for the wireless force measurement system of the total knee arthroplasty,” in *2010 Annual International Conference of the IEEE Engineering in Medicine and Biology Society (EMBC)*, (Buenos Aires, Argentina), pp. 3539–3542, september 2010.
- [21] M. E. Hardwick, P. A. Pulido, D. D. D’Lima, and C. W. Colwell, “e-knee : the electronic knee prosthesis,” *Orthopaedic Nursing*, vol. 25(5), pp. 326–329, 2006.

- [22] A. Arami, M. Simoncini, O. Atasoy, W. Hasenkamp, A. Bertsch, E. Meurville, S. Tanner, P. Renaud, C. Dehollain, P. A. Farine, B. M. Jolles, K. Aminian, and P. Ryser, “Instrumented knee prosthesis for force and kinematics measurements,” *IEEE Transactions on Automation Science and Engineering*, vol. 10, pp. 615–624, 2013.
- [23] A. Mundermann, C. O. Dyrby, D. D. D’Lima, C. W. Colwell, and T. P. Andriacchi, “In vivo knee loading characteristics during activities of daily living as measured by an instrumented total knee replacement,” *Journal of Orthopaedic Research*, vol. 26(9), pp. 1167–1172, 2008.
- [24] S. Almouahed, M. Gouriou, C. Hamitouche, E. Stindel, and C. Roux, “Design and evaluation of instrumented smart knee implant,” *IEEE Transactions on Biomedical Engineering*, vol. 58(4), pp. 971–982, 2011.
- [25] C. Lahuec, S. Almouahed, M. Arzel, D. Gupta, C. Hamitouche, M. Jezequel, E. Stindel, and C. Roux, “A self-powered telemetry system to estimate the post-operative instability of a knee implant,” *IEEE Transactions on Biomedical Engineering*, vol. 58(3), pp. 822–825, 2011.
- [26] S. Almouahed, M. Gouriou, C. Hamitouche, E. Stindel, and C. Roux, “The use of piezoceramics as electrical energy harvesters within instrumented knee implant during walking,” *IEEE/ASME Transactions on Mechatronics*, vol. 16(5), pp. 799–807, 2011.
- [27] T. Koshino, T. Murase, and T. Saito, “Medial opening-wedge high tibial osteotomy with use of porous hydroxyapatite to treat medial compartment osteoarthritis of the knee,” *Journal of Bone and Joint Surgery*, vol. 85A(1), pp. 78–85, 2003.
- [28] J. M. Wright, H. C. Crockett, D. P. Slawski, M. W. Madsen, and R. E. Windsor, “High tibial osteotomy,” *Journal of the American Academy of Orthopaedic Surgeons*, vol. 13, pp. 279–289, 2005.
- [29] G. Puddu, M. Cipolla, G. Cerullo, V. Franco, and E. Gianni, “Which osteotomy for a valgus knee?,” *International Orthopaedics*, vol. 34(2), pp. 239–247, 2009.
- [30] C. Sherman and M. E. Cabanela, “Closing wedge osteotomy of the tibia and the femur in the treatment of gonarthrosis,” *International Orthopaedics*, vol. 34(2), pp. 173–184, 2010.
- [31] A. Collo, S. Almouahed, P. Poignet, C. Hamitouche, and E. Stindel, “Towards a dynamic tibial component for postoperative fine-tuning adjustment of knee ligament imbalance,” in *Proceedings of the International Conference on Biomedical Electronics and Devices (Biodevices 2013)*, (Barcelona, Spain), pp. 95–102, february 2013.

- [32] “Genesis 2 system versatility.” Smith and Nephew Richards Inc. - Genesis 2 Total Knee System, april 1997.
- [33] “Iso standard 14243-1, implants for surgery - wear of total knee-joint prostheses - part 1 : Loading and displacement parameters for wear-testing machines with load control and corresponding environmental conditions for test.” International Organisation for Standardization, 2009.
- [34] D. D. D’Lima, N. Steklov, S. Patil, and C. W. Colwell, “The mark coventry award : in vivo knee forces during recreation and exercise after knee arthroplasty,” *Clinical Orthopaedics and Related Research*, vol. 466(11), pp. 2605–2611, 2008.
- [35] D. D. D’Lima, B. J. Fregly, S. Patil, N. Steklov, and C. W. Colwell, “Knee joint forces : prediction, measurement, and significance,” *Proceedings of the Institution of Mechanical Engineers, Part H : Journal of Engineering in Medicine*, vol. 226(2), pp. 95–102, 2012.
- [36] C. P. Townsend, S. W. Arms, and M. J. Hamel, “Remotely powered, multichannel, microprocessor based telemetry systems for smart implantable total knee implant,” in *Proceedings of SPIE’s 6th Annual International Conference on Smart Structures and Materials*, (Newport Beach, California, USA), march 1999.
- [37] S. W. Arms, M. J. Hamel, and C. P. Townsend, “Multi-channel structural health monitoring network, powered and interrogated using electromagnetic fields,” in *International SAMPE Symposium and Exhibition - Society for the Advancement of Material and Process Engineering*, (Baltimore, Maryland, USA), june 2007.
- [38] D. Crescini, E. Sardini, and M. Serpelloni, “An autonomous sensor for force measurements in human knee implants,” in *Proceedings of the Euroensors XXIII Conference*, (Lausanne, Switzerland), pp. 718–721, september 2009.
- [39] D. Crescini, E. Sardini, and M. Serpelloni, “Design and test of an autonomous sensor for force measurements in human knee implants,” *Sensors and Actuators A : Physical*, vol. 166(1), pp. 1–8, 2011.
- [40] O. Atasoy and C. Dehollain, “A study for remote powering of a knee prosthesis through inductive link,” in *2010 Conference on Ph.D. Research in Microelectronics and Electronics (PRIME)*, (Berlin, Germany), pp. 1–4, august 2010.
- [41] A. Collo, P. Poignet, C. Hamitouche, S. Almouahed, and E. Stindel, “A miniaturised actuation system embedded in an instrumented knee implant for postoperative ligament imbalance correction,” in *Proceedings of the 36th Annual International Conference of the IEEE Engineering in Medicine and Biology Society (EMBC 2014)*, (Chicago, Illinois, USA), pp. 6211–6214, august 2014.
- [42] “Iso standard 68-1, iso general purpose screw threads - basic profile - part 1 : Metric screw threads.” International Organisation for Standardization, 1998.

- [43] J. L. Fanchon, *Guide de Mécanique : Sciences et Technologies Industrielles*. Paris, France : Nathan, 2001.
- [44] Lily-Bearings, “F2-6m thrust ball bearings.” <http://www.lily-bearing.com/en/miniature/f2-6m.htm>, 2014. [Online; accessed 12-May-2014].
- [45] AST-Bearings, “F3-8m thrust ball bearings.” <http://www.astbearings.com/product.html?product=F3-8M>, 2014. [Online; accessed 12-May-2014].
- [46] AST-Bearings, “F5-12m thrust ball bearings.” <http://www.astbearings.com/product.html?product=F5-12M>, 2014. [Online; accessed 12-June-2014].
- [47] “Minilub - revêtement lubrifiant.” Metallisation Nord Industrie - <http://www.mni-hi-tech.com>, 2014.
- [48] “Iso standard 261, iso general purpose metric screw threads - general plan.” International Organisation for Standardization, 1998.
- [49] Faulhaber, “Miniature drive systems - adm0620-2r-v2-05.” <http://www.micromo.com/ecatalog/page245.html>, 2014. [Online; accessed 12-May-2014].
- [50] Faulhaber, “Miniature drive systems - precision gearheads - 06/1 k 1024 :1.” <http://www.micromo.com/ecatalog/page294.html>, 2014. [Online; accessed 12-May-2014].
- [51] T. P. Schmalzried, E. S. Szuszczewicz, M. R. Northfield, K. H. Akizuki, R. E. Frankel, G. Belcher, and H. C. Amstutz, “Quantitative assessment of walking activity after total hip or knee replacement,” *Journal of Bone and Joint Surgery*, vol. 80, pp. 54–59, 1998.
- [52] “Adl-force 5 simulator user manual.” AMTI Force and Motion, november 2010.
- [53] “Iso standard 14243-3, implants for surgery - wear of total knee-joint prostheses - part 3 : Loading and displacement parameters for wear-testing machines with displacement control and corresponding environmental conditions for test.” International Organisation for Standardization, 2004.
- [54] Tekscan, “Flexiforce elf user manual.” <http://www.tekscan.com/flexible-force-sensors>, august 2013.

Un des objectifs principaux de l'Arthroplastie Totale du Genou (ATG) est la mise en place de conditions appropriées de tension ligamentaire au niveau des deux ligaments collatéraux de l'articulation. Cette étape, qui est effectuée manuellement par le chirurgien, détermine directement la fonctionnalité de l'implant prothétique et sa durée de vie postopératoire. Au cours des deux dernières décennies, plusieurs outils ont été développés en tant qu'outils d'aide au chirurgien pour la phase d'équilibrage ligamentaire. En dépit de cela, les imprécisions peropératoires sont pratiquement inévitables et risquent de donner lieu à des complications postopératoires. Dans le pire des cas, une reprise chirurgicale devient nécessaire pour rétablir des conditions d'équilibre optimales. Dans ce contexte, cette thèse a pour objectif l'étude, la conception et l'analyse d'un modèle original de prothèse instrumentée de genou qui soit capable de détecter toute condition de laxité ligamentaire postopératoire et, si nécessaire, de la compenser.

Un système d'actionnement miniaturisé embarqué dans l'embase tibiale a été proposé pour ajuster l'inclinaison du plateau tibial de façon à retendre un ligament collatéral trop relâché. Cette opération, réalisée avant la survenue de complications plus graves, est suffisante pour rétablir des conditions d'équilibre optimales sans besoin d'une seconde intervention chirurgicale. Pour ce faire, une structure mécanique a été conçue et dimensionnée de façon à répondre aux besoins cliniques tout en faisant face aux contraintes de biocompatibilité imposées par un milieu biologique tel que celui du genou. L'analyse du modèle mécanique du système d'actionnement proposé a confirmé son bon rendement; les simulations effectuées sur le modèle 3D de l'implant ont permis d'en optimiser la conception. Suite à la fabrication d'un prototype à taille réelle de l'implant proposé, des essais expérimentaux ont été conduits à l'aide d'un simulateur du genou pour valider le principe de fonctionnement du système d'actionnement et pour évaluer les performances lors de la marche. Les résultats très prometteurs de la phase de validation expérimentale ont également fourni des indications précieuses pour l'orientation et la suite de travaux futurs.

Mots-clés : Prothèse Instrumentée de Genou, Déséquilibre ligamentaire, Système d'actionnement, Structure mécanique miniaturisée

Collateral ligaments tensioning is a key achievement of Total Knee Arthroplasty (TKA). This stage, which directly determines the postoperative knee joint function and the implant lifespan, cannot be standardised for all patients and highly relies on the surgeons experience and perception. Over the last twenty-five years, the design of instrumented knee prostheses has been accepted as a way forward to provide the surgeon with useful pre- and intraoperative assistance. Nevertheless, suboptimal collateral ligaments tension values are practically unavoidable and may lead to severe postoperative complications; in the worst-case scenario, revision surgery might be necessary already a few years after primary TKA. In such framework, this work aims to propose a novel instrumented knee implant able to detect collateral ligaments laxity conditions right after primary TKA and, if needed, compensate for any detected inaccuracy in the postoperative period.

A miniaturised actuation system embedded in the tibial baseplate can be employed to adjust the inclination of the tibial tray and re-tighten a too lax collateral ligament. Such correcting action, carried out to restore optimal balance conditions before the occurrence of more severe complications, is intended to improve the prosthesis lifespan and, contextually, reduce the need for revision surgery. To this end, a compact and robust mechanical structure was dimensioned in order to fulfil the aforementioned clinical needs while facing with technical and technological limitations. Smart design choices resulted in a good system efficiency, as proved by the mechanical model static force analysis. Simulations run on the implant 3D model allowed to perform useful design optimisations and to estimate the components robustness properties. Upon fabrication of the proposed instrumented tibial component full-scale prototype, stability and force sensors tests on a knee simulator were defined to evaluate the actuation system working principle and assess the effectiveness of the proposed design choices under normal working conditions. The very promising results of the experimental validation stage also provided precious indications for future work and improvements.

Keywords : Instrumented Knee Prosthesis, Knee Ligament Imbalance, Actuation System, Miniaturised Mechanical Device